Spring 2022 – Systems Biology of Reproduction
Discussion Outline – Gonadal Developmental Systems Biology
Michael K. Skinner – Biol 475/575
CUE 418, 10:35-11:50 am, Tuesday & Thursday
February 17, 2022
Week 6

Gonadal Developmental Systems Biology

Primary Papers:

1. Soto and Ross (2021) Reproduction 161:239-253
2. Ben Maamar, et al. (2017) Scientific Reports 7:44184
3. Nilsson, et al. (2013) BMC Genomics 14:496

Discussion

Student 13: Reference #1 above

- What is the technical approach?
- What specific transcriptome observations were made?
- Why is the similarity in cow and human germline development?

Student 14: Reference# 2 above

- What are the technology used and objectives?
- What environmental exposure was used?
- What impacts on human fetal development and germ cells were observed?

Student 16: Reference #3 above

- What is the experimental and systems approach?
- What is a cluster analysis?
- What gene networks were identified for primordial follicle assembly?

REPRODUCTION
RESEARCH

Similarities between bovine and human germline development revealed by single-cell RNA sequencing

Delia Alba Soto and Pablo Juan Ross

Department of Animal Science, University of California, Davis, California, USA

Correspondence should be addressed to P J Ross; Email: pross@ucdavis.edu

Abstract

The germ cell lineage ensures the creation of new individuals and perpetuates the genetic information across generations. Primordial germ cells are pioneers of gametes and exist transiently during development until they differentiate into oogonia in females, or spermatogonia in males. Little is known about the molecular characteristics of primordial germ cells in cattle. By performing single-cell RNA-sequencing, quantitative real-time PCR, and immunofluorescence analyses of fetal gonads between 40 and 90 days of fetal age, we evaluated the molecular signatures of bovine germ cells at the initial stages of gonadal development. Our results indicate that at 50 days of fetal age, bovine primordial germ cells were in the early stages of development, expressing genes of early primordial germ cells, including transcriptional regulators of human germline specification (e.g. *SOX17*, *TFAP2C,* and *PRDM1*). Bovine and human primordial germ cells also share expression of *KIT*, *EPCAM*, *ITGA6*, and *PDPN* genes coding for membrane-bound proteins, and an asynchronous pattern of differentiation. Additionally, the expression of members of Notch, Nodal/Activin, and BMP signaling cascades in the bovine fetal ovary, suggests that these pathways are involved in the interaction between germ cells and their niche. Results of this study provide insights into the mechanisms involved in the development of bovine primordial germ cells and put in evidence similarities between the bovine and human germline.

Reproduction (2021) **161** 239–253

Introduction

The specification of primordial germ cells (PGCs), the progenitors of sperm and eggs, occurs around the onset of gastrulation by the inductive signaling of bone morphogenetic proteins (BMP) on a group of cells that are initially destined toward a somatic mesodermal fate (Lawson *et al.* 1999, Saitou *et al.* 2002, Kobayashi *et al.* 2017, Chen *et al.* 2019). Even though the signaling pathways that operate during PGC specification are conserved across mammals (Nikolic *et al.* 2016), the origin of the signaling molecules, the key transcriptional regulators, and their hierarchy are divergent between species (Kojima *et al.* 2017).

In mice, the period of PGC development lasts around 7 days. This process is initiated by BMP4 signaling on WNT-primed cells, which activates PRDM1 (also known as BLIMP1) and PRDM14. Together with TFAP2C, a direct target of PRDM1, these genes act in combination to induce PGC fate (Ohinata *et al.* 2005, Yamaji *et al.* 2008). The PRDM1-PRDM14-TFAP2C tripartite genetic network acts to repress the somatic mesodermal program, induce re-expression of pluripotency genes, initiate expression of PGC genes, and prompt genome-wide epigenetic reprogramming (Saitou *et al.* 2002, Yabuta *et al.* 2006, Seki *et al.* 2007); all key events involved in the specification of PGCs. After specification, PGCs follow guidance cues that will ultimately lead them to the genital anlage. Upon colonization of the undifferentiated developing gonad, PGCs undergo synchronous mitotic divisions with incomplete cytokinesis, forming nests of interconnected germ cells (Pepling & Spradling 1998). The PGC development period ends when female PGCs enter meiotic prophase or male PGCs enter mitotic quiescence (McLaren & Southee 1997). In the ovary, meiosis initiation is triggered by retinoic acid signaling which in the testis is antagonized by the cytochrome P450 activity of Sertoli cells (Bowles *et al.* 2006, Koubova *et al.* 2006).

In humans, the period of PGC development lasts around 7 weeks (from week 2 to week 9 of fetal development) (Tang *et al.* 2015). Activation of BMP signaling leads to upregulation of PRDM1, which in primates and pigs, is triggered by SOX17, a key regulator of PGC specification (Irie *et al.* 2015, Kobayashi *et al.* 2017, Kojima *et al.* 2017). BMP signaling initially upregulates TFAP2C independently from SOX17, which in combination with PRDM1 establish the gene expression program of human PGCs (Kojima *et al.* 2017). Upon specification, human PGCs migrate and colonize the genital ridge to extensively proliferate until they enter meiosis asynchronously in females (Anderson *et al.* 2007) or enter mitotic quiescence and undergo meiosis after puberty in males (Tang *et al.* 2015).

ISSN 1470–1626 (paper) 1741–7899 (online)
https://doi.org/10.1530/REP-20-0313
Online version via https://rep.bioscientifica.com

Despite the advances in mice and humans, PGC specification and development in livestock species are largely unknown. Similar to humans, the period of bovine PGC development lasts around 6 weeks (from week 2 to week 8 of fetal development) (Lavoir *et al.* 1994, Wrobel & Süß 1998). At 40 days of fetal development, the undifferentiated bovine gonad undergoes sexual differentiation, and then female germ cells initiate meiosis between 70 and 80 days of fetal age (Erickson 1966). At the molecular level, bovine PGCs are characterized by nonspecific alkaline phosphatase (AP) activity (Wrobel & Süß 1998), expression of well-conserved germline markers such as the tyrosine-kinase receptor KIT (also known as cKIT) (Kritzenberger & Wrobel 2004), and the RNA-binding proteins NANOS3 (Ideta *et al.* 2016), DDX4 (also known as VASA) (Pennetier *et al.* 2004, Bartholomew & Parks 2007, Luo *et al.* 2013) and DAZL (Hummitzsch *et al.* 2013). However, the molecular signatures that characterize the bovine germline during early gonadal development have not been elucidated, due in part to the challenges associated with studying PGCs. During their initial development, PGCs are embedded in the developing embryo in small numbers (Barton *et al.* 2016, Cantú & Laird 2017) and even though human and mice PGCs can be purified by cell sorting, antibodies to successfully target and isolate bovine PGCs are not commercially available. To overcome this limitation and elucidate the molecular signatures that characterize the bovine germline during early gonadal development, we performed single-cell RNA-sequencing (scRNA-seq), quantitative real-time PCR (RT-qPCR), and immunofluorescence analyses of fetal gonads between 40 and 90 days of age. At day 50 bovine PGCs were in early stages of development and shared with the human germline expression of transcriptional regulators and surface markers, and an asynchronous progression of differentiation.. Bovine PGCs and their somatic counterparts expressed members of the BMP, Activin/Nodal, and Notch signaling cascades, suggesting that these pathways may have roles in coordinating the events of gonad development in cattle.

Materials and methods

Tissue collection and processing

Bovine fetuses were obtained from a local abattoir and transported on ice to the laboratory within 3 h of retrieval. Fetuses were inspected for normal development and the crown-rump length (CRL) was measured to estimate gestational age (DesCôteaux *et al.* 2009). Gonads were identified based on their location within the abdominal cavity, anatomy, and relationship with neighboring organs (mesonephros and/or kidneys). Tissues retrieved for histology were fixed in 4% paraformaldehyde for 24 h at 4°C and stepwise dehydrated through an ethanol gradient and processed in a VIP Tissue Tech processor (Sakura Finetek). Tissue was then embedded in paraffin, sectioned at 5 µm thickness and stained with hematoxylin and eosin (H&E). Gonads collected for immunostaining analyses were fixed in 4% paraformaldehyde for 5 h at 4°C, washed and transferred to 30% sucrose until embedding in Tissue-Tek optimal cutting temperature (OCT) compound (4883, Sakura Finetek). Cryoblocks were sectioned at 10 µm thickness and tissue sections were stored at −20°C until staining. Gonads retrieved for scRNA-seq were washed in ice-cold PBS and slow frozen in DMEM containing 20% FBS and 10% DMSO using a freezing device (5100-0001, Thermo Scientific). Fetal ovaries and testes harvested for quantitative RT-PCR were snap-frozen in liquid nitrogen and stored at −80°C until RNA was extracted. Samples utilized in this study are listed in Table 1.

Immunofluorescence analysis

Cryosections were washed to remove the OCT compound before unmasking for 10 min in a steamer in 10 mM sodium citrate buffer, pH 6.0. Blocking was performed by incubating the tissue sections with 0.3 mM glycine and 10% normal donkey serum for 1 h, at room temperature. Tissue sections were then incubated overnight at 4°C with the following primary antibodies: anti-PRDM1 (1:50; 14-5963-80, Invitrogen), anti-OCT4 (1:500; sc-8628, Santa Cruz Biotechnology), anti-DAZL (1:500; Ab34139, Abcam), anti-DDX4 (1:500; Ab13840, Abcam). Secondary antibody incubation was performed for 1 h at room temperature and Hoechst 33342 was used for counterstaining. Tissue sections were mounted using ProLong Gold Antifade (P36934, Invitrogen) and images captured using

Table 1 List of bovine fetuses harvested for this study.

CRL (cm)	**Sex**	**Estimated fetal age** (days)	**Analysis**
2	N/A	40	H&E
2	Male	40	IMF
2.5	Male	45	IMF
3	Female	45–50	IMF
3	Male	45–50	RT-qPCR
3.5	Female	50	AP
3.5	Female	50	RT-qPCR
4	Female	50	scRNA-seq
4	Female	50	scRNA-seq
4.5	Female	50	H&E
4.5	Female	50	RT-qPCR
5.5	Female	50–60	RT-qPCR
5.5	Male	50–60	RT-qPCR
6	Female	60	IMF
6.3	Male	60	IMF & AP
8	Male	60–70	RT-qPCR
8.3	Female	60–70	RT-qPCR
11	Female	80	RT-qPCR
11	Male	80	RT-qPCR
12	Male	80	IMF & AP
14	Female	90	RT-qPCR
14	Male	90	RT-qPCR
15.5	Female	90	IMF
16	Female	90	IMF

AP, detection of alkaline phosphatase activity; CRL, crown-rump length; H&E, hematoxylin and eosin staining; IMF, immunofluorescence staining; N/A, not available; RT-qPCR, quantitative real-time PCR; scRNA-seq: single-cell RNA-sequencing.

a Leica TCS SP8STED 3X laser-scanning confocal microscope. Image processing was performed using ImageJ (v2.0.0-rc-69/1.52n). Immunostaining of mesonephros was utilized as negative control when germline-specific proteins were detected.

Alkaline phosphatase staining

Detection of AP activity was performed using the Alkaline Phosphatase Staining Kit II (00-0055; Stem-gent) adapting the manufacturer's protocol for tissue sections. Briefly, cryosections were washed in PBS supplemented with 0.05% Tween 20 and incubated with freshly prepared AP Substrate Solution (provided with the kit) in the dark at room temperature for 15 min. The reaction was stopped by washing tissue sections in PBS and stained sections were mounted in ClearMount mounting medium (MMC0112, American MasterTech). Imaging was performed using a Q Imaging camera on an Olympus BH2 microscope.

Sex determination by polymerase chain reaction

Fetuses less than 50 days of fetal age (4 cm CRL) were sexed by PCR targeting the DEAD box helicase 3 gene (*DDX3X/DDX3Y*), which allows discrimination between X and Y chromosomes based on amplicon size (Gokulakrishnan *et al.* 2012). DNA extraction was performed using the DNeasy Blood and Tissue Kit (69504, Qiagen) according to manufacturer's protocol. DNA was quantified using a NanoDrop 2000C Spectrophotometer (Thermo Scientific) and amplified using the Go Taq Hot Start Green Master Mix. Amplicons were observed by agarose gel electrophoresis stained with ethidium bromide. Genomic DNA from adult testes and ovaries were used as controls.

cDNA preparation and quantitative RT-PCR

Total RNA was extracted using the RNeasy Mini Kit (74104, Qiagen) and DNase treated with the RNase-Free DNase Set (79254, Qiagen). After extraction, RNA was quantified using the Qubit RNA BR Assay Kit (Q10211, Invitrogen) and reverse transcribed using SuperScript III Reverse Transcriptase (18080044, Invitrogen) according to the manufacturer's protocols.

Evaluation of gene expression was performed using PowerUp SYBR Green Master Mix (A25742, Applied Biosystems) on a QuantStudio 3 Real-Time PCR System (A28137, Applied Biosystems). The Primer Quest tool (Integrated DNA Technologies) was used to design primers (Table 2) spanning an exon–exon junction. Samples were run in technical duplicates and relative expression was calculated by the delta Ct method, normalizing values to the HMBS housekeeping gene. cDNA from adult testes and ovaries were used as controls.

Fetal gonad dissociation for single cell RNA-sequencing

Slow-frozen gonads from two independent replicates of approximately 50 days of fetal age (4 cm CRL) were removed from liquid nitrogen and thawed at 37°C in a water bath. Gonads were then rinsed in ice-cold PBS, minced into ~0.1 mm pieces and incubated in Collagenase Type IV (800 U/mL) (LS004186, Worthington) supplemented with DNase I (6 U/mL) (04536282001, Roche Applied Science) at 37°C in a prewarmed orbital shaker for 10 min at 150 rpm. After dissociation, the cell suspension was filtered and dead cells were removed by magnetic bead sorting using a Dead Cell Removal Kit (13009010, Miltenyi) following the manufacturer's protocol. Viable cells resuspended in 0.4% BSA were submitted on ice to the UC Davis DNA Technologies & Expression Analysis Core for library preparation and sequencing.

10× Genomics library preparation and sequencing

Cells were captured using a 10× Chromium controller targeting 10,000 cells per sample. Libraries were prepared using the Chromium Single Cell 3′ v2 chemistry for sample 1 and v3 chemistry for sample 2 according to the manufacturer's protocol. Sequencing was performed in an Illumina HiSeq 4000 platform as 150 base paired-end.

Mapping, cell quality control and downstream analyses

Demultiplexing of raw reads and mapping to the bovine reference genome (ARS-UCD1.2.96) was performed using the Cell Ranger software (v3.0.2). Reads were filtered and counted through the Cell Ranger Count pipeline. The R package Seurat (v3.1.0.9003) was used for sample integration, quality control,

Table 2 Sequence of primer sets used for qPCR.

Gene	Forward primer sequence	Reverse primer sequence	Tm (°C)	Amplicon size (bp)
DDX4	GAAGGTGATAGCTCTGGTTTCT	GTCTTGATAACCGCCTCTCTT	62	99
HMBS	CTTCACCATTGGAGCTGTCT	TAGTTCCTACCACACTCTTCTCT	62	116
NANOS3	TGTGCAGGTTCCAAAGGT	GTCTCCTTAGGCAGAAGTTGAG	62	81
PRDM1	CCACATGAATGCCAGGTTTG	TGCACTGGTAAGGTTTCTCTC	62	97
PRDM14	GGACAAGGGTGACAGGAAAT	TCCCGCATGTAGAACACTTG	62	128
POU5F1	AACGAGAATCTGCAGGAGATATG	TCTCACTCGGTTCTCGATACT	62	87
SOX2	CATTAACGGCACACTGCCCC	TGAAAATGTCTCCCCCGCCC	62	76
SOX17	AAGATGCTGGGCAAGTCG	CGGTACTTGTAGTTGGGATGG	62	116
TFAP2C	CGACATGGCACACCAGAT	GGAAATAGGACCTTTGCGAATAAC	62	94
DDX3	AGGAAGCCAGGAAAGTAA	CATCCACGTTCTAAGTCT	58	184 and 208

Tm, melting temperature.

and secondary analyses (Stuart *et al.* 2019). Quality check of datasets and cell filtering was based on 4 criteria: number of detected genes, number of unique molecular identifiers, percentage of mitochondrial genes, and percentage of ribosomal genes. Cells that passed the selection criteria (cells containing 200 to 6000 reads and <5% of mitochondrial genes) were used for downstream analysis (Supplementary Fig. 1A, see section on supplementary materials given at the end of this article). Integration and normalization of the two replicates was performed by identifying 'anchors' across datasets. Dimensionality reduction was performed by uniform manifold approximation and projection (UMAP) and differential gene expression was performed using non-parametric Wilcoxon rank sum test, which is part of the standard Seurat pipeline. Functional clustering of gene ontology (GO) term enrichment of differentially expressed genes was performed using DAVID (Huang *et al.* 2009). The integration of bovine and human data sets was performed using the human UMI count data from http://github.com/zorrodong/germcell (Li *et al.* 2017). Only female cells expressing 2000 to 10,000 genes and 100,000 to 1,100,000 transcripts were kept for integration, resulting in 970 total cells. Integration of the bovine and human datasets was also performed by the identification of 'anchors' using R package Seurat (v3.1.5.9003) (Stuart *et al.* 2019) and variations due cell cycle heterogeneity were regressed out. The identification of candidate surface marker genes was performed using the computational framework COMET (Delaney *et al.* 2019) using their stand-alone software package.

Data availability

Accession numbers for the 10×X Genomics single cell RNA-seq data that support the findings of this study are openly available at https://www.ncbi.nlm.nih.gov/geo/, GEO accession: GSE162952. Code availability of the custom scripts used can be found on GitHub at https://github.com/deliasoto/Bovine_scRNA-seq.

Results

Morphology and alkaline phosphatase activity of bovine fetal gonads

We evaluated the anatomical relationship of the developing gonad with the mesonephros between 40 and 50 days of fetal age (2–4.5 cm CRL) by H&E staining. At 40 days of fetal age (Supplementary Fig. 2A and B), the gonads were identified by their ventral location to the mesonephros, one of the biggest organs in the abdominal cavity at this stage. Around 10 days later (Supplementary Fig. 2C and D), gonads had tripled in size and grown out from the mesonephros. Similar to other mammals, bovine PGCs possess temporary AP activity that is lost upon differentiation (Gropp & Ohno 1966, Lavoir *et al.* 1994). We detected nonspecific AP activity throughout the fetal gonad in ovaries and testes (Supplementary Fig. 2E, F and G). In ovaries at 50 days of fetal age (3.5 cm CRL), AP positive cells were detected throughout the whole organ, but the surface epithelium seemed to be AP negative. In testes, positive cells in the seminiferous tubules progressively lost AP activity between 60 and 80 days of development (6-12 cm CRL), whereas somatic cells in the interstitium remained AP positive. Thus, in female and male fetal gonads, germ cells were masked by the positive AP reaction of the surrounding cells, confirming the lack of specificity of AP staining that others have described (Gropp & Ohno 1966, Lavoir *et al.* 1994, Wrobel & Süß 1998). Even though bovine fetal gonads can be easily identified after 40 days of development, AP activity is not an appropriate germ cell marker as it is unspecific and germ cells lose AP expression over time.

Single-cell RNA-sequencing of 50 days old bovine fetal ovaries

Since specific surface markers and antibodies to sort the different cell populations of the bovine fetal gonad are not available, we performed scRNA-seq on dissociated fetal gonads to capture the molecular signatures of the bovine germline and its niche. A total of 19,499 cells from two independent replicates of approximately 50 days of fetal age (4 cm CRL) were sequenced obtaining 564,587,528 sequence reads, with 64,039 and 22,332 mean reads per cell in sample 1 and 2, respectively (Supplementary Fig. 1A). After filtering out cell doublets and low-quality cells, 15,548 cells were used for clustering. We identified 11 cell clusters with all clusters being represented in each replicate (Supplementary Fig. 1B). Cluster identity was assigned based on the expression of well-conserved marker genes (Fig. 1A and B) and functional GO term enrichment (Supplementary Table 1). Cells allocated to cluster 5 were identified as PGCs based on the expression of pluripotency and germline-specific genes such as *NANOG*, *OCT4* (also known as POU5F1), *NANOS3*, and *EPCAM* (Fig. 1B and C). PGCs represented 10.8% of the cells present in the fetal gonad. Clusters 0, 1, and 2 expressed genes associated with stromal (*NR5A1* and *COL1A2)* and epithelial (*KRT19* and *MSLN*) cell populations of the fetal ovary (Jameson *et al.* 2012, Mork *et al.* 2012, Hummitzsch *et al.* 2013), and respectively represented 51.7, 20.1, 17.5% of the cells restricted to the somatic and germ cell compartment. GO analysis indicated that clusters 0, 1, and 2 showed specific enrichment for terms such as collagen and extracellular matrix, translation and cell–cell adhesion, and cell proliferation, respectively (Supplementary Table 1). Thus, we identified clusters 0, 1, and 2 as stromal cells, quiescent epithelial cells and proliferative epithelial cells, respectively (Fig. 1B and C). Clusters 3, 4, 6, 7, 8, 9, and 10 represented 29.7% of the total cells analyzed and corresponded to endothelial cells, erythrocytes,

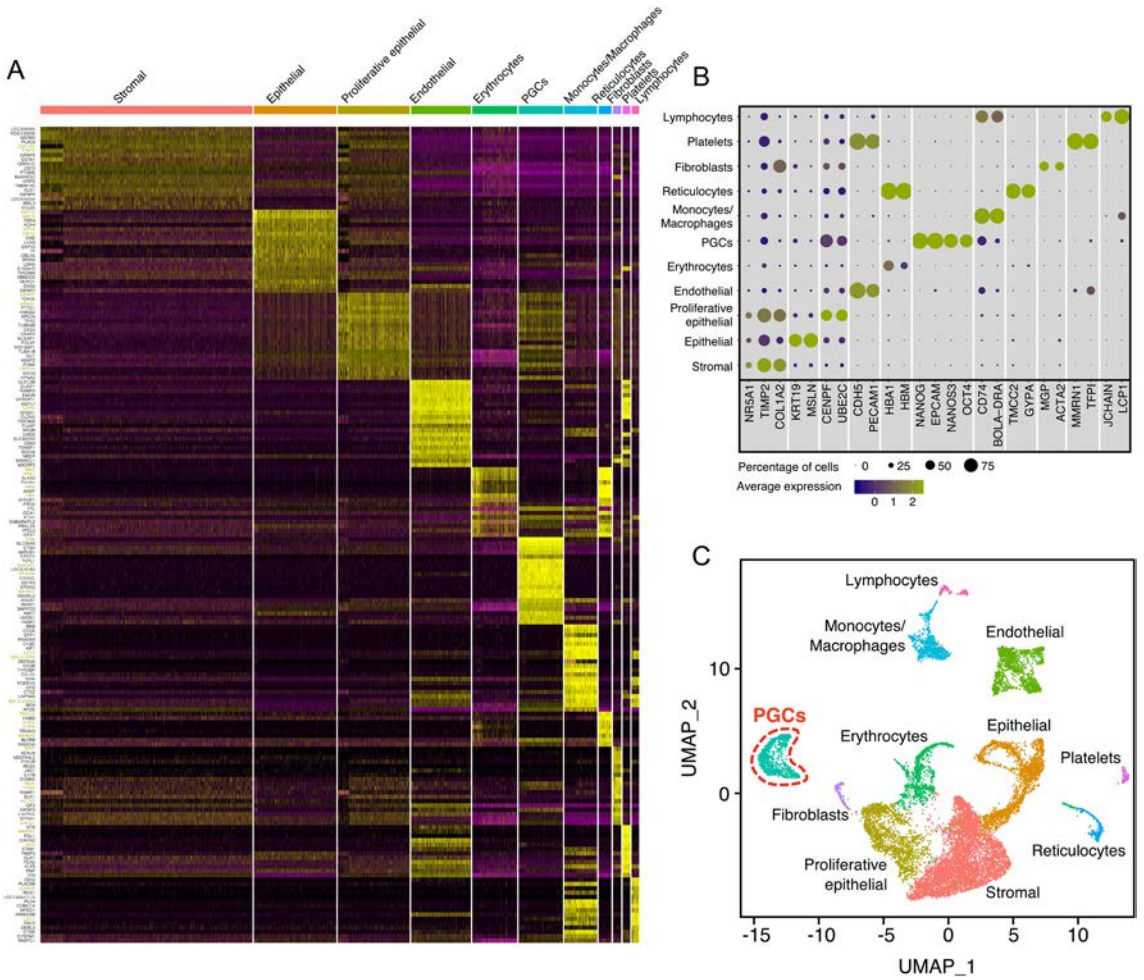

Figure 1 Cell populations detected by scRNA-seq in the bovine fetal ovary at 50 days of fetal age. (A) Heatmap of differentially expressed genes in each cell cluster. Genes used for cluster identification are colored in yellow. (B) Dot plot of the average level of expression (dot color) and percentage of positive cells (dot size) expressing specific marker genes in each cell cluster. (C) Identity of cell populations in UMAP projection.

monocytes/macrophages, reticulocytes, fibroblasts, platelets, and lymphocytes, respectively (Fig. 1C). This analysis demonstrated that different cell populations, including PGCs, can be identified in the bovine fetal gonad by scRNA-seq.

Evaluation of the gene expression profile of the somatic compartment (clusters 0, 1 and 2) (Supplementary Fig. 3) showed high expression of genes involved in the development of the genital ridge (*WT1*, *GATA4*, *SF1*, *EMX2* and *LHX9*) (Luo *et al.* 1994, Miyamoto *et al.* 1997, Birk *et al.* 2000, Hammes *et al.* 2001, Kusaka *et al.* 2010, Hu *et al.* 2013). On the other hand, genes associated with pre-granulosa cells (*LGR5*, *RSP01*, *WNT4*, *FOXL2* and *FST*) (Jorgez *et al.* 2004, Mork *et al.* 2012, Rastetter *et al.* 2014, Zheng *et al.* 2014) presented only low expression in around 5.5% of the cells. These results indicate that the somatic cells of 50 days old (4 cm CRL) bovine fetal gonads are largely undifferentiated and starting the transition toward supportive cells.

Molecular profiling of the bovine germline during early fetal development

scRNA-seq data indicated that at 50 days of fetal age (4 cm CRL) most of the cells in the PGC cluster (98.7%) expressed at least one marker of pluripotency including *OCT4* (72.5%), *NANOG* (95.2%), and *SALL4* (47.2%), or at least one marker of early PGCs development (95.5%) including *NANOS3* (80.2%), *KIT* (69%), and *AP* (57.6%). A smaller subset of cells (21.1%) expressed genes that characterize pre-meiotic late-stage PGCs including *DAZL* (6.3%), *DDX4* (16%), and *STRA8* (0.5%) (Fig. 2A and Table 3). Marker co-expression analysis showed that 76% of the cells allocated to the PGC cluster shared expression of pluripotency and early markers, with 21% also co-expressing late PGCs markers (Fig. 2B), indicating that most PGCs in day 50 fetuses are still in early stages of differentiation, with a subset of cells transitioning toward a more advanced stage.

To confirm the early stage of bovine PGCs at 50 days of fetal age (4 cm CRL) and assess the developmental

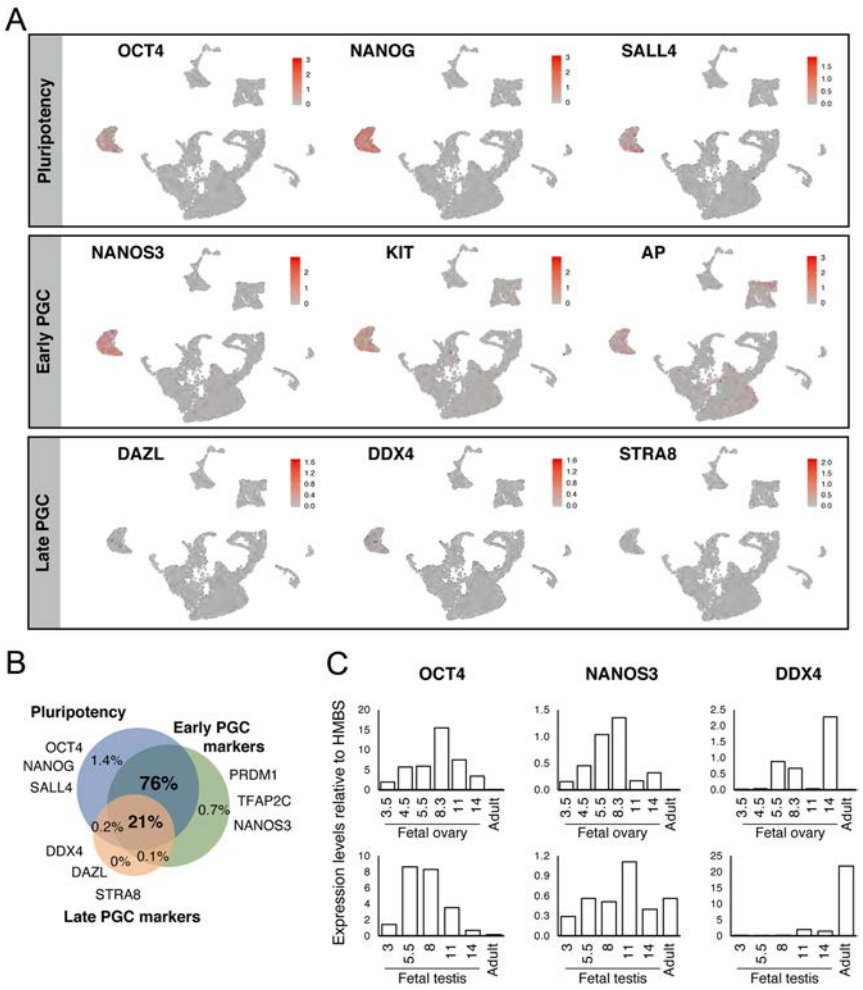

Figure 2 Gene expression profile of bovine PGCs. (A) Level of expression of pluripotency, early and late markers of PGC development in cells of the bovine gonad. (B) Venn diagram of the co-expression of pluripotency, early, and late markers of PGCs development in bovine PGCs. (C) Relative expression of *OCT4*, *NANOS3* and *DDX4* in fetal gonads between 45 and 90 days of fetal age and adult testes and ovaries. Numbers in fetal samples represent crown-rump length in cm.

timeline of the bovine germline, we analyzed expression of well-known markers of early and late PGC at different stages of development by RT-qPCR and immunofluorescence (Figs 2C and 3). Detection of *OCT4, NANOS3,* and *DDX4* in fetal gonads by RT-qPCR (Fig. 2C) corroborated the findings from scRNA-seq. *OCT4* and *NANOS3* presented a similar pattern of expression, characterized by a progressive increase during the first 2–3 months of gonad development, likely reflecting PGC proliferation. *OCT4* and *NANOS3* expression decreased after this period (Fig. 2C). *NANOS3* was not detected in adult ovaries, but was expressed in the adult testes, which is consistent with its role during spermatogenesis (Lolicato *et al.* 2008). Expression of *DDX4* increased after 50 days of development (4 cm CRL) reaching its highest expression in the adult testis (Fig. 2C). Immunofluorescence analyses (Figs 3 and 6) indicated that PRDM1 and OCT4 were equally expressed in female and male PGCs early in development (40–70 days or 2–7 cm CRL). Upon progression of differentiation, PRDM1 and OCT4 were first downregulated in males while in females their expression persisted in germ cells located at the ovarian cortex. DAZL protein was first detected at 60 days (6 cm CRL) of development and rapidly became broadly expressed in the germline, especially in males. DAZL detection persisted at 80-90 days (12–16 cm CRL), in spermatogonia and oogonia inside the seminiferous tubules and ovigerous cords, respectively. DDX4 was only detected in the fetal gonads after day 80 of fetal development (12 cm CRL), following DAZL upregulation. Overall, RT-qPCR and immunofluorescence analyses confirmed scRNA-seq results indicating that at day 50 of fetal age (4 cm CRL), bovine PGCs are mostly in early stages of development.

Similarities between bovine and human germline development

Given the early developmental stage of day 50 bovine PGCs, we evaluated the presence of known transcriptional regulators involved in human germline commitment. The signaling cascade that triggers specification of the human germline has been well studied. *PRDM1*, *PRDM14*, and *TFAP2C* form a key

Table 3 Gene expression profile of female bovine PGCs at 50 days of fetal age.

Genes	PGC cluster	
	Number of positive cells	Percentage of positive cells
Pluripotency		
OCT4	854	72.5
NANOG	1121	95.2
SALL4	556	47.2
KLF4	128	10.9
LIN28A	59	5.0
DPPA3	0	0.0
SOX2	0	0.0
Early PGCs		
PRDM1	794	67.4
PRDM14	44	3.7
TFAP2C	1006	85.4
SOX17	1116	94.7
SOX15	1008	85.6
NANOS3	945	80.2
ALPL	679	57.6
DND1	3	0.3
Late PGCs		
DDX4	188	16.0
DAZL	74	6.3
PIWIL2	23	2.0
Meiosis		
STRA8	6	0.5
SYCP1	5	0.4
SYCP2	261	22.2
SYCP3	479	40.7
REC8	29	2.5
STAG3	9	0.8
Oocyte		
NOBOX	1	0.1
FIGLA	1	0.1
ZP3	57	4.8
GDF9	4	0.3
Surface proteins		
KIT	813	69.0
EPCAM	1133	96.2
PDPN	1110	94.2
ITGA6	409	34.7

transcriptional network that commands specification of the germline in different species (Ohinata *et al.* 2005, Yamaji *et al.* 2008, Kobayashi *et al.* 2017, Sybirna *et al.* 2020). Specifically in humans, the SRY-Box proteins SOX17 and SOX15 also play an important role in germline development (Guo *et al.* 2015, Tang *et al.* 2015, Kobayashi *et al.* 2017, Kojima *et al.* 2017, Chen *et al.* 2018, 2019). Bovine PGCs expressed *PRDM1*, *TFAP2C*, *SOX17*, and *SOX15* transcription factors (Fig. 4A). *PRDM14* was only detected in a few cells, which is consistent with observations in human PGCs (Guo *et al.* 2015, Irie *et al.* 2015, Tang *et al.* 2015, Kobayashi *et al.* 2017) and *SOX2*, which is only re-activated in mouse PGCs (Western *et al.* 2005, Perrett *et al.* 2008, Campolo *et al.* 2013), was not detected. We confirmed expression of *PRDM1*, *TFAP2C*, *SOX17*, *SOX2,* and *PRDM14* by RT-qPCR in fetal gonads (Fig. 4B). Levels of *PRDM1*, *TFAP2C,* and *SOX17* increased until days 60–70 of development (approximately 8 cm CRL) and then decreased steadily. Interestingly, *PRDM14* shared a similar pattern of expression with *PRDM1*, *TFAP2C*, and *SOX17*, especially in fetal ovaries. Expression of SOX2 was almost undetectable in all the fetal samples evaluated, confirming results of scRNA-seq analysis.

Integration of our dataset with a publicly available single-cell transcriptome of human fetal gonadal cells (FGCs) of 5–26 weeks of development (Li *et al.* 2017), showed that 50 days old bovine PGCs clustered together with early human germ cells (Mitotic) (Fig. 5A). Bovine PGCs and human mitotic FGCs had a similar gene expression profile, especially for genes involved in germline specification and pluripotency, and genes that characterize early and late PGC development (Fig. 5B). Our scRNA-seq results also revealed that bovine PGCs expressed genes coding for the surface proteins *EPCAM* (96.2%), *PDPN* (94.2%), *KIT* (69%), and *ITGA6* (34.7%) (Table 3), which are also present in human FGCs (Fig. 5C) (Sasaki *et al.* 2016, Chen *et al.* 2018). These findings further confirm the similar germline-specific molecular profiles between these two species.

We performed prediction of marker panels by COMET which ranks single or multiple marker genes for identification of cell populations of interest. In line with previous results, *EPCAN, KIT* and *PDPN* appeared among the top ranked markers to identify bovine PGCs (Supplementary Fig. 4A and Supplementary Table 3). Interestingly *CD9*, which has a role during fertilization (Umeda *et al.* 2020) and is present in 99.7% of the cells in the PGC cluster and ranked the fifth best marker for PGC identification and isolation. Reliable approaches for the isolation of gonadal somatic cells could be possible using single marker genes (Supplementary Fig. 4B) or by positive and negative selection of marker pairs (Supplementary Fig. 4C).

Exploring the distribution of OCT4 and DAZL in whole ovaries from 40- to 90 day-old fetuses (Fig. 6), we found a progressive loss of OCT4 expression from the center of the ovary outwards to the periphery, while DAZL expression persisted during differentiation, as others have described (Hummitzsch *et al.* 2013). At 40 days of age, few OCT4-positive cells were detected in the ovary. OCT4-positive cells dramatically increased 20 days later and at day 90 OCT4 was only expressed in cells confined to the vicinity of the surface epithelium. Expression of DAZL was first detected at 60 days of age in cells of the medulla and ovarian cortex. DAZL-positive cells localized in the same pattern of cells expressing OCT4; in fact, all the DAZL-positive cells detected at 60 days co-expressed OCT4. Overall, the expression pattern of germline transcriptional regulators, germline-specific, pluripotency, and cell surface markers, and the asynchronous pattern of differentiation detected in the bovine germline, revealed important similarities in the development of bovine and human germ cells.

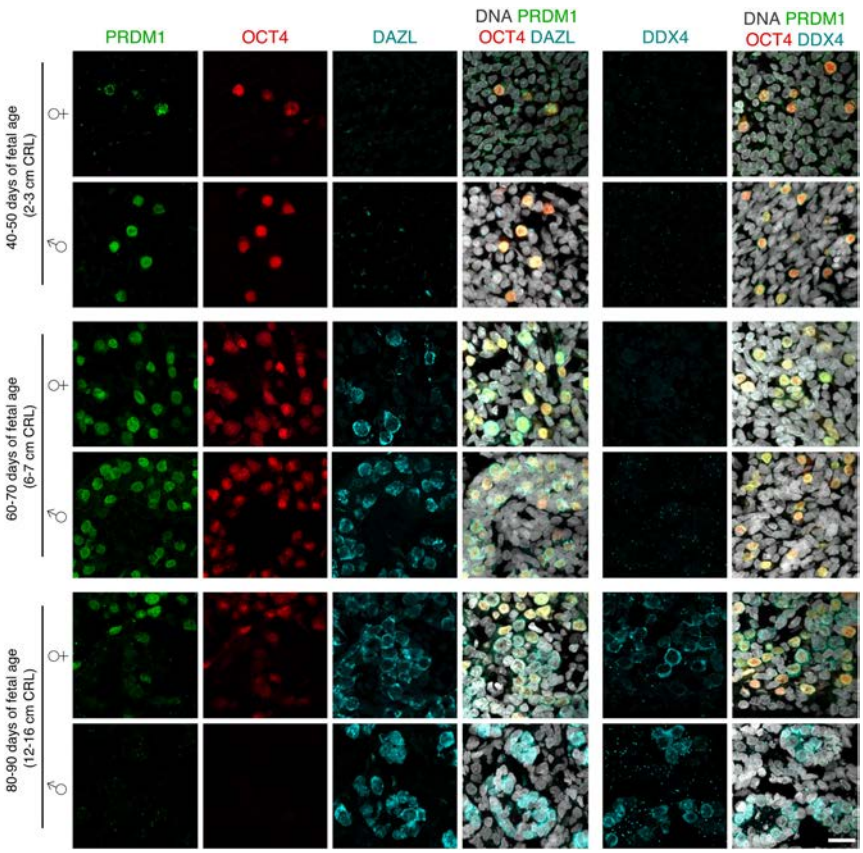

Figure 3 Expression of well-conserved germ cell markers in bovine fetal gonads. Immunofluorescence for PRDM1, OCT4, DAZL, and DDX4 in gonads from 40 to 90 days of fetal age. Nuclear staining was performed using Hoechst 33342. Scale bar 20 µm. OCT4 and PRDM1 detection was confined to the nuclei of PGCs, and DAZL and DDX4 to the cytoplasm. This is in agreement with their roles as transcriptional regulators and RNA-binding proteins, respectively.

Expression of mediators of different signaling pathways in the bovine fetal ovary

Our data confirmed that bovine PGCs express the *KIT* receptor (Kritzenberger & Wrobel 2004), while gonadal somatic cells expressed the *KIT* ligand (KITLG, also known as SCF) (Fig. 7), consistent with previous findings (reviewed by Driancourt *et al.* 2000).

It has been suggested that bone morphogenetic protein (BMP), Nodal, and Notch signaling cascades have roles in the initial development of the human germline (Li *et al.* 2017). We identified expression of *BMP2* and *BMP4* ligands in different cell populations, particularly in PGCs (Fig. 7). *BMP4* was more broadly expressed than *BMP2*, and it was among the top differentially expressed genes detected in the PGC cluster (Supplementary Table 2). Receptors (*ACVR1*, *BMPR1A*) and effector (*SMAD5)* of BMP signaling were detected in several cell groups at different levels of expression. Notably, most of the cells expressing *ACVR1*, *BMPR1A* or *SMAD5* corresponded to stromal cells, epithelial cells, and PGCs.

The *Nodal* ligand was detected only in a few PGCs, but receptors (*ACVR1C*, *ACVR2A*) and nuclear effectors (*SMAD2* and *SMAD3*) of the Nodal cascade, were present in several cell clusters with a higher number of positive cells in the stromal, epithelial, and PGC clusters. Since Nodal and Activin are both members of the TGFβ superfamily of signaling molecules, and signal through the same mediators (reviewed by Pauklin & Vallier 2015), we evaluated the expression of the subunits I*INHA*, *INHBA*, and *INHBB*) (Fig. 7) that form Activins (A, B, and AB), as well as Inhibins (A, B, and AB). We detected expression of the three Inhibin subunits in our dataset, with specific enrichment in stromal cells and epithelial cells.

Members of notch signaling members were found at varying levels of expression in many of the cell populations analyzed (Fig. 7). The Notch ligand *DLL3* was mostly detected in PGCs, and the receptors *NOTCH2*, *NOTCH3*, the effector *RBPJ* (also known as CBF1), which cooperates with Notch intracellular domain to promote transcription, and the target gene *HES1*, were abundant in stromal and/or epithelial cells. The consistent expression of mediators of KIT, BMP, Nodal/Activin, and Notch signaling in PGCs and supporting somatic cells of the bovine fetal gonad, suggest that these pathways may be involved in the interaction between bovine PGCs and their niche.

Discussion

Obtaining a pure population of PGCs for molecular profiling is challenging. Previous means used to identify bovine PGCs included AP activity, KIT expression, detection of specific lectins, and histological features. AP activity and KIT expression are unspecific methods

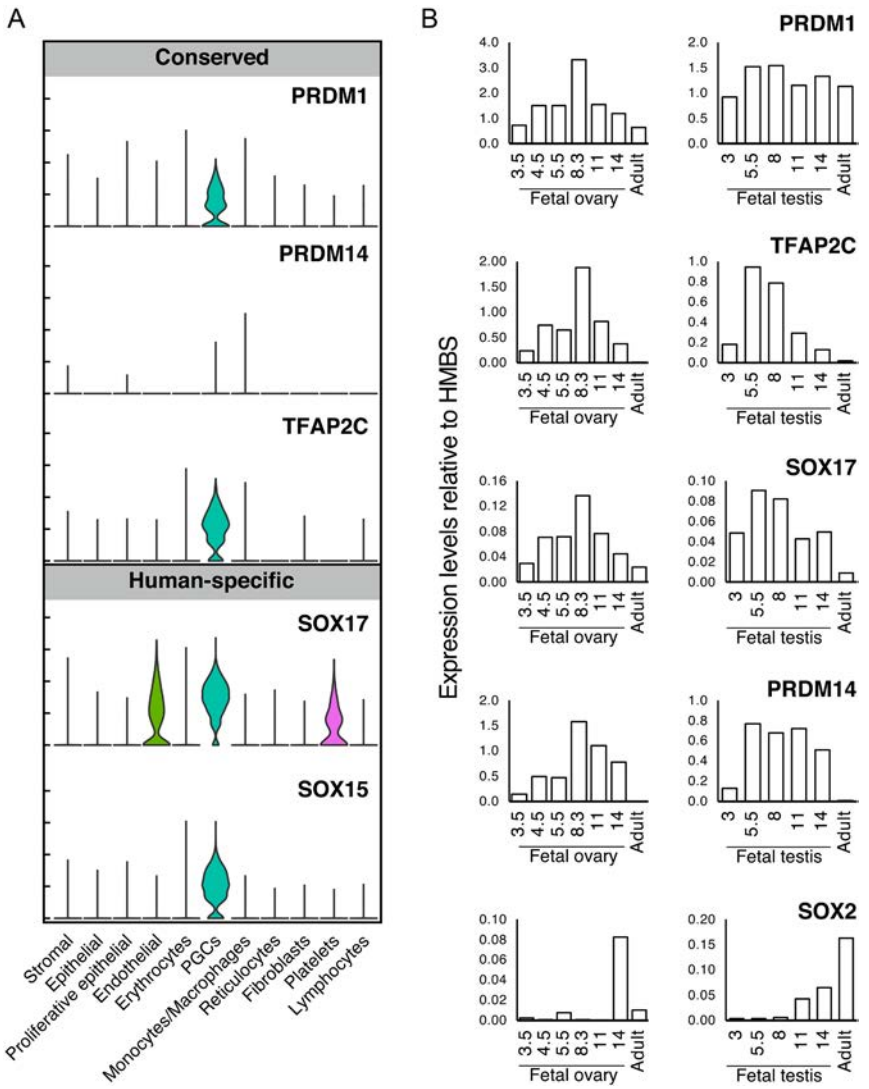

Figure 4 Expression of transcriptional regulators of germline development in bovine PGCs. (A) Violin plots of common (*PRDM1, PRDM14* and *TFAP2C*), and species-specific genes with a function in human (*SOX15* and *SOX17*) germline development. (B) Relative expression of *PRDM1*, *TFAP2C*, *SOX17*, *SOX2*, and *PRDM14* in fetal gonads between 45 and 90 days of fetal age, and adult testes and ovaries. Numbers in fetal samples represent crown-rump length in cm.

to identify germ cells, as they are also present in hematopoietic cells and gonadal somatic cells (Ohno & Gropp 1965, Lavoir *et al.* 1994, Kritzenberger & Wrobel 2004). Similar to other species, bovine PGCs have a characteristic morphology that allows their identification (Leichthammer *et al.* 1990, Wrobel & Süß 1998); however, identification of cells by morphology is impractical, considering the time required for tissue dissociation and manual cell selection. Targeting specific lectins on bovine PGCs does not offer a great advantage either, as glycan-binding antibodies have weak affinity for their target, leading to poor sensitivity (Haab 2012). DDX4 is a germline-specific marker frequently used for sorting human germ cells, but since the expression of a membrane-bound isoform of DDX4 in pre-meiotic germ cells is debatable, the use of commercially available anti-DDX4 antibodies for sorting purposes has shown conflicting outcomes (Woods & Tilly 2013, Zarate-Garcia *et al.* 2016, Wagner *et al.* 2020). Therefore, by performing scRNA-seq, we overcame the limiting step of cell sorting and obtained the transcriptional landscape of bovine PGCs and of different cell groups within the fetal ovary.

The relatively undifferentiated state of bovine PGCs captured by scRNA-seq and the positive expression of master regulators of human germline commitment suggest that the signaling network governing bovine PGC specification might be similar to what has been described in humans. Our scRNA-seq data indicated that at 50 days of fetal age, the transcriptional profile of bovine PGCs is characterized by the expression of *PRDM1*, *TFAP2C*, *SOX17*, *SOX15*, *SALL4*, *LIN28A*, *KLF4*, and *ITGA6* (Table 3), with *SOX17* being one of the top differentially expressed genes (Supplementary Table 2), and lacking *SOX2* expression (Fig. 5B). Therefore, bovine PGCs seem to possess a transcriptional network similar to human PGCs. It has been postulated that SOX17 exerts its critical function in the development of the human germline by regulating gene expression as a binding partner of OCT4 (Tang *et al.* 2016). Expression of SOX17 and SOX2 are mutually exclusive in human

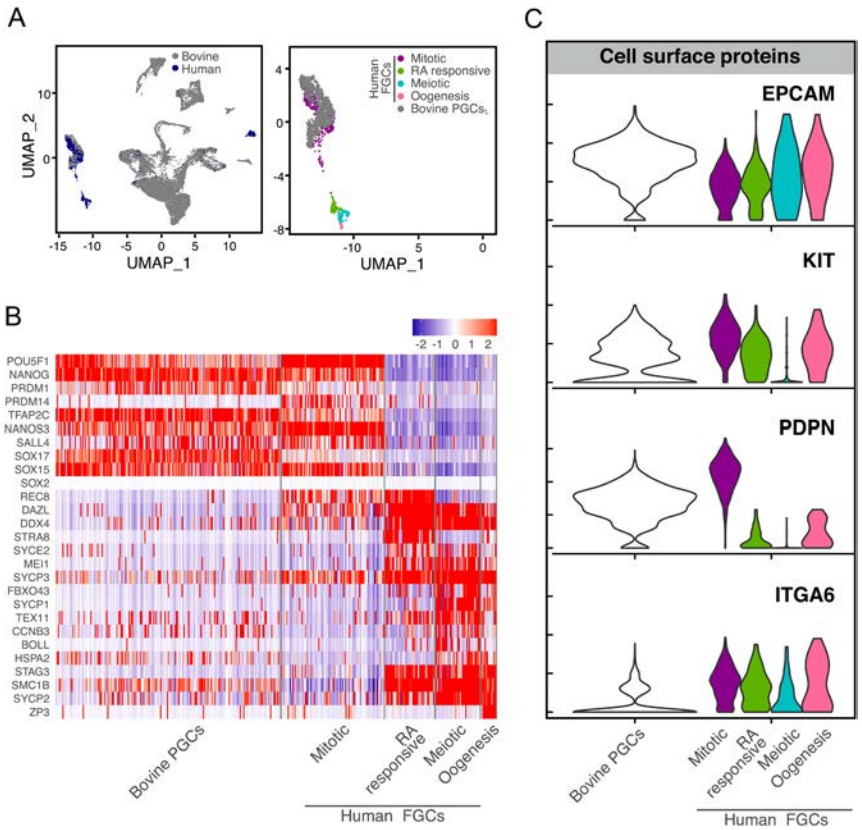

Figure 5 Similarities between bovine and human PGCs transcriptional profile. (A) Integration of scRNA-seq data from bovine (50 days) and human (5–26 weeks) fetal germ cells at different stages of differentiation (Li *et al.* 2017). (B) Comparison of the expression of germline-specific genes between bovine PGCs and human fetal germ cells (Li *et al.* 2017). (C) Expression of *EPCAM*, *KIT*, *PDPN*, and *ITGA6* genes coding for membrane-bound proteins in bovine PGCs and human fetal germ cells (Li *et al.* 2017). FGCs, fetal germ cells; RA, retinoic acid.

PGCs and downregulation of SOX2 is required for PGC-like cell differentiation *in vitro* (Lin *et al.* 2014). OCT4 switches binding partners from SOX2 to SOX17, and regulates the expression of endoderm genes during mouse primitive endoderm differentiation (Aksoy *et al.* 2013). Interestingly, targets of the SOX17-OCT4 partnership are PRDM1 and SALL4 (Aksoy *et al.* 2013), which are both also expressed in bovine PGCs (Table 3). Therefore, our data support the notion that there might be a correspondence between embryonic structure and usage of transcription factors, and that SOX17 may be critical in determining PGC fate in species that develop as bilaminar discs, such as pigs, primates and cattle (Kobayashi & Surani 2018). It will be of interest in the future to evaluate the requirement for SOX17 in the development of the bovine germline.

Unlike PRDM1, which seems to have a conserved role in PGC fate across mammals, PRDM14 function seems to be less explicit. In mouse PGCs, PRDM14 is involved in repressing the somatic program, upregulating germline-specific genes, and promoting epigenetic reprogramming (Saitou *et al.* 2002, Yabuta *et al.* 2006, Seki *et al.* 2007). Instead in human PGCs the role of PRDM14 is less understood. Since in fetal gonads PRDM14 has a cytoplasmic location (Irie *et al.* 2015) and its knockdown did not affect PGC-like cell specification (Sugawa *et al.* 2015) it has been suggested that PRDM14 is dispensable for human PGC fate. However, a recent report put in evidence the crucial role of PRDM14 in the differentiation of human PGC-like cells by inducing a rapid and comprehensive loss of endogenous PRDM14 protein (Sybirna *et al.* 2020). Thus, we compared the expression profile of *PRDM14* in bovine and human PGCs and interestingly, only a small group of bovine PGCs expressed PRDM14. This difference could be attributed to a different role of PRDM14 in bovine PGC fate, or possible to the different scRNA-seq platform used between datasets.

The transcriptome of bovine PGCs revealed the expression of genes coding for membrane-bound proteins that could be of utility for cell sorting. Besides the *KIT* receptor (Kritzenberger & Wrobel 2004), bovine PGCs also expressed *PDPN*, *EPCAM*, and *ITGA6*. Even though these markers do not seem to be specific to the germline, they may be a good alternative to the also unspecific KIT receptor, especially if they are targeted simultaneously. KIT, AP, PDPN, EPCAM, and ITGA6 have also been used to sort or quantify gonadal and *in vitro* generated germ cells in humans (Guo *et al.* 2015, Irie *et al.* 2015, Sasaki *et al.* 2015, Kobayashi *et al.* 2017, Li *et al.* 2017, Yokobayashi *et al.* 2017, Chen *et al.* 2018).

Different signaling pathways have roles in regulating the delicate interaction between PGCs and gonadal somatic cells. BMP signaling has a well-known role in determining germline fate and regulating follicular development (reviewed by Rossi *et al.* 2016). BMP4 and BMP7, secreted from theca and granulosa cells, are important for the primordial to primary follicle

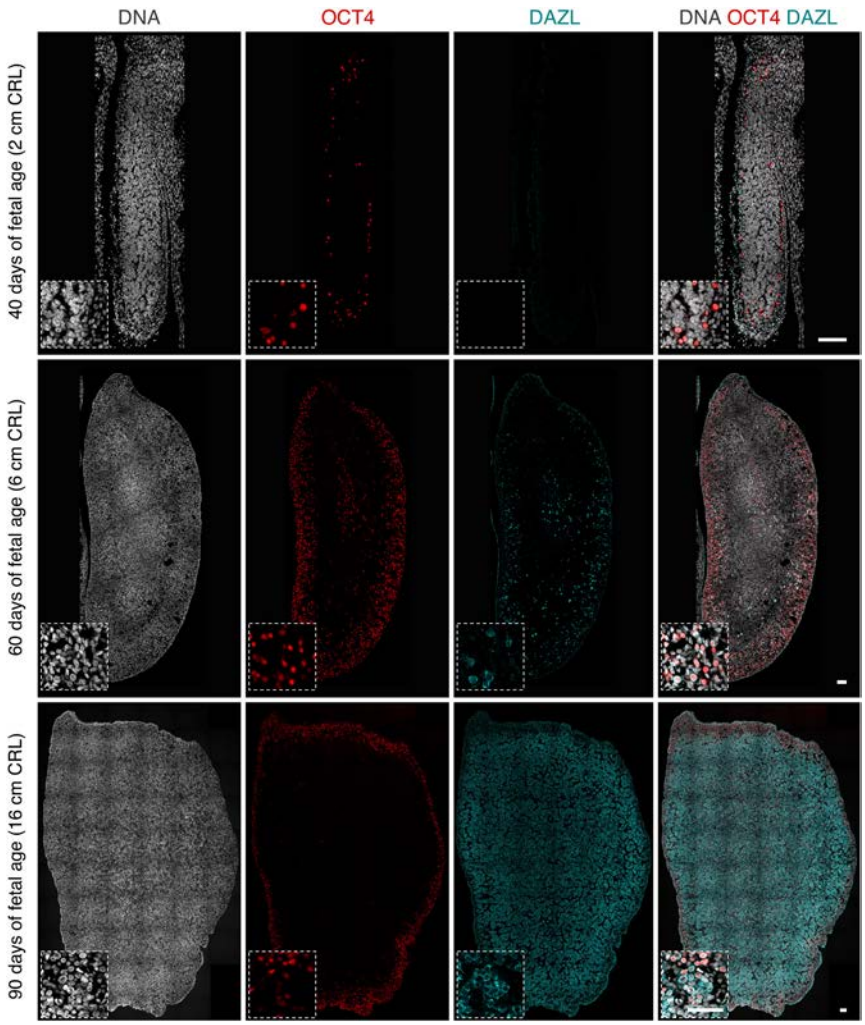

Figure 6 Expression of germ cell markers in whole bovine ovaries. Immunofluorescence for OCT4 and DAZL in the developing ovary. Histological sections were imaged at 20× and pictures were merged to inspect a complete section of the ovary. Nuclear staining was performed using Hoechst 33342. Scale bars 100 µm.

transition (Lee *et al.* 2001, Nilsson & Skinner 2003). Granulosa cells of human fetal ovaries are characterized by having high expression of BMP2, which possibly plays a role during the mitosis-meiosis transition of germ cells (Li *et al.* 2017). In the bovine fetal gonad, we detected *BMP2* and *BMP4* ligands in germ cells, and *BMP7* highly expressed in a small group of cells in the somatic compartment. Receptors and mediators of BMP signaling were present in stromal cells, epithelial cells, and PGCs. These results suggest that BMP signaling operates two-ways between PGCs and the somatic compartment in the bovine fetal ovary. Human PGCs might induce differentiation of other germ cells through activation of the Nodal/Activin signaling pathway (Li *et al.* 2017). Our results indicate that Nodal/Activin signaling may also be active in different cell populations of the fetal ovary, but mainly in stromal cells, epithelial cells, and PGCs. We hypothesize that neither Activins nor Nodal ligands are the main drivers of activation of the cascade, but rather, that Inhibins are the ligands that trigger activation of Activin/Nodal pathway in the bovine fetal ovary. Recently the role of the Notch pathway in the development of the mammalian ovary has begun to be elucidated (Vanorny & Mayo 2017). Notch activation in somatic cells of the mouse fetal ovary is required for germ cell nest breakdown, follicle assembly (Xu & Gridley 2013, Vanorny *et al.* 2014), and meiosis entry (Feng *et al.* 2014). Our scRNA-seq results show high expression of the *DLL3* ligand in PGCs, and expression of the *NOTCH2* receptor and the target gene *HES1* in somatic cells, in agreement with findings in the human fetal gonad (Li *et al.* 2017). Therefore, these results suggest that Notch signaling plays an important role during gonad development, which is conserved among the mouse, human, and cow.

Another difference between mouse and human germ cells development is the pattern by which differentiation proceeds. In the mouse fetal ovary, meiosis progresses in a rostro-caudal wave (Bowles *et al.* 2006, Koubova *et al.* 2006) while in the human fetal ovary meiosis occurs radially (Anderson *et al.* 2007). Interestingly, our data indicate similarities between the bovine and human germline in terms of spatio-temporal differentiation. In fetal ovaries, we

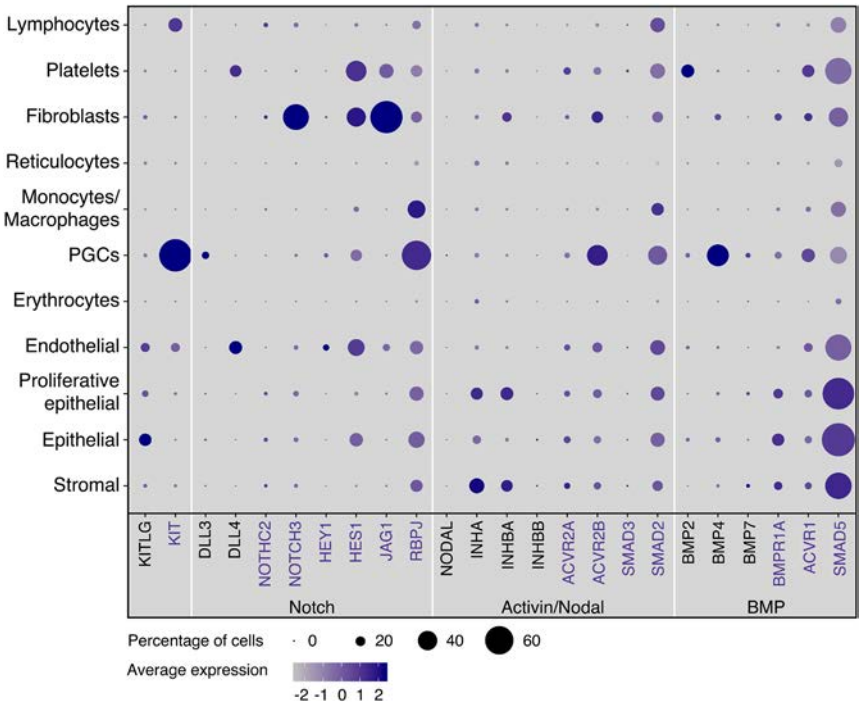

Figure 7 Gene expression of members of different signaling pathways in the bovine fetal ovary. Dot plot of the average level of expression (dot color) and percentage of positive cells in each cell cluster (dot size). Genes in black represent ligands. Genes in purple represent receptors, effectors, or targets of each signaling cascade.

detected a progressive downregulation of OCT4 from the center to the periphery. Germ cells in seminiferous tubules also progressively lost expression of OCT4, and only few OCT4-positive cells remained among DAZL/DDX4-positive cells at day 80 of development. This is in agreement with characterizations of the developing human testis, where differentiation is asynchronous and germ cells expressing early and late markers coexist inside the same seminiferous tubule (Anderson *et al.* 2007, Sohni *et al.* 2019). These results may indicate that the progression of bovine PGC differentiation is asynchronous and that germ cells at different stages of differentiation coexist in the fetal gonad, similar to what has been reported for the human ovary (Anderson *et al.* 2007).

Conclusions

Results from this work offer new insights into the mechanisms that govern gonadal and germline development in cattle. The data we report here is a useful resource to understand the different cell compartments of the developing gonad, the reciprocal relationship between germ cells and their niche, and the factors that may affect germ cell development. Further, results from this study may provide the basis for developing approaches for *in vitro* differentiation of bovine gametes from pluripotent stem cells. The similarities we found in the transcriptional profile of human and bovine PGCs confirm that mouse biology can only be partially extrapolated to other mammalian species and indicate that cattle may be a suitable model to study the specification and commitment of PGCs in humans.

Supplementary materials

This is linked to the online version of the paper at https://doi.org/10.1530/REP-20-0313.

Declaration of interest

The authors declare that there is no conflict of interest that could be perceived as prejudicing the impartiality of the research reported.

Funding

This work was supported by UC Davis Chancellor's Fellowship to P J R and USDA program W-4171 and NRSP8. D A S was supported by a doctoral scholarship from CONICYT within the funding program Becas Chile.

Author contribution statement

D A S was involved in the conception and design, performing experiments, data collection, data analysis, bioinformatics, data interpretation, and manuscript writing. P J R contributed to teh conception and design, financial support, data interpretation, and manuscript writing.

Acknowledgements

The authors thank the UC Davis DNA Tech Core for support with single cell sample preparation, Prof Anna Denicol for technical recommendations, Carly Guiltinan for proofreading and Ingrid Brust-Mascher for assistance with confocal microscopy.

References

Aksoy I, Jauch R, Chen J, Dyla M, Divakar U, Bogu GK, Teo R, Leng Ng CK, Herath W, Lili S *et al.* 2013 Oct4 switches partnering from Sox2 to Sox17 to reinterpret the enhancer code and specify endoderm. *EMBO Journal* **32** 938–953. (https://doi.org/10.1038/emboj.2013.31)

Anderson RA, Fulton N, Cowan G, Coutts S & Saunders PTK 2007 Conserved and divergent patterns of expression of DAZL, VASA and OCT4 in the germ cells of the human fetal ovary and testis. *BMC Developmental Biology* **7** 136. (https://doi.org/10.1186/1471-213X-7-136)

Bartholomew RA & Parks JE 2007 Identification, localization, and sequencing of fetal bovine VASA homolog. *Animal Reproduction Science* **101** 241–251. (https://doi.org/10.1016/j.anireprosci.2006.09.017)

Barton LJ, LeBlanc MG & Lehmann R 2016 Finding their way: themes in germ cell migration. *Current Opinion in Cell Biology* **42** 128–137. (https://doi.org/10.1016/j.ceb.2016.07.007)

Birk OS, Caslano DE, Wassif CA, Cogilatl T, Zhaos L, Zhao Y, Grinberg A, Huang SP, Kreidberg JA, Parker KL et al. 2000 The LIM homeobox gene Lhx9 is essential for mouse gonad formation. *Nature* **403** 909–913. (https://doi.org/10.1038/35002622)

Bowles J, Knight D, Smith C, Wilhelm D, Richman J, Mamiya S, Yashiro K, Chawengsaksophak K, Wilson MJ, Rossant J *et al.* 2006 Retinoid signaling determines germ cell fate in mice. *Science* **312** 596–600. (https://doi.org/10.1126/science.1125691)

Campolo F, Gori M, Favaro R, Nicolis S, Pellegrini M, Botti F, Rossi P, Jannini EA & Dolci S 2013 Essential role of Sox2 for the establishment and maintenance of the germ cell line. *Stem Cells* **31** 1408–1421. (https://doi.org/10.1002/stem.1392)

Cantú AV. & Laird DJ 2017 A pilgrim's progress: seeking meaning in primordial germ cell migration. *Stem Cell Research* **24** 181–187. (https://doi.org/10.1016/j.scr.2017.07.017)

Cao J, Spielmann M, Qiu X, Huang X, Ibrahim DM, Hill AJ, Zhang F, Mundlos S, Christiansen L, Steemers FJ *et al.* 2019 The single-cell transcriptional landscape of mammalian organogenesis. *Nature* **566** 496–502. (https://doi.org/10.1038/s41586-019-0969-x)

Chen D, Liu W, Zimmerman J, Pastor WA, Kim R, Hosohama L, Ho J, Aslanyan M, Gell JJ, Jacobsen SE *et al.* 2018 The TFAP2C-regulated OCT4 naive enhancer is involved in human germline formation. *Cell Reports* **25** 3591.e5–3602.e5. (https://doi.org/10.1016/j.celrep.2018.12.011)

Chen D, Sun N, Hou L, Kim R, Faith J, Aslanyan M, Tao Y, Zheng Y, Fu J, Liu W *et al.* 2019 Human primordial germ cells are specified from lineage-primed progenitors. *Cell Reports* **29** 4568.e5–4582.e5. (https://doi.org/10.1016/j.celrep.2019.11.083)

Delaney C, Schnell A, Cammarata LV, Yao-Smith A, Regev A, Kuchroo VK & Singer M 2019 Combinatorial prediction of marker panels from single cell transcriptomic data. *Molecular Systems Biology* **15** e9005. (https://doi.org/10.15252/msb.20199005)

DesCôteaux L, Gnemmi G & Colloton J 2009 *Practical Atlas of Ruminant and Camelid Reproductive Ultrasonography*. Ames, Iowa: Wiley-Blackwell. (https://doi.org/10.1002/9781119265818)

Driancourt MA, Reynaud K, Cortvrindt R & Smitz J 2000 Roles of KIT and KIT LIGAND in ovarian function. *Reviews of Reproduction* **5** 143–152. (https://doi.org/10.1530/ror.0.0050143)

Erickson BH 1966 Development and radio-response of the prenatal bovine ovary. *Reproduction* **11** 97–105. (https://doi.org/10.1530/jrf.0.0110097)

Feng YM, Liang GJ, Pan B, Qin XS, Zhang XF, Chen CL, Li L, Cheng SF, De Felici M & Shen W 2014 Notch pathway regulates female germ cell meiosis progression and early oogenesis events in fetal mouse. *Cell Cycle* **13** 782–791. (https://doi.org/10.4161/cc.27708)

Gokulakrishnan P, Kumar RR, Sharma BD, Mendiratta SK & Sharma D 2012 Sex determination of cattle meat by polymerase chain reaction amplification of the DEAD box protein (DDX3X/DDX3Y) gene. *Asian-Australasian Journal of Animal Sciences* **25** 733–737. (https://doi.org/10.5713/ajas.2012.12003)

Gropp A & Ohno S 1966 The presence of a common embryonic blastema for ovarian and testicular parenchymal (follicular, interstitial and tubular) cells in cattle, Bos taurus. *Zeitschrift für Zellforschung und Mikroskopische Anatomie* **74** 505–528. (https://doi.org/10.1007/BF00496841)

Guo F, Yan L, Guo H, Li L, Hu B, Zhao Y, Yong J, Hu Y, Wang X, Wei Y *et al.* 2015 The transcriptome and DNA methylome landscapes of human primordial germ cells. *Cell* **161** 1437–1452. (https://doi.org/10.1016/j.cell.2015.05.015)

Haab BB 2012 Using lectins in biomarker research: addressing the limitations of sensitivity and availability. *Proteomics: Clinical Applications* **6** 346–350. (https://doi.org/10.1002/prca.201200014)

Hammes A, Guo JK, Lutsch G, Leheste JR, Landrock D, Ziegler U, Gubler MC & Schedl A 2001 Two splice variants of the Wilms' tumor 1 gene have distinct functions during sex determination and nephron formation. *Cell* **106** 319–329. (https://doi.org/10.1016/s0092-8674(01)00453-6)

Huang da W, Sherman BT & Lempicki RA 2009 Systematic and integrative analysis of large gene lists using DAVID bioinformatics resources. *Nature Protocols* **4** 44–57. (https://doi.org/10.1038/nprot.2008.211)

Hummitzsch K, Irving-Rodgers HF, Hatzirodos N, Bonner W, Sabatier L, Reinhardt DP, Sado Y, Ninomiya Y, Wilhelm D & Rodgers RJ 2013 A new model of development of the mammalian ovary and follicles. *PLoS ONE* **8** e55578. (https://doi.org/10.1371/journal.pone.0055578)

Hu YC, Okumura LM & Page DC 2013 Gata4 Is Required for Formation of the Genital Ridge in Mice. *PLoS Genetics* **9** 1003629. (https://doi.org/10.1371/journal.pgen.1003629)

Ideta A, Yamashita S, Seki-Soma M, Yamaguchi R, Chiba S, Komaki H, Ito T, Konishi M, Aoyagi Y & Sendai Y 2016 Generation of exogenous germ cells in the ovaries of sterile NANOS3-null beef cattle. *Scientific Reports* **6** 24983. (https://doi.org/10.1038/srep24983)

Irie N, Weinberger L, Tang WWC, Kobayashi T, Viukov S, Manor YS, Dietmann S, Hanna JH & Surani MA 2015 SOX17 is a critical specifier of human primordial germ cell fate. *Cell* **160** 253–268. (https://doi.org/10.1016/j.cell.2014.12.013)

Jameson SA, Natarajan A, Cool J, DeFalco T, Maatouk DM, Mork L, Munger SC & Capel B 2012 Temporal transcriptional profiling of somatic and germ cells reveals biased lineage priming of sexual fate in the fetal mouse gonad. *PLoS Genetics* **8** e1002575. (https://doi.org/10.1371/journal.pgen.1002575)

Jorgez CJ, Klysik M, Jamin SP, Behringer RR & Matzuk MM 2004 Granulosa Cell-Specific Inactivation of Follistatin Causes Female Fertility Defects. *Molecular Endocrinology* **18** 953–967. (https://doi.org/10.1210/me.2003-0301)

Kobayashi T & Surani MA 2018 On the origin of the human germline. *Development* **145** dev150433. (https://doi.org/10.1242/dev.150433)

Kobayashi T, Zhang H, Tang WWC, Irie N, Withey S, Klisch D, Sybirna A, Dietmann S, Contreras DA, Webb R *et al.* 2017 Principles of early human development and germ cell program from conserved model systems. *Nature* **546** 416–420. (https://doi.org/10.1038/nature22812)

Kojima Y, Sasaki K, Yokobayashi S, Sakai Y, Nakamura T, Yabuta Y, Nakaki F, Nagaoka S, Woltjen K, Hotta A *et al.* 2017 Evolutionarily distinctive transcriptional and signaling programs drive human germ cell lineage specification from pluripotent stem cells. *Cell Stem Cell* **21** 517.e5–532.e5. (https://doi.org/10.1016/j.stem.2017.09.005)

Koubova J, Menke DB, Zhou Q, Cape B, Griswold MD & Page DC 2006 Retinoic acid regulates sex-specific timing of meiotic initiation in mice. *PNAS* **103** 2474–2479. (https://doi.org/10.1073/pnas.0510813103)

Kritzenberger M & Wrobel KH 2004 Histochemical in situ identification of bovine embryonic blood cells reveals differences to the adult haematopoietic system and suggests a close relationship between haematopoietic stem cells and primordial germ cells. *Histochemistry and Cell Biology* **121** 273–289. (https://doi.org/10.1007/s00418-004-0629-5)

Kusaka M, Katoh-Fukui Y, Ogawa H, Miyabayashi K, Baba T, Shima Y, Sugiyama N, Sugimoto Y, Okuno Y, Kodama R et al. 2010 Abnormal epithelial cell polarity and ectopic Epidermal Growth Factor Receptor (EGFR) expression induced in Emx2 KO Embryonic Gonads. *Endocrinology* **151** 5893–5904. (https://doi.org/10.1210/en.2010-0915)

Lavoir MC, Basrur PK & Betteridge KJ 1994 Isolation and identification of germ cells from fetal bovine ovaries. *Molecular Reproduction and Development* **37** 413–424. (https://doi.org/10.1002/mrd.1080370408)

Lawson KA, Dunn NR, Roelen BAJ, Zeinstra LM, Davis AM, Wright CVE, Korving JPWFM & Hogan BLM 1999 Bmp4 is required for the generation of primordial germ cells in the mouse embryo. *Genes and Development* **13** 424–436. (https://doi.org/10.1101/gad.13.4.424)

Lee WS, Otsuka F, Moore RK & Shimasaki S 2001 Effect of bone morphogenetic protein-7 on folliculogenesis and ovulation in the rat1. *Biology of Reproduction* **65** 994–999. (https://doi.org/10.1095/biolreprod65.4.994)

Leichthammer F, Baunack E & Brem G 1990 Behavior of living primordial germ cells of livestock in vitro. *Theriogenology* **33** 1221–1230. (https://doi.org/10.1016/0093-691X(90)90040-Z)

Li L, Dong J, Yan L, Yong J, Liu X, Hu Y, Fan X, Wu X, Guo H, Wang X *et al.* 2017 Single-cell RNA-seq analysis maps development of human germline cells and gonadal niche interactions. *Cell Stem Cell* **20** 858. e4–873.e4. (https://doi.org/10.1016/j.stem.2017.03.007)

Lin IY, Chiu FL, Yeang CH, Chen HF, Chuang CY, Yang SY, Hou PS, Sintupisut N, Ho HN, Kuo HC *et al.* 2014 Suppression of the SOX2 neural effector gene by PRDM1 promotes human germ cell fate in embryonic stem cells. *Stem Cell Reports* **2** 189–204. (https://doi.org/10.1016/j.stemcr.2013.12.009)

Lolicato F, Marino R, Paronetto MP, Pellegrini M, Dolci S, Geremia R & Grimaldi P 2008 Potential role of Nanos3 in maintaining the undifferentiated spermatogonia population. *Developmental Biology* **313** 725–738. (https://doi.org/10.1016/j.ydbio.2007.11.011)

Luo X, Ikeda Y & Parker KL 1994 A cell-specific nuclear receptor is essential for adrenal and gonadal development and sexual differentiation. *Cell* **77** 481–490. (https://doi.org/10.1016/0092-8674(94)90211-9)

Luo H, Zhou Y, Li Y & Li Q 2013 Splice variants and promoter methylation status of the bovine vasa homology (Bvh) gene may be involved in bull spermatogenesis. *BMC Genetics* **14** 58. (https://doi.org/10.1186/1471-2156-14-58)

McLaren A & Southee D 1997 Entry of mouse embryonic germ cells into meiosis. *Developmental Biology* **187** 107–113. (https://doi.org/10.1006/dbio.1997.8584)

Miyamoto N, Yoshida M, Kuratani S, Matsuo I & Aizawa S 1997 Defects of urogenital development in mice lacking Emx2. Development 124 1653–1664.

Mork L, Maatouk D, McMahon JA, Guo JJ, Zhang P, McMahon AP, McMahon JA & Capel B 2012 Temporal differences in granulosa cell specification in the ovary reflect distinct follicle fates. *Biology of Reproduction* **87** 128–128. (https://doi.org/10.1095/biolreprod.111.095208)

Nikolic A, Volarevic V, Armstrong L, Lako M & Stojkovic M 2016 Primordial germ cells: current knowledge and perspectives. *Stem Cells International* **2016** 1741072. (https://doi.org/10.1155/2016/1741072)

Nilsson EE & Skinner MK 2003 Bone morphogenetic protein-4 acts as an ovarian follicle survival factor and promotes primordial follicle development. *Biology of Reproduction* **69** 1265–1272. (https://doi.org/10.1095/biolreprod.103.018671)

Ohinata Y, Payer B, O'Carroll D, Ancelin K, Ono Y, Sano M, Barton SC, Obukhanych T, Nussenzweig M, Tarakhovsky A *et al.* 2005 Blimp1 is a critical determinant of the germ cell lineage in mice. *Nature* **436** 207–213. (https://doi.org/10.1038/nature03813)

Ohno S & Gropp A 1965 Embryological basis for germ cell chimerism in mammals. *Cytogenetics* **4** 251–261. (https://doi.org/10.1159/000129862)

Pauklin S & Vallier L 2015 Activin/nodal signalling in stem cells. *Development* **142** 607–619. (https://doi.org/10.1242/dev.091769)

Pennetier S, Uzbekova S, Perreau C, Papillier P, Mermillod P & Dalbiès-Tran R 2004 Spatio-temporal expression of the germ cell marker genes MATER, ZAR1, GDF9, BMP15,andVASA in adult bovine tissues, oocytes, and preimplantation embryos1. *Biology of Reproduction* **71** 1359–1366. (https://doi.org/10.1095/biolreprod.104.030288)

Pepling ME & Spradling AC 1998 Female mouse germ cells form synchronously dividing cysts. *Development* **125** 3323–3328.

Perrett RM, Turnpenny L, Eckert JJ, O'Shea M, Sonne SB, Cameron IT, Wilson DI, Meyts ER-D & Hanley NA 2008 The early human germ cell lineage does not express SOX2 during in vivo development or upon in vitro culture1. *Biology of Reproduction* **78** 852–858. (https://doi.org/10.1095/biolreprod.107.066175)

Rastetter RH, Bernard P, Palmer JS, Chassot AA, Chen H, Western PS, Ramsay RG, Chaboissier MC & Wilhelm D 2014 Marker genes identify three somatic cell types in the fetal mouse ovary. *Developmental Biology* **394** 242–252. (https://doi.org/10.1016/j.ydbio.2014.08.013)

Rossi RODS, Costa JJN, Silva AWB, Saraiva MVA, Van Den Hurk R & Silva JRV 2016 The bone morphogenetic protein system and the regulation of ovarian follicle development in mammals. *Zygote* **24** 1–17. (https://doi.org/10.1017/S096719941400077X)

Saitou M, Barton SC & Surani MA 2002 A molecular programme for the specification of germ cell fate in mice. *Nature* **418** 293–300. (https://doi.org/10.1038/nature00927)

Sasaki K, Yokobayashi S, Nakamura T, Okamoto I, Yabuta Y, Kurimoto K, Ohta H, Moritoki Y, Iwatani C, Tsuchiya H *et al.* 2015 Robust in vitro induction of human germ cell fate from pluripotent stem cells. *Cell Stem Cell* **17** 178–194. (https://doi.org/10.1016/j.stem.2015.06.014)

Sasaki K, Nakamura T, Okamoto I, Yabuta Y, Iwatani C, Tsuchiya H, Seita Y, Nakamura S, Shiraki N, Takakuwa T *et al.* 2016 The germ cell fate of cynomolgus monkeys is specified in the nascent amnion. *Developmental Cell* **39** 169–185. (https://doi.org/10.1016/j.devcel.2016.09.007)

Seki Y, Yamaji M, Yabuta Y, Sano M, Shigeta M, Matsui Y, Saga Y, Tachibana M, Shinkai Y & Saitou M 2007 Cellular dynamics associated with the genome-wide epigenetic reprogramming in migrating primordial germ cells in mice. *Development* **134** 2627–2638. (https://doi.org/10.1242/dev.005611)

Sohni A, Tan K, Song HW, Burow D, de Rooij DG, Laurent L, Hsieh TC, Rabah R, Hammoud SS, Vicini E *et al.* 2019 The neonatal and adult human testis defined at the single-cell level. *Cell Reports* **26** 1501.e4–1517.e4. (https://doi.org/10.1016/j.celrep.2019.01.045)

Stuart T, Butler A, Hoffman P, Hafemeister C, Papalexi E, Mauck WM, Hao Y, Stoeckius M, Smibert P & Satija R 2019 Comprehensive integration of single-cell data. *Cell* **177** 1888.e21–1902.e21. (https://doi.org/10.1016/j.cell.2019.05.031)

Sugawa F, Araúzo Bravo MJ, Yoon J, Kim KP, Aramaki S, Wu G, Stehling M, Psathaki OE, Hübner K & Schöler HR 2015 Human primordial germ cell commitment in vitro associates with a unique PRDM14 expression profile. *EMBO Journal* **34** 1009–1024. (https://doi.org/10.15252/embj.201488049)

Sybirna A, Tang WWC, Pierson Smela M, Dietmann S, Gruhn WH, Brosh R & Surani MA 2020 A critical role of PRDM14 in human primordial germ cell fate revealed by inducible degrons. *Nature Communications* **11** 1282. (https://doi.org/10.1038/s41467-020-15042-0)

Tang WWC, Dietmann S, Irie N, Leitch HG, Floros VI, Bradshaw CR, Hackett JA, Chinnery PF & Surani MA 2015 A unique gene regulatory network resets the human germline epigenome for development. *Cell* **161** 1453–1467. (https://doi.org/10.1016/j.cell.2015.04.053)

Tang WWC, Kobayashi T, Irie N, Dietmann S & Surani MA 2016 Specification and epigenetic programming of the human germ line. *Nature Reviews: Genetics* **17** 585–600. (https://doi.org/10.1038/nrg.2016.88)

Umeda R, Satouh Y, Takemoto M, Nakada-Nakura Y, Liu K, Yokoyama T, Shirouzu M, Iwata S, Nomura N, Sato K *et al.* 2020 Structural insights into tetraspanin CD9 function. *Nature Communications* **11** 1606. (https://doi.org/10.1038/s41467-020-15459-7)

Vanorny DA & Mayo KE 2017 The role of Notch signaling in the mammalian ovary. *Reproduction* **153** R187–R204. (https://doi.org/10.1530/REP-16-0689)

Vanorny DA, Prasasya RD, Chalpe AJ, Kilen SM & Mayo KE 2014 Notch signaling regulates ovarian follicle formation and coordinates follicular growth. *Molecular Endocrinology* **28** 499–511. (https://doi.org/10.1210/me.2013-1288)

Wagner M, Yoshihara M, Douagi I, Damdimopoulos A, Panula S, Petropoulos S, Lu H, Pettersson K, Palm K, Katayama S *et al.* 2020 Single-cell analysis of human ovarian cortex identifies distinct cell populations but no oogonial stem cells. *Nature Communications* **11** 1147. (https://doi.org/10.1038/s41467-020-14936-3)

Western P, Maldonado-Saldivia J, van den Bergen J, Hajkova P, Saitou M, Barton S & Surani MA 2005 Analysis of Esg1 expression in pluripotent cells and the germline reveals similarities with Oct4 and Sox2 and differences between human pluripotent cell lines. *Stem Cells* **23** 1436–1442. (https://doi.org/10.1634/stemcells.2005-0146)

Woods DC & Tilly JL 2013 Isolation, characterization and propagation of mitotically active germ cells from adult mouse and human ovaries. *Nature Protocols* **8** 966–988. (https://doi.org/10.1038/nprot.2013.047)

Wrobel KH & Süß F 1998 Identification and temporospatial distribution of bovine primordial germ cells prior to gonadal sexual differentiation. *Anatomy and Embryology* **197** 451–467. (https://doi.org/10.1007/s004290050156)

Xu J & Gridley T 2013 Notch2 is required in somatic cells for breakdown of ovarian germ-cell nests and formation of primordial follicles. *BMC Biology* **11** 13. (https://doi.org/10.1186/1741-7007-11-13)

Yabuta Y, Kurimoto K, Ohinata Y, Seki Y & Saitou M 2006 Gene expression dynamics during germline specification in mice identified by quantitative single-cell gene expression profiling1. *Biology of Reproduction* **75** 705–716. (https://doi.org/10.1095/biolreprod.106.053686)

Yamaji M, Seki Y, Kurimoto K, Yabuta Y, Yuasa M, Shigeta M, Yamanaka K, Ohinata Y & Saitou M 2008 Critical function of Prdm14 for the establishment of the germ cell lineage in mice. *Nature Genetics* **40** 1016–1022. (https://doi.org/10.1038/ng.186)

Yokobayashi S, Okita K, Nakagawa M, Nakamura T, Yabuta Y, Yamamoto T & Saitou M 2017 Clonal variation of human induced pluripotent stem cells for induction into the germ cell fate. *Biology of Reproduction* **96** 1154–1166. (https://doi.org/10.1093/biolre/iox038)

Zarate-Garcia L, Lane SIR, Merriman JA & Jones KT 2016 FACS-sorted putative oogonial stem cells from the ovary are neither DDX4-positive nor germ cells. *Scientific Reports* **6** 27991. (https://doi.org/10.1038/srep27991)

Zheng W, Zhang H, Gorre N, Risal S, Shen Y & Liu K 2014 Two classes of ovarian primordial follicles exhibit distinct developmental dynamics and physiological functions. *Human Molecular Genetics* **23** 920–928. (https://doi.org/10.1093/hmg/ddt486)

Received 5 June 2020
First decision 8 July 2020
Revised manuscript received 11 November 2020
Accepted 1 December 2020

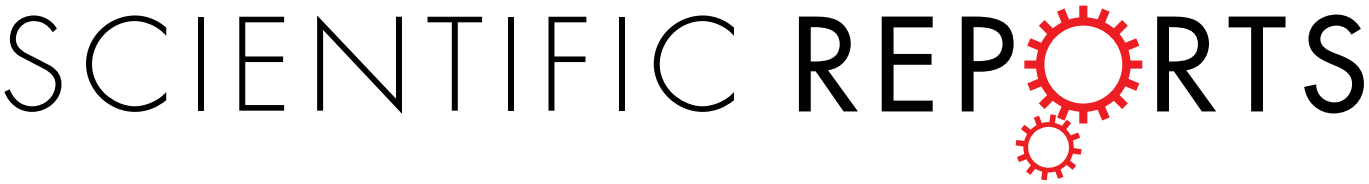

OPEN

Ibuprofen results in alterations of human fetal testis development

Millissia Ben Maamar[1], Laurianne Lesné[1], Kristin Hennig[2], Christèle Desdoits-Lethimonier[1], Karen R. Kilcoyne[3], Isabelle Coiffec[1], Antoine D. Rolland[1], Cécile Chevrier[1], David M. Kristensen[1,4], Vincent Lavoué[5], Jean-Philippe Antignac[2], Bruno Le Bizec[2], Nathalie Dejucq-Rainsford[1], Rod T. Mitchell[3], Séverine Mazaud-Guittot[1,*] & Bernard Jégou[1,6,*]

Received: 21 October 2016
Accepted: 03 February 2017
Published: 10 March 2017

Among pregnant women ibuprofen is one of the most frequently used pharmaceutical compounds with up to 28% reporting use. Regardless of this, it remains unknown whether ibuprofen could act as an endocrine disruptor as reported for fellow analgesics paracetamol and aspirin. To investigate this, we exposed human fetal testes (7–17 gestational weeks (GW)) to ibuprofen using *ex vivo* culture and xenograft systems. Ibuprofen suppressed testosterone and Leydig cell hormone INSL3 during culture of 8–9 GW fetal testes with concomitant reduction in expression of the steroidogenic enzymes *CYP11A1*, *CYP17A1* and *HSD17B3*, and of *INSL3*. Testosterone was not suppressed in testes from fetuses younger than 8 GW, older than 10–12 GW, or in second trimester xenografted testes (14–17 GW). *Ex vivo*, ibuprofen also affected Sertoli cell by suppressing AMH production and mRNA expression of *AMH*, *SOX9*, *DHH*, and *COL2A1*. While PGE2 production was suppressed by ibuprofen, PGD2 production was not. Germ cell transcripts *POU5F1*, *TFAP2C*, *LIN28A*, *ALPP* and *KIT* were also reduced by ibuprofen. We conclude that, at concentrations relevant to human exposure and within a particular narrow 'early window' of sensitivity within first trimester, ibuprofen causes direct endocrine disturbances in the human fetal testis and alteration of the germ cell biology.

Analgesics, including paracetamol and non-steroidal anti-inflammatory drugs (NSAIDs) such as aspirin and ibuprofen, are among the most widely used and environmentally prevalent pharmaceutical drugs in the world[1]. They are regarded as extremely effective medications and are widely used for self-medication, including by pregnant women during early pregnancy[2–4]. During pregnancy, analgesics are generally taken to relieve migraine, pain, and fever, but are also used in inflammatory conditions and are frequently used during preterm labor[1,5–8]. These medications are known to cross the placenta and to be present in meconium, neonatal urine, and in breast milk, indicating painkiller transmission from the mother to the fetus and to neonates[9–15]. Attention has recently been focused on the associations between analgesic use during the second and third trimesters of pregnancy and a number of unwanted effects in children. These include low birthweight, risk of premature closure of the ductus arteriosus, cardiac defects, decreased fetal and neonatal renal function, and asthma[16–20]. Concerns have also been raised recently about the use of over-the-counter painkillers during the first and second trimesters of pregnancy and an association with congenital cryptorchidism, the most frequent congenital reproductive disorder in newborn boys[7,8,21,22], as well as with shorter anogenital distance (AGD) in male infants[23,24], the latter being a biomarker for androgen action during fetal life. A series of studies undertaken *in utero* in the rat and *ex vivo* in rat and human fetal testes and in xenografted mouse models have shown that paracetamol and the NSAIDs aspirin and indomethacin can disrupt the testicular endocrine system. These disruptive endocrine effects may highlight analgesic involvement in fetal maldescended testes[1,7,25–28].

[1]Institut national de la santé et de la recherche médicale (Inserm), Institut de recherche en santé, environnement et travail (Irset – Inserm UMR 1085), Université de Rennes 1, 9 Avenue Léon Bernard, F-35000 RENNES, France. [2]LUNAM Université, Oniris, USC INRA 1329, Laboratoire d'Etude des Résidus et Contaminants dans les Aliments (LABERCA), Nantes, F-44307, France. [3]MRC Centre for Reproductive Health, University of Edinburgh, Queens Medical Research Institute, 47 Little France Crescent, Edinburgh, EH16 4TJ, UK. [4]Laboratorium of Genomic and Molecular Biomedicine, Department of Biology, University of Copenhagen, Ole Maaløes Vej 5, DK-2200 Copenhagen N, Denmark. [5]CHU de Rennes, Service de Gynécologie, Hôpital Sud, 16, boulevard de Bulgarie, F-35700 Rennes, France. [6]Ecole des hautes études en santé publique (EHESP), Avenue Léon Bernard, F-35043 RENNES, France. *These authors contributed equally to this work. Correspondence and requests for materials should be addressed to B.J. (email: bernard.jegou@inserm.fr)

Ibuprofen is the only of the 3 most common over-the-counter painkiller with paracetamol and aspirin, whose endocrine disruptive potential has not yet been investigated *ex vivo*. This is despite the fact that its consumption has continued to increase even though aspirin consumption has decreased[1,6]. The percentage of pregnant women reporting ibuprofen use averages 10%, but this varies widely across studies, ranging from 0.5% to over 28%[3,6,7,16,29–34]. In addition to cryptorchidism[7], ibuprofen use by pregnant women has also been associated with hypospadias[35], another congenital abnormality featuring a midline fusion defect of the male ventral urethra. The latter association was not found in another study[36]. Cryptorchidism and hypospadias are associated disorders and although some cases arise from genetic syndromes, most cases remain idiopathic[37]. However, both cryptorchidism and hypospadias most probably reflect subnormal levels of androgens during the development of the male urogenital tract[38,39].

In this study, we investigated whether ibuprofen disrupts the endocrine system and the differentiation of the human fetal testis during the first and second trimesters of pregnancy. We used a combination of an organotypic culture system (Fetal Gonad Assay; FEGA) based on culturing human fetal testes fragments, and a human fetal testes xenograft system. These approaches, have been separately used for the study of endocrine-disrupting substances[26,27,40,41], but never integrated in the same series of experiments. In the FEGA system, after 1 to 3 days of exposure to ibuprofen at 10^{-7}–10^{-4} M, we assessed the gross morphology, endocrine function, and gene expression for the main cell types of the first trimester human fetal testis *ex vivo*, whilst the xenograft system was used to determine the effect of prolonged (7 day) ibuprofen exposure on the endocrine function of the second trimester testis.

Results

Ibuprofen and Leydig cell morphology and function. No apparent changes in general morphology or Leydig cell marker expression was seen in the ibuprofen-exposed FEGA explants as compared to the non-exposed (Fig. 1A–C).

In the 7–7.9 gestational week (GW) 10^{-5} M ibuprofen-treated testes, no significant effect was observed on testosterone levels when compared to the non-treated testes (Fig. 1D). By contrast, when the 8–9.9 GW testes were exposed *ex vivo* to ibuprofen, a significant dose-dependent testosterone decrease was seen after 72 h of exposure (slope $\beta = -0.076$, $p < 0.0001$); the pairwise comparisons versus the control condition evidenced an effect with 10^{-5} M (−32.3%; $p < 0.001$ and with 10^{-4} M (−35.6%; $p < 0.01$) (Fig. 1E). In the 8–9.9 GW testes, we also observed time- and dose-dependent effects of ibuprofen (after 24 h, slope $\beta = -0.052$, $p < 0.0001$; after 48 h, slope $\beta = -0.081$, $p < 0.0001$; after 72 h, slope $\beta = -0.085$, $p < 0.0001$), with the decrease of testosterone occurring after only 24 h of exposure: −12.8% with 10^{-5} M ($p < 0.01$); and −24.6% with 10^{-4} M ($p < 0.001$). This dose-dependent decrease was amplified after 48 h (−19.8 and −49%, respectively; both $p < 0.001$), and further amplified after 72 h (−29.3% and −55.3%, respectively; both $p < 0.001$) (Fig. 1F). In contrast, no effect was observed *ex vivo* on testosterone levels in the 10–12 GW testes for doses of ibuprofen of 10^{-7}–10^{-4} M (Fig. 1G).

Given the apparent specific time window for testosterone reduction during the mid-late first trimester, we then investigated the effect of ibuprofen exposure during the second trimester (14–17 GW) using the xenograft system. Exposure to a 7 day therapeutic regimen of ibuprofen (10 mg/kg, 3 times daily) did not affect testosterone production from the human fetal testis as determined by both host mouse seminal vesicle weight (14.63 mg *versus* 13.21 mg; p = 0.62; n = 4 Fig. 1H) and plasma testosterone (0.84 *versus* 0.82 ng/ml; p = 0.85; n = 4; Fig. 1I) in host mice. Similarly, plasma 5-dihydrotestosterone (5α-DHT) was unaffected by exposure to ibuprofen (3.26 *versus* 2.44 ng/ml; p = 0.56; n = 4; Fig. S1). Mean plasma ibuprofen concentration 1 hour after the final dose in ibuprofen-exposed host mice was 2.78 ± 0.55 μg/ml and undetectable in vehicle-exposed controls (Fig. S1)

Using gas chromatography-tandem mass spectrometry (GC/MS-MS), we then measured the entire complement of detectable steroids both in the FEGA testis explants themselves and in the media after 48 h of exposure to 10^{-5} M of ibuprofen in the 8–9.9 GW testes (Fig. 2A,B). Our results reveal that in this fetal age-range, only 3 steroids were found to be above the threshold of the GC/MS-MS technique in the non-treated fetal testis: pregnenolone (1.39 ± 0.7 ng/mg of testicular tissue); dehydroepiandrosterone (DHEA) (1.7 ± 1.1 ng/mg of testicular tissue); and testosterone (54.4 ± 25.7 ng/mg of testicular tissue). Levels of these 3 steroids in the explants were not significantly affected by ibuprofen at 10^{-5} M (data not shown). Parallel investigation in the corresponding culture media allowed us to detect, for the first time in humans, 6 steroids in the control (*i.e.* unexposed) condition in both the Δ5 and Δ4 steroid pathways: - Δ5, 17-hydroxy-pregnenolone (17-OH-preg) (4.3 ± 1.9 ng/mL); DHEA (21.3 ± 4.7 ng/mL) (Fig. 2A); - Δ4, 17-hydroxy-progesterone (17-OH-prog) (9.6 ± 5.9 ng/mL); androstenedione (183.7 ± 97.0 ng/mL); testosterone (1597.8 ± 722.5 ng/mL); and 5-dihydrotestosterone (5α-DHT) (7.1 ± 8.0 ng/mL of culture media) (Fig. 2B). Of these, the potent androgens testosterone and α-DHT were found to be significantly inhibited by 10^{-5} M of ibuprofen (36.8 and 70.2%, respectively at $p < 0.01$). The levels of the other androgen androstenedione were also reduced (−41.2%), but this was not statistically significant at $p < 0.05$ (Fig. 2B).

After 48 h of exposure to ibuprofen, the expression of 3 genes that encode for steroidogenic enzymes was markedly decreased: by 48.6% ($p < 0.05$) for *CYP11A1,* by 82% ($p < 0.001$) for *CYP17A1,* and by 70.4% ($p < 0.05$) for *HSD17B3* (Fig. 2C). By contrast, the mRNA levels of *HSD3B2* and *SRD5A3,* 2 other genes which encode enzymes of the steroidogenic pathway, as well as the mRNA levels of *BZRP* and *STAR,* the 2 genes encoding proteins involved in cholesterol transport to the mitochondria, were not affected by exposure to ibuprofen (Fig. 2C).

The other key fetal Leydig cell-produced hormone investigated was INSL3. For explants from 8–12 week gestation fetuses, INSL3 levels were dose-dependently and significantly decreased after 72 h of exposure to ibuprofen at doses ranging from 10^{-7}–10^{-4} M, (slope $\beta = -0.155$, $p = 0.007$) (Fig. 3A). At 10^{-5} M the decrease of INSL3 (−39%) was significant ($p < 0.05$), but at 10^{-4} M no significant difference was observed. To assess whether a window of sensitivity exists, we again divided the fetuses into 2 age groups, 8–9.9 GW and 10–12 GW. In fact, there was a significant dose-response decrease in INSL3 levels for the 10–12 GW age group (slope $\beta = -0.181$, $p = 0.03$) (Fig. 3B,C). In addition to decreased INSL3 production, after 48 h of culture with 10^{-5} M of ibuprofen,

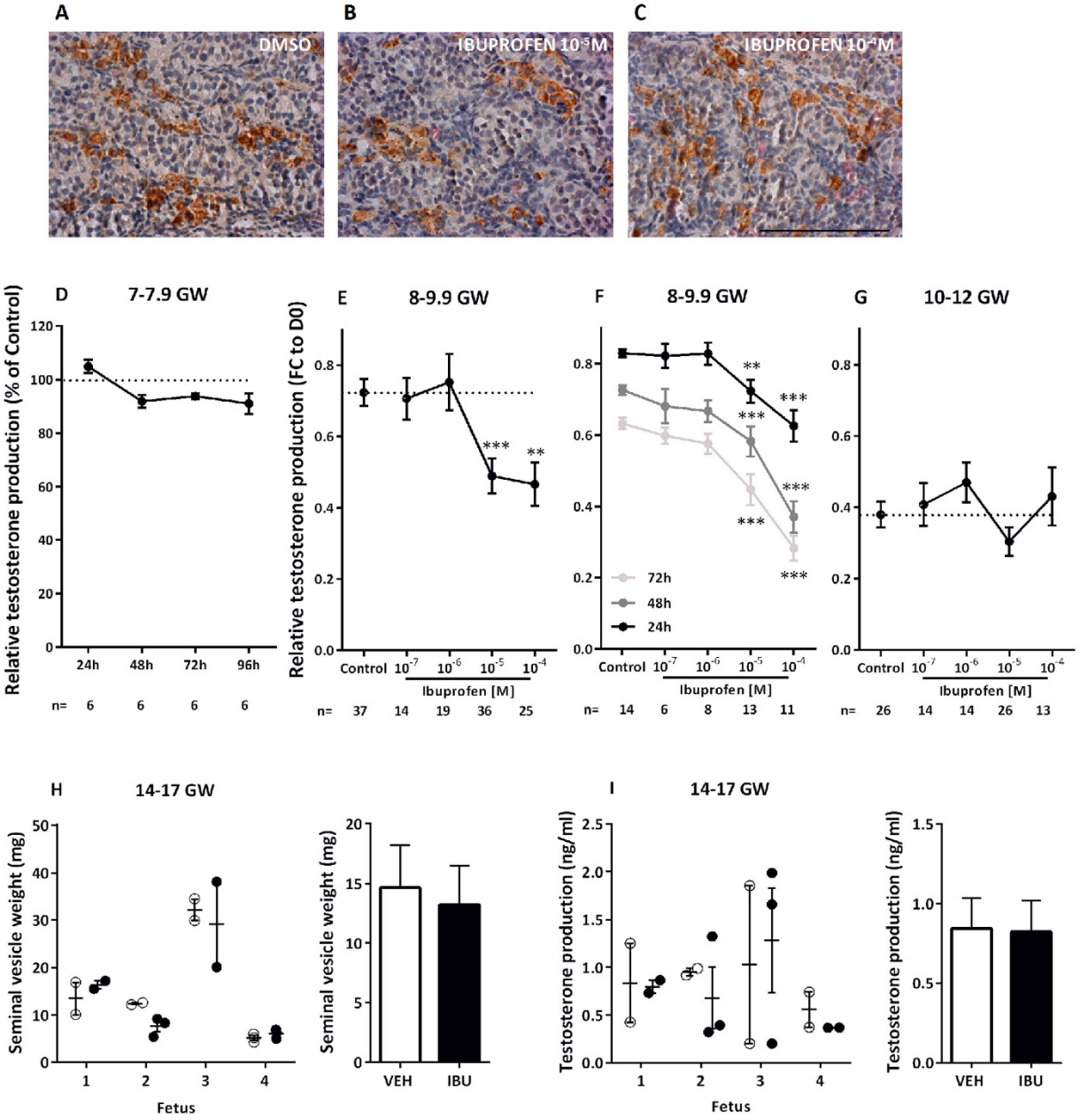

Figure 1. Ibuprofen and Leydig cell steroidogenic function. (**A–C**) Representative images of CYP11A1 immunostaining in explants of a 7.9 gestational week (GW) human fetal testis cultured with DMSO or ibuprofen. CYP11A1 appears brown (3,3′-diaminobenzidine tetrahydrochloride staining), and sections were counterstained with hematoxylin. Scale bar = 100 μm. (**D**) Testosterone production as a function of culture duration in 7–7.9 GW human fetal testes in the presence of DMSO (Control) or 10^{-5} M of ibuprofen. Results are expressed as fold change from the respective control testis (% of Control). Values are means ± SEM of 6 testes from 6 different fetuses. Repeated measures analysis of variance (ANOVA) on ranks was performed ($p = 0.172$). (**E–G**) Testosterone production after culture of 8-9.9 GW (**E**,**F**) and 10–12 GW human fetal testes (**G**) in the presence of DMSO (Control) or 10^{-7}–10^{-4} M of ibuprofen for 72 h (**E**,**G**) and for 24, 48 and 72 h (**F**). Results are expressed as fold change from the first day of culture (FC to D0). Values are means ± SEM of 14–37 testes from 14–37 fetuses for the 8–9.9 GW group, 6–14 testes from 6–14 fetuses for the 8–9.9 GW at 24, 48 and 72 h group, and 13–21 testes from 13–21 fetuses for 10–12 GW. ANOVAs with a random fetus effect were performed using unstructured covariance matrices. A Wilcoxon test was also performed for pairwise comparisons (**$p < 0.01$, ***$p < 0.001$). (**H**) Seminal vesicle weight and (**I**) plasma testosterone production in host mice carrying human fetal testis xenografts (14–17 GW; n = 4 fetuses) after 7 days (7d) of exposure to vehicle (Corn Oil; open circles) or ibuprofen (10 mg/kg 3 times daily; closed circles) with overall mean ± SEM for vehicle (white bars) and ibuprofen (black bars). Values are means ± SEM from 4 fetuses. Data analyzed by two-way ANOVA.

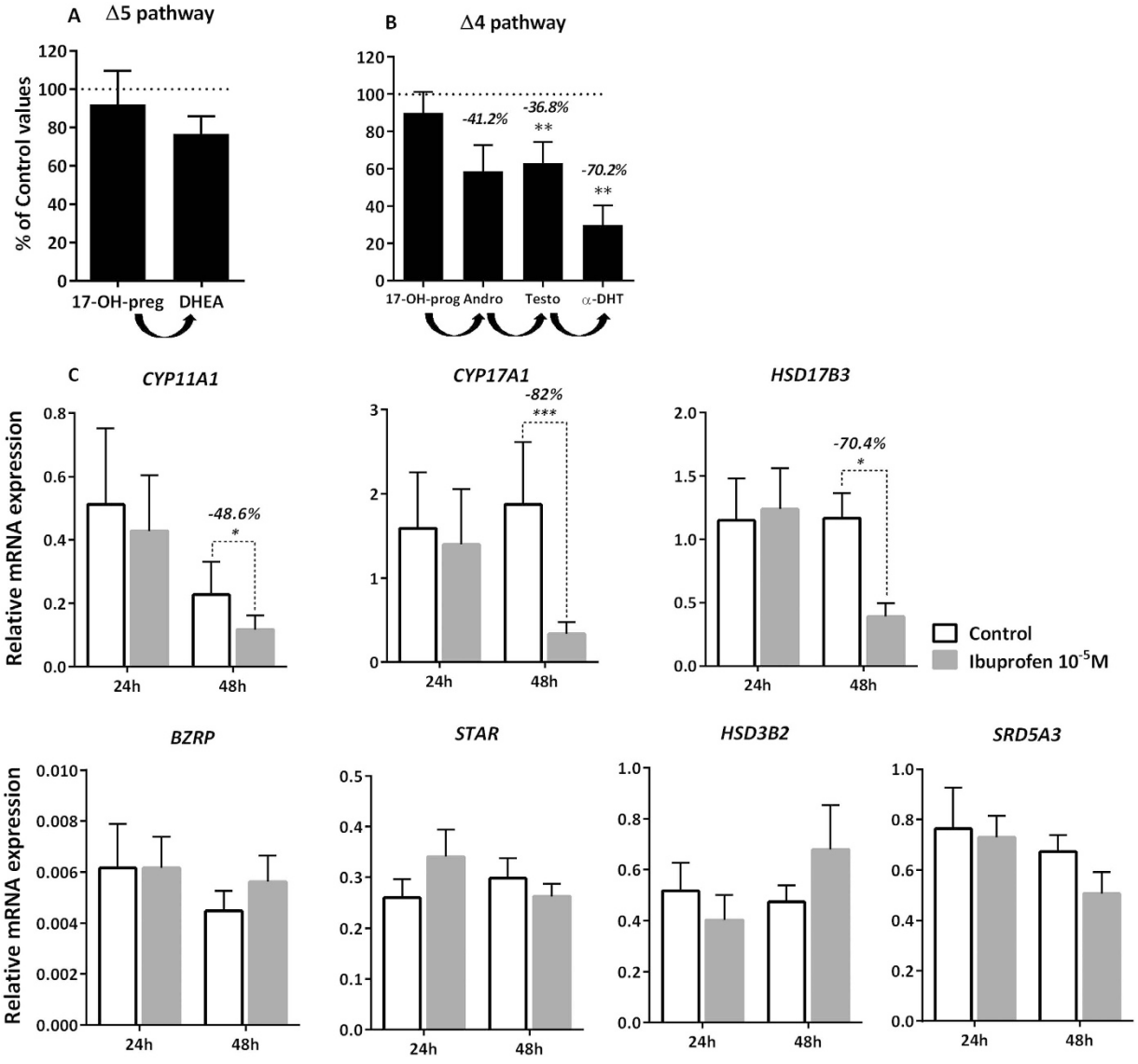

Figure 2. Ibuprofen and global steroidogenesis. (**A**,**B**) Global analysis of ibuprofen effects on the Δ5 (**A**) and Δ4 pathways (**B**) of testosterone production using GC-MS/MS. Human fetal testis explants (8–9.9 GW) were incubated for 48 h with DMSO (Control) or 10^{-5} M of ibuprofen. Steroid precursors of the Δ5 and Δ4 pathways were measured by GC-MS/MS in the media. Values are mean ± SEM of 8 fetuses pooled in 5 independent experiments, and are expressed as the percentage of variation from the control. $^{**}p < 0.01$ by non-parametric signed rank Wilcoxon test on paired data. (**C**) Quantitative RT-PCR of *BZRP*, *STAR*, *CYP11A1, CYP17A1, HSD17B3, HSD3B2* and *SRD5A3* was performed on control testes (white bars) and testes treated with 10^{-5} M of ibuprofen (grey bars) for 24 and 48 h. Each column shows a pool of 11–15 fetal testes. Each bar represents the mean ± SEM of the fold change in target gene expression relative to the reference gene *RPLP0*. A non-parametric signed rank Wilcoxon test on paired data was performed ($^{*}p < 0.05$, $^{**}p < 0.01$, $^{***}p < 0.001$).

INSL3 transcripts were also repressed by 57.1% ($p < 0.001$) (Fig. 3D). As in previous studies[26,42], INSL3 production appears to have substantial interindividual variability.

Ibuprofen and Sertoli cell morphology and function. No apparent change in Sertoli cell number or topographical organization was observed in FEGA explants after exposure to 10^{-5} M or 10^{-4} M of ibuprofen, based on expression of AMH or cytokeratin 18 (KRT18) a marker of the immature Sertoli cell intermediate filaments, (Fig. 4A–F). This was further demonstrated by an unchanged Sertoli cell density after 72 h of exposure to 10^{-5} M of ibuprofen (Fig. 4G).

When the testes from the youngest human fetuses (7–7.9 GW) were exposed to 10^{-5} M of ibuprofen, a significant decrease in AMH was seen from 48 h of culture onwards (−31.1% at 48 h ($p < 0.05$), −53.0% at 72 h ($p < 0.0001$), and −38.1% at 96 h ($p < 0.05$)) (Fig. 4H). When fetuses of 8–12 GWs were analyzed together, a dose-dependent suppression of AMH production was observed (slope $\beta = -0.294$, $p < 0.0001$), with −38.4% ($p < 0.001$) at 10^{-5} M and −76.2% ($p < 0.001$) at 10^{-4} M (Fig. 4I). The dose-dependent decrease of AMH levels

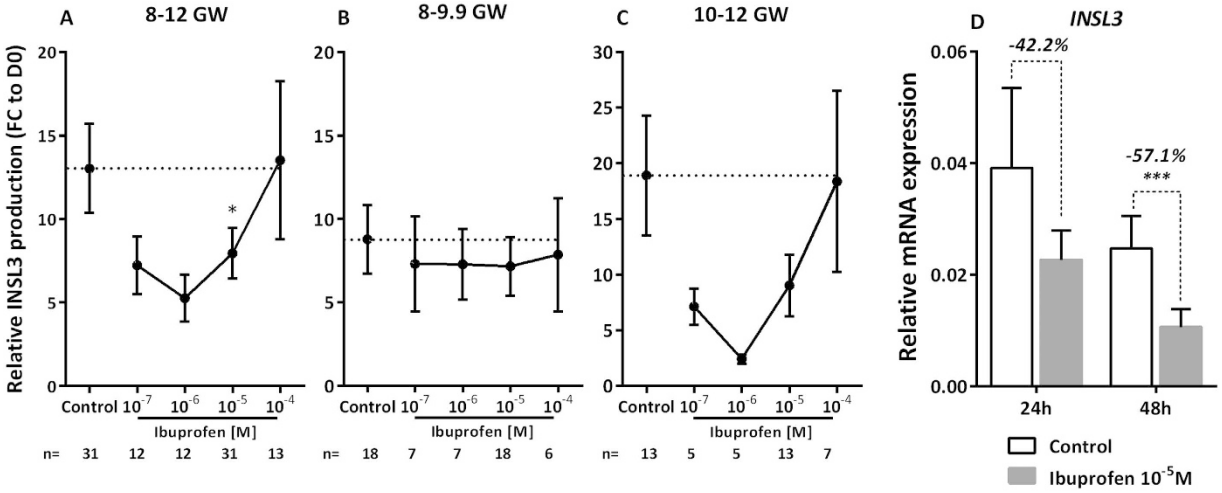

Figure 3. Ibuprofen and production of INSL3 by Leydig cells. (**A**–**C**) Ibuprofen and INSL3 production after exposure to ibuprofen during 72 h of human fetal testis culture at (**A**) 8–12 gestational weeks (GW), (**B**) 8–9.9 GW, and (**C**) 10–12 GW. Results are expressed as fold change from the first day of culture (FC to D0). Values are means ± SEM ($n = 12$–31 testes from 12–31 fetuses). ANOVAs with a random fetus effect were performed using unstructured covariance matrices. A Wilcoxon test was performed for pairwise comparisons. (*$p < 0.05$). (**D**) Quantitative RT-PCR for *INSL3* was performed on control testes (white bars) and testes treated with 10^{-5} M of ibuprofen (grey bars) for 24 and 48 h. Each column is made up of a pool of 11–15 fetal testes. Each bar represents the mean ± SEM of the fold change in target gene expression relative to *RPLP0* reference gene. A non-parametric signed rank Wilcoxon test on paired data was performed (***$p < 0.001$).

was also seen both in the 8–9.9 GW group (slope $\beta = -0.295$, $p < 0.0001$), with −31.0% ($p < 0.05$) at 10^{-7} M, −54.8% ($p < 0.001$) at 10^{-5} M and −66.7% ($p < 0.001$) with 10^{-4} M (Fig. 4J) and in the 10–12 GW group (slope $\beta = -0.291$, $p = 0.003$) (Fig. 4K). In accordance with these findings, the expression of *AMH* mRNA was found to be suppressed by ibuprofen exposure in hFEGA: −42.1% at 24 h and −89.9% ($p < 0.001$) at 48 h (Fig. 5). As with *AMH* mRNA, the mRNA of *SOX9*, a specific marker of the differentiation of Sertoli cells, was repressed after ibuprofen exposure: −43.3% ($p < 0.001$) at 24 h; and −59.7% ($p < 0.001$) at 48 h. The mRNA expression of the 2 *SOX9* targets investigated *DHH* and *COL2A1* was decreased by −51.3% ($p < 0.01$) and −61.7% ($p < 0.01$) at 24 h; and −79.8% ($p < 0.001$) and 79.6% ($p < 0.001$), respectively (Fig. 5).

We also investigated the effect of ibuprofen exposure on AMH production in the second trimester human fetal testis using the xenograft system. In contrast to the results in the first trimester testis there was no significant difference in AMH production in second trimester xenografts exposed to ibuprofen compared to vehicle-exposed controls (0.75 *versus* 1.34 ng/ml; $p = 0.038$; Fig. 4L).

Ibuprofen alters germ cell markers. Neither the morphology nor the density of the germ cells appeared altered after 72 h of exposure to 10^{-5} and 10^{-4} M of ibuprofen (Fig. 6A–D). This contrasted with the expression of 5 germ cell genes which were repressed after 48 h of ibuprofen exposure: *POU5F1,* a transcription factor essential for the pluripotency maintenance in embryonic stem cells[43], was significantly decreased by 57.2% ($p < 0.01$); *TFAP2C,* a factor believed to regulate the expression of several genes involved in cell growth and differentiation[44], was also significantly decreased by 67.9% ($p < 0.001$); *LIN28A,* which regulates the germ cell pool[45], was significantly decreased by 32.9% ($p < 0.05$); *ALPP* and *KIT*, which are typical markers of germ cells[46,47], were significantly decreased by 91.8% ($p < 0.05$) and 72.7% ($p < 0.05$), respectively (Fig. 6E).

Ibuprofen suppresses the production of prostaglandin PGE2, but not that of PGD2. Cyclooxygenase enzymes (COX1 and COX2) are responsible for catalyzing the formation of prostaglandins from arachidonic acid, and ibuprofen is classically known to inhibit these enzymes[48,49]. We therefore assayed the prostaglandins PGD2 and PGE2, both previously found to be produced by the human fetal testis[26]. At all ages investigated, ibuprofen did not have a significant effect on PGD2 levels (Fig. 7A–C). In contrast, an ibuprofen-induced dose-dependent inhibition of PGE2 levels was demonstrated (slope $\beta = -0.109$, $p = 0.03$). Furthermore, significant inhibitory effects on PGE2 levels were observed in the 8–12 GW fetal testes after 72 h of exposure to 10^{-5} and 10^{-4} M of ibuprofen (−31.6%, $p < 0.01$ at 10^{-5} M; and −32.7%, $p < 0.01$ at 10^{-4} M) (Fig. 7D). This ibuprofen-suppressive effect was more pronounced in the 8–9.9 GW fetal testes under the same conditions: −29.7% at 10^{-7} M; −36.5% at 10^{-6} M; −51.4% ($p < 0.01$) at 10^{-5} M; and −42.0% ($p < 0.05$) at 10^{-4} M (Fig. 7E), again with a significant dose-dependent suppression of PGE2 production (slope $\beta = -0.122$, $p = 0.02$). In the 10–12 GW testes, no significant inhibition of PGE2 was seen (Fig. 7F). However, high levels of PGE2 were observed when the 10–12 GW testes were exposed to the lowest doses of ibuprofen (+128.1% at 10^{-7} M, $p < 0.05$ and +78.1% at 10^{-6} M, $p < 0.01$).

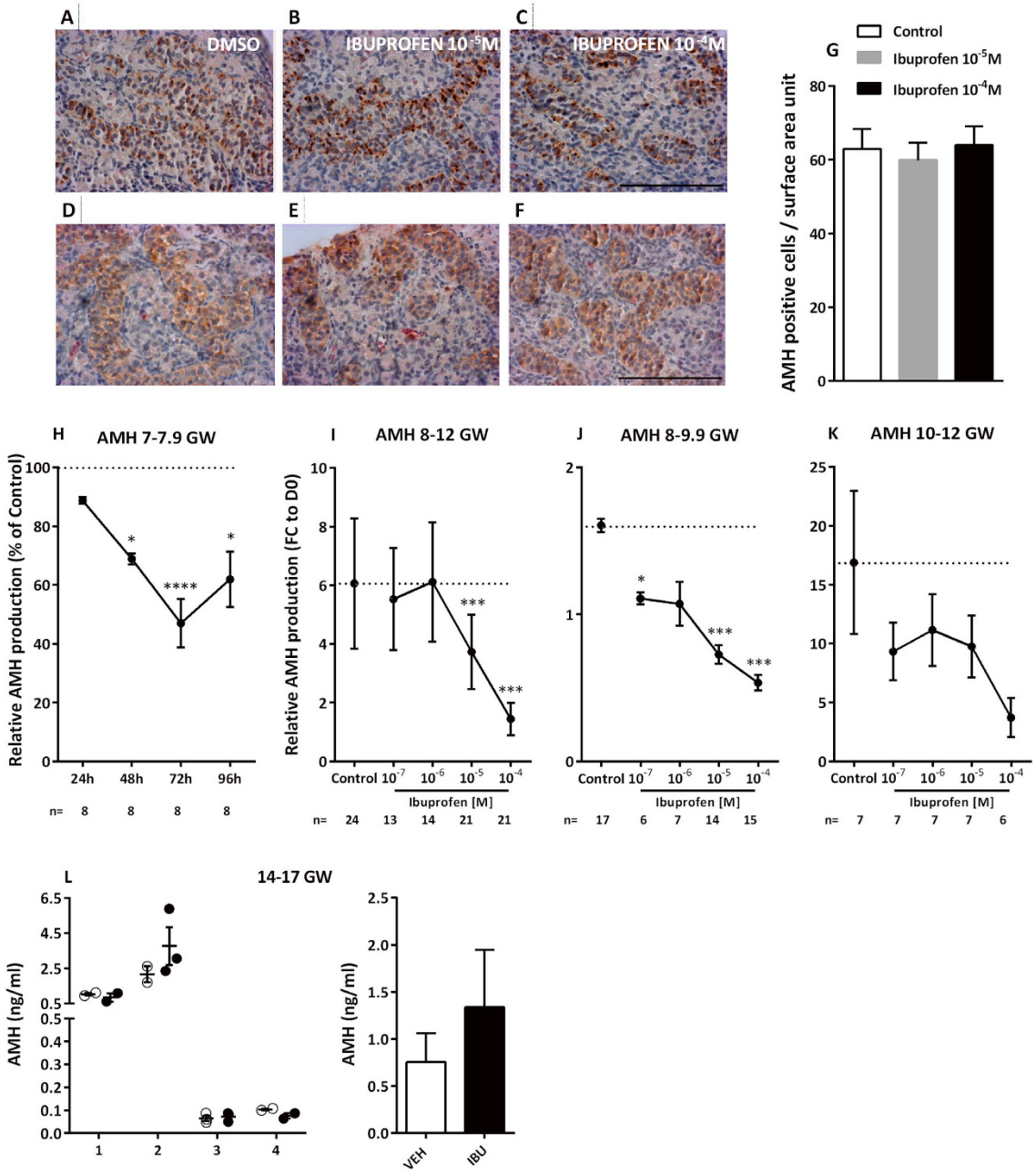

Figure 4. Ibuprofen and Sertoli cell function. (**A**–**F**) Representative images of KRT18 (**A**–**C**) and AMH (**D**–**F**) immunostaining in cultured explants of 7–7.9-gestational week (GW) human fetal testis. KRT18 and AMH appear brown (3,3-diaminobenzidine tetrahydrochloride staining), and sections were counterstained with hematoxylin. Scale bar = 100 μm. (**G**) Sertoli cell numbers were determined by counting AMH-positive cells in control testes (white bars) and testes treated with 10^{-5}M (grey bars) and 10^{-4}M (black bars) of ibuprofen for 72 h. Data are presented as the number of cells per surface area unit (0.01 mm^2) (means ± SEM) based on 1 or 2 explants per treatment in 7 fetuses. A Wilcoxon test was performed for pairwise comparisons. (**H**) AMH production after 24, 48, and 72 h of exposure to DMSO (Control) or 10^{-5}M of ibuprofen in 7–7.9 GW human fetal testes. Results are expressed as fold changes from the control testis (% of Ctrl). Values are means ± SEM for 7 testes from 7 fetuses. Repeated measures analysis of variance (ANOVA) on ranks was performed (*$p < 0.05$, ****$p < 0.0001$). (**I**–**K**) AMH production after culture of 8–12 GW (**I**); 8–9.9 GW (**J**); and 10–12 GW (**K**) human fetal testes in the presence of the control solvent DMSO (Control) or 10^{-7}–10^{-4}M of ibuprofen. Results are expressed as fold change from the first day of culture (FC to D0). Values are means ± SEM of 6–17 testes from 6–17 fetuses for the 8–9.9 GW, and of 6–7 testes from 6–7 fetuses for the 10–12 GW. ANOVAs with a random fetus effect were performed using unstructured covariance matrices. A Wilcoxon test was performed for pairwise comparisons (*$p < 0.05$; ***$p < 0.001$). (**L**) Plasma AMH in individual host mice carrying human fetal testis xenografts (14–17 GW; n = 4 fetuses) after 7d exposure to vehicle (Corn Oil; open circles) or ibuprofen (10 mg/kg 3 times daily; closed circles) with overall mean ± SEM for vehicle (white bars) and ibuprofen (black bars). Data analyzed by two-way ANOVA.

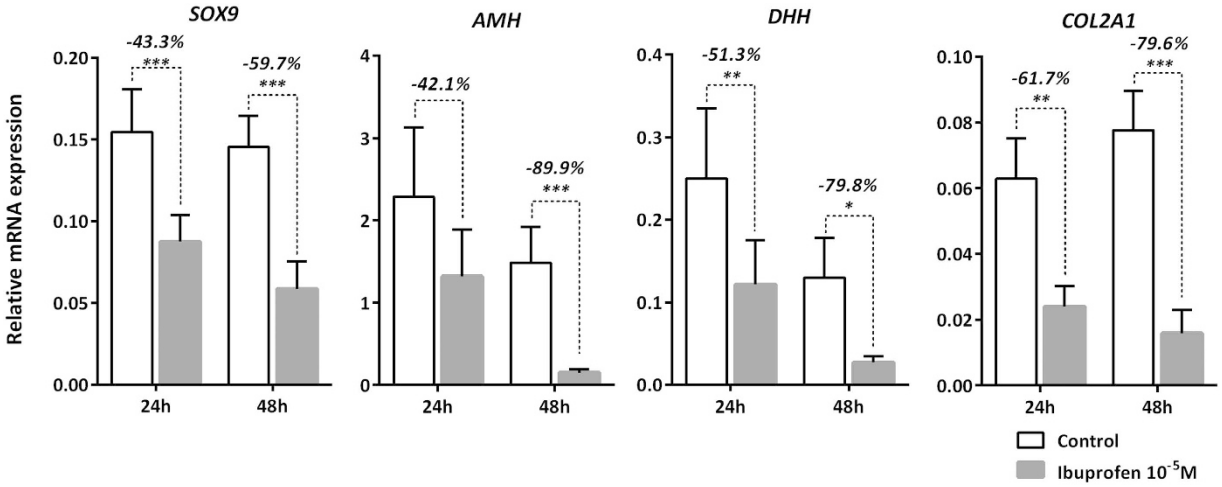

Figure 5. Ibuprofen and Sertoli cell markers. Quantitative RT-PCR for *SOX9, AMH, DHH* and *COL2A1* were performed on control testes (white bars) and testes treated with 10^{-5}M of ibuprofen (grey bars) at 24 or 48 h of culture. Each column represents a pool of 11–15 fetal testes. Each bar shows the mean ± SEM of the fold change in target gene expression relative to the *RPLP0* reference gene. A non-parametric signed rank Wilcoxon test on paired data was performed (*$p < 0.05$; **$p < 0.01$; ***$p < 0.001$).

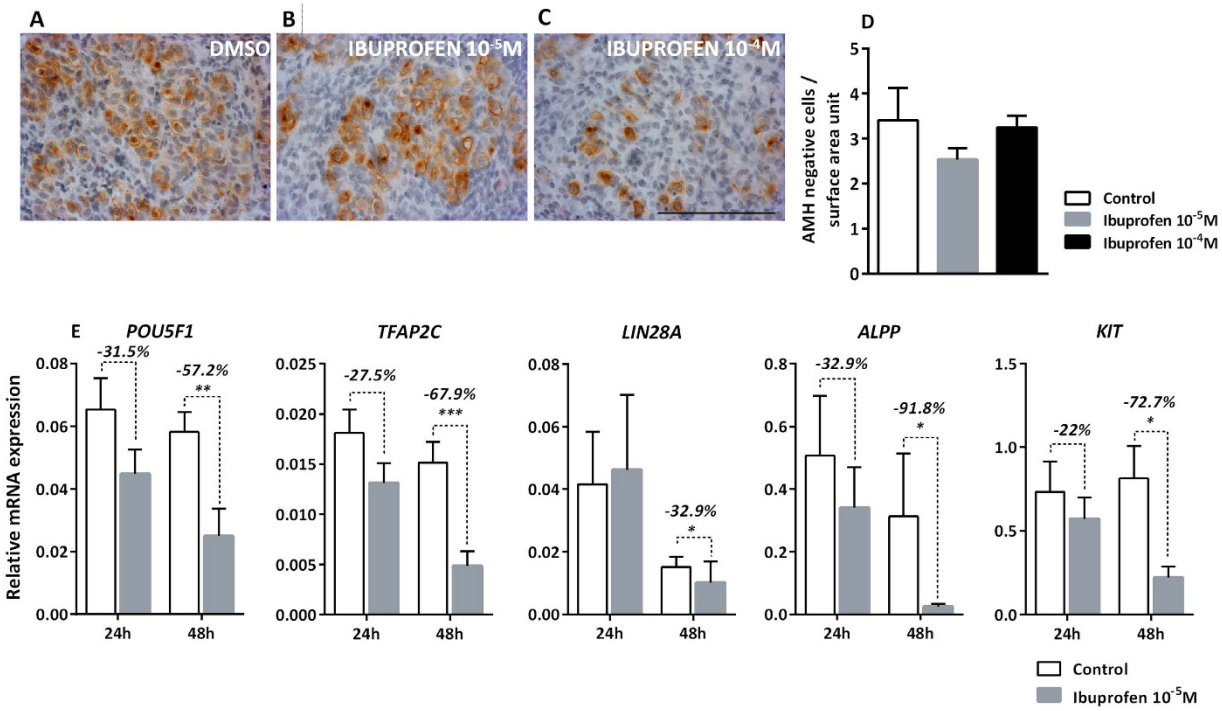

Figure 6. Ibuprofen and germ cells. (**A**–**C**) Representative images of M2A immunostaining in cultured explants of an 8.6-gestational week (GW) human fetal testis. M2A appears brown (3,3′-diaminobenzidine tetrahydrochloride staining), and sections were counterstained with hematoxylin. Scale bar = 100 μm. (**D**) Numbers of germ cells were determined by counting AMH-negative cells after culturing human fetal testis ($n = 7$ testes from 7 fetuses) in the presence of 0.01% of DMSO (Control, white bars) or 10^{-5}M (grey bars) or 10^{-4}M (black bars) of ibuprofen. Data are presented as the number of cells per surface area unit (0.01 mm^2) (means ± SEM) based on 1 or 2 explants per treatment from 7 fetuses. A non-parametric signed rank Wilcoxon test on paired data was performed. (**E**) Quantitative RT-PCR for *POU5F1*, *TFAP2C, LIN28A, ALPP* and *KIT* was performed on control testes (white bars) and testes treated with 10^{-5}M of ibuprofen (grey bars) at 24 or 48 h of culture. Each column shows a pool of 11 or 15 fetal testes. Each bar represents the mean ± SEM of the fold change in target gene expression relative to the *RPLP0* reference gene. A non-parametric signed rank Wilcoxon test on paired data was performed (*$p < 0.05$, **$p < 0.01$; ***$p < 0.001$).

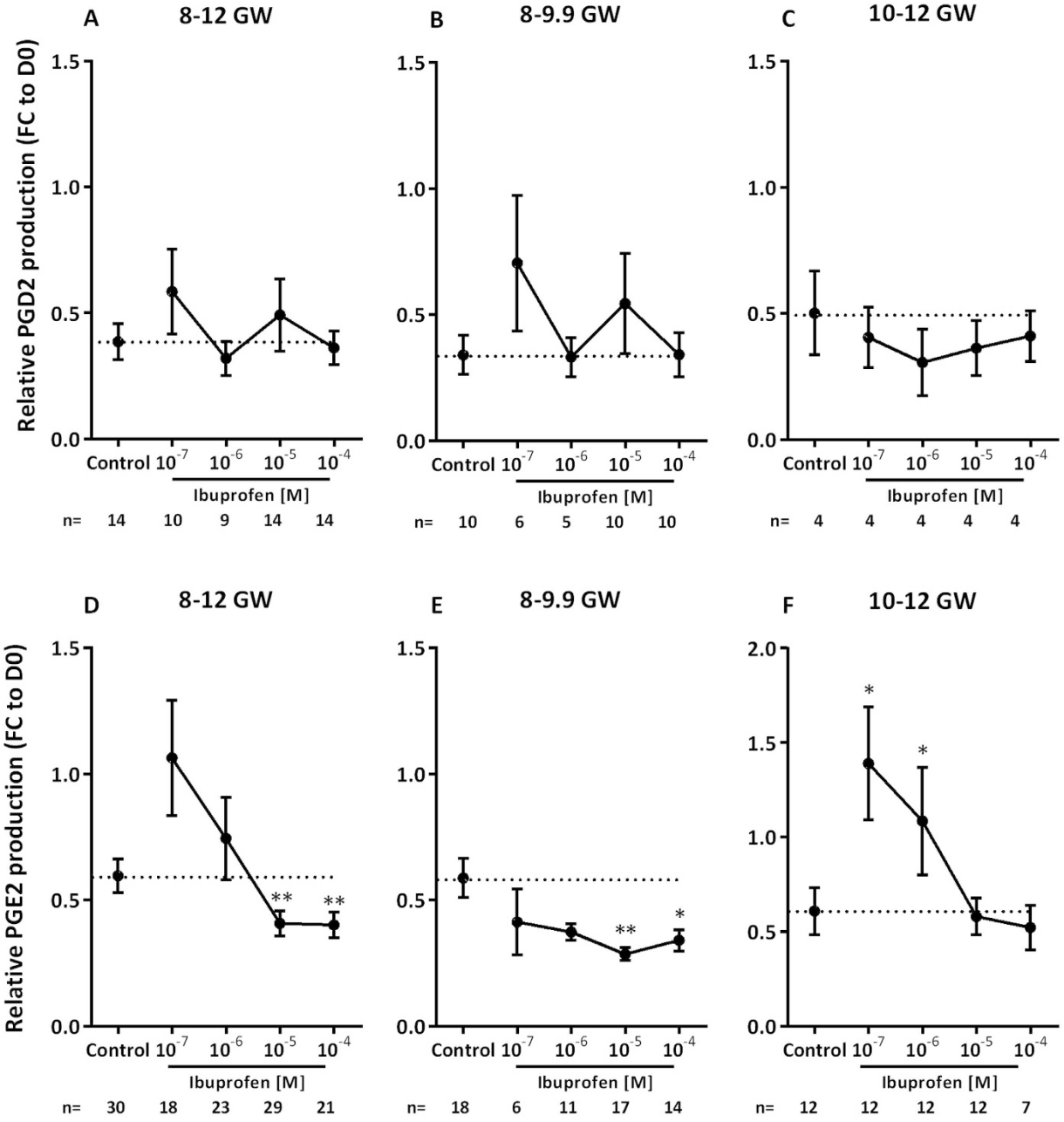

Figure 7. Effect of ibuprofen on human fetal testis PGD2 and PGE2 production. (**A**–**C**) PGD2 concentrations after 72 h of culture of 8 to 12 gestational week (GW) (**A**), 8–9.9 GW (**B**), and 10–12 GW (**C**) human fetal testes in the presence of the solvent DMSO (Control) or 10^{-7}–10^{-4} M of ibuprofen. (**D**–**F**) PGE2 concentrations after 72 h of culture of 8–12 GW (**D**), 8–9.9 GW (**E**), and 10–12 GW (**F**) human fetal testes in the presence of DMSO (Control) or 10^{-7}–10^{-4} M of ibuprofen. Results are expressed as fold change from the first day of culture (FC to D0) for both PGD2 and PGE2 productions. Data are means ± SEM ($n = 4$–10 testes from 4–10 fetuses for PGD2; $n = 6$–18 testes from 6–18 fetuses for PGE2). ANOVAs with a random embryo effect were performed using unstructured covariance matrices. A Wilcoxon test was performed for pairwise comparisons (*$p < 0.05$, **$p < 0.01$).

Discussion

The 3 most frequently consumed mild analgesics during the first trimester of pregnancy are paracetamol (also known as acetaminophen) and the NSAIDs aspirin and ibuprofen[1]. Several recent epidemiological studies have reported that the consumption of ibuprofen during the first trimester is associated with an increased risk of cryptorchidism and/or hypospadias[7,8,33]. In animals and humans, these congenital abnormalities are considered complex disorders involving either rare genetic traits, or abnormal endocrine activity or production in fetal testes[37–39,50–52]. Since the *in utero* assessment of ibuprofen's effects on the development and function of human fetal testes is impossible for obvious ethical reasons, we developed an *ex vivo* model system which has already proven

to be useful for studying the effects of paracetamol, NSAIDs (aspirin and indomethacin) and environmental chemicals (bisphenol A) on the human fetal testis during the first trimester[26,40]. In addition, as a complementary tool of investigation, we utilized a xenograft system which has been shown to model the effects of prolonged exposure to therapeutic doses of analgesics in the human testis during the second trimester[27].

The present study demonstrates, through the use of the FEGA, that concentrations which are equivalent to or even lower than peak plasma levels of ibuprofen[53,54] markedly affect the biology of the 2 major human fetal testicular somatic cell populations, as well as of the germ cells, and that these effects occur during specific periods of human fetal testis development. This occurred without any obvious changes in the number of these cells or in the general morphology of the testis at any age. Thus, ibuprofen markedly decreased testosterone levels and steroidogenesis at large. This inhibitory effect was observed using both the immunoassay of testosterone and GC/MS-MS analysis, and was found to be dose-, time- and age-dependent. Of note is that this appeared restricted to the 8–9.9 GW fetal testes. Androgens play an essential role in the masculinization of the urogenital tract[55]. This narrow window of ibuprofen sensitivity corresponding to the younger fetal ages investigated is similar to that previously observed for aspirin and indomethacin[26]. This likely reflects the fact that Leydig cells go through markedly different steps of differentiation and thus biological states[56], some of which appear to be resistant to ibuprofen's anti-androgenic effects. Indeed, we were able to demonstrate that testosterone production was not reduced by exposure to ibuprofen in late first trimester human fetal testis (10–12 GW) in the *ex vivo* culture system, nor in second trimester human fetal testis (14–17 GW) using the xenograft approach. The ibuprofen-induced testosterone inhibition during the specific 8–99 GW time window contrasts greatly with the effects observed in previous studies in aspirin- and indomethacin-treated fetal testes *ex vivo*. In fact, we found that the latter NSAIDs actually stimulate human testis testosterone levels[26], rather than suppressing them as in the case of ibuprofen. Another striking difference is that, while paracetamol was previously found to reduce both plasma levels of testosterone and the weight of androgen-dependent seminal vesicles in the xenograft model-system[27], ibuprofen had no effect in the xenograft-system model as revealed here. These differences are likely to reflect the different nature and thus mechanisms of action of the two analgesics considered, ibuprofen being a NSAID while paracetamol is not.

The present work also reveals that at least 3 steps of steroidogenesis are significantly affected *ex vivo* by ibuprofen, as it suppressed the transcripts encoding CYP11A1, CYP17A1, and HSD17B3. CYP11A1 is important as it catalyzes the first reaction of steroidogenesis (*i.e.* the conversion of cholesterol to pregnenolone). CYP17A1 catalyzes 17α-hydroxylation of progesterone and pregnenolone, and also converts 17α-hydroxypregnenolone to DHEA and 17α-hydroxyprogesterone to androstenedione. CYP17A1 is typically regarded as a key determinant of testosterone production, susceptible to both androgen production regulation and perturbation[57,58]. HSD17B3 catalyzes the ultimate conversion of androstenedione to testosterone, androstenedione being the first androgen produced in the downstream chain line of steroidogenesis. The present study represents the first GC/MS-MS global analysis of fetal testicular steroidogenesis demonstrating that, in addition to suppression of testosterone, the effect of ibuprofen on the expression of CYP17A1 also negatively impacted androstenedione and to a greater extent 5α-DHT. Further supporting evidence for ibuprofen being an anti-androgenic compound is the observation that low doses of this NSAID (5–6 mg/kg/day for 35 days) inhibited plasma levels of testosterone in adult male mice[59]. Ibuprofen has also been shown to inhibit the human UDP-glucuronosyltransferases UGT2B15 and UGT2B17, and the latter is very important for glucuronidation and testosterone excretion[60].

It is important to note that not only androgens were impacted by ibuprofen but also INSL3, which is the peptidic hormone produced by Leydig cells and which was dose-dependently inhibited by ibuprofen. In accordance with this, *INSL3* expression levels were also suppressed by ibuprofen. *Insl3 k*nock-out mice are cryptorchid[50,61] and some mutations of the human *INSL3* gene have been associated with cases of cryptorchidism[38]. The first phase of testicular descent which occurs in humans between 8 and 17 GW is controlled by INSL3[28,38,51,62]. In a previous study, 8–12 GW human fetal testes treated with paracetamol had reduced INSL3 production[26], and in the present study ibuprofen exposure in testis explants at the same gestational age for 72 h induced significant alterations in INSL3 production. These findings support the hypothesis that ibuprofen-induced suppression of INSL3 expression and production could be related to the increased risk of cryptorchidism in boys whose mothers were exposed to ibuprofen during pregnancy[7].

Interestingly, ibuprofen also induced a dose-dependent suppression of AMH production in the human fetal testis *ex vivo*. To the best of our knowledge, ibuprofen is the first endocrine disruptor which is found to display direct suppressive action on the endocrine function of the human (and other mammalian) fetal Sertoli cells. However, the reduced AMH production following ibuprofen exposure was restricted to the first trimester testis during a specific period from 7–9.9 GW. Exposure in late first trimester (10–12 GW) explants and in second trimester (14–17 GW) xenografts did not result in a significant change in AMH production although the variability between samples clearly increased in the late first trimester. In addition, there was a large variability in AMH production between fetuses for the second trimester xenografts which was accounted for using two-factor analysis as previously described[27]. The difference observed here between the FEGA *ex vivo* (*i.e.* decreased levels of AMH) and the xenograft model system (*i.e.* no change in AMH levels) could result from the age-difference of the fetal testes used; it also cannot be excluded, however, that the intrinsic difference of the two assay-systems discussed before[28] could also account for it. Taken together, the results obtained *ex vivo* indicate that there exist specific 'windows of sensitivity' during which certain Sertoli cell function may be affected by exposure to ibuprofen. It is likely that the ibuprofen suppression of *SOX9* mRNA expression evidenced in this study along with several of its known targets (*AMH, DHH, COL2A1*), represents the basis by which ibuprofen also suppresses AMH.

Our study reveals not only that ibuprofen disturbs the endocrine homeostasis of the testis, in both the Sertoli and Leydig cells, but also that exposure to this NSAID markedly alters the expression of the germ cells genes *POU5F1*, *TFAP2C*, *LIN28A*, *ALPP*, and *KIT*. These genes are expressed in a population of mitotic fetal germ cells named gonocytes. NSAIDs have been shown to promote cell cycle arrest and apoptosis thereby decreasing the initiation and/or progression of various cancers (colorectal, bladder, skin, esophageal adenocarcinoma,

Cell type	Hormone	Paracetamol	Ibuprofen	Aspirin	Indomethacin
Leydig cell	Testosterone	⇔	↘[1]	↗	↗
	INSL3	↘	↘	⇔	⇔
Sertoli cell	AMH	⇔	↘	↗	⇔
Unknown	PGD2	⇔	⇔	⇔	⇔
	PGE2	↘	↘ or ↗[2]	↘	↘

Table 1. Summary of the endocrine-disrupting signatures of each tested analgesic *ex vivo*. Data for paracetamol, aspirin and indomethacin come from[26]. [1]After 24, 48 and 72 h of exposure. [2] ↘ In the 8–9.9 GW and 8–12 GW testes at 10^{-5} and 10^{-4} M; ↗ in the 10–12 GW testes at 10^{-7} and 10^{-6} M.

ovarian)[63–66]. Whether ibuprofen effects occur by similar mechanisms remains to be established. In addition, whether ibuprofen-induced alteration of germ cell gene expression results from a direct effect of this NSAID on the human gonocytes, or if it is secondary to the marked suppression of the endocrine function of both Sertoli and Leydig cells is also unknown.

PGD2 and PGE2, the 2 prostaglandins investigated in this study, are thought to be involved in the differentiation of the fetal testis. In fact, exposing mouse testis explants (11, 12, and 14 days post-coitum) to PGE2 prevented the differentiation of testis cords[67]. Furthermore, mice deficient in *Ptgds,* which encodes the lipocalin-type prostaglandin D2 synthase enzyme responsible for PGD2 synthesis, display unilateral cryptorchidism[68]. However, here, we show that exposure to ibuprofen had no significant effect on PGD2 production. In contrast, ibuprofen induced marked changes in PGE2 levels. It is interesting to note that, as in our previous study on paracetamol, aspirin, and indomethacin, human fetal testis PGD2 production appears to be much less sensitive to the effects of ibuprofen than PGE2[26]. The precise mechanism of action underlying the inhibitory effect of ibuprofen on PGE2 production remains to be explored. PGE2 is known to modulate immune and inflammatory responses through its receptors EP1 to EP4[69], and EP2 has recently been detected within the rat fetal testis[70]. It also remains to be determined what the consequences of ibuprofen-induced suppression of PGE2 might be on the human fetal testis biology and development. It would be important to understand which testicular cell type(s) is/are responsible for PGE2 production and which ones express the receptor for PGE2 within the human fetal testis.

Of all the analgesics that we have tested so far using our *ex vivo* human fetal testis system[26], ibuprofen appears to be the agent which alters the human fetal endocrine balance with the widest range of effects as it affects all the major testicular cell types. Interestingly, paracetamol, aspirin, indomethacin, and ibuprofen each display their own endocrine-disrupting signatures (Table 1). The only unequivocally shared effect observed with these 4 analgesics is their inhibitory action on prostaglandin E2 production in 8–9.9 GW fetuses. However, whereas paracetamol and aspirin did not have any effect on testosterone production at this stage of gestation, the same group of testes treated with ibuprofen had lower testosterone production. Several other differences between analgesic effects also exist: ibuprofen - unlike aspirin but similar to paracetamol - suppresses INSL3 production. Furthermore, aspirin increased AMH production whereas paracetamol had no such effect, and ibuprofen showed a dose-response inhibition of this Sertoli cell produced hormone (Table 1). Taken together, these observations indicate that each drug has its own mechanism of action within the human fetal testis. Due to the different analgesic-induced biological signatures induced within the fetal testis, it is likely that this explains why when pregnant women simultaneously use more than one analgesic (paracetamol, aspirin, and ibuprofen), the risk of cryptorchidism observed is almost 10 times higher (odds ratio 2 fold versus 17 fold) than when a single painkiller is used[7]. Likewise, simultaneous use of both paracetamol and NSAIDs was found to be associated with significantly shorter AGD in boys, while exposure to paracetamol only was not significantly associated with shorter AGD[24]. In any case, the different therapeutic indications and contra-indications of these medications, *i.e.* paracetamol and of the NSAIDs, also reflect their different structures and properties. The present data complement our previous findings, which show that analgesics can behave as endocrine disruptors during key stages of the development of the urogenital tract[26]. This study provides new mechanistic explanations for the increased risk of cryptorchidism and hypospadias observed after *in utero* exposure to these medications by different groups.

In conclusion we show that exposure to therapeutic levels of ibuprofen during specific 'windows of sensitivity' can result in multiple effects on Sertoli-, Leydig- and germ-cell development and function in the human fetal testis. This includes effects on production of several testicular hormones during the first trimester. These findings are based on the results of 2 different model systems of human fetal testis development. Whilst they cannot be directly translated into recommendations for the use of ibuprofen in humans they provide experimental support to the epidemiological association between analgesic use and the development of male reproductive disorders, evidence that would support the avoidance of ibuprofen use during the first trimester where practicable.

Materials and Methods

Ethics statement. First trimester (7–12 gestational week) and second trimester (14–17 gestational week) human fetuses were obtained from abortions performed at the Rennes Sud Hospital in Rennes, France and the Royal Infirmary of Edinburgh, Edinburgh, UK, respectively. None of the pregnancy terminations were due to fetal abnormalities. Women gave written informed consent as per the legal procedures put in place by the French national biomedical research agency (authorization #PFS09-011; Agence de la Biomédecine) and the Declaration of Helsinki – Ethical Principles for Medical Research Involving Human Subjects. All experiments were performed in accordance with relevant guidelines and regulations. Ethical approval for the study was obtained from Rennes

Sud Hospital local ethics committee (notice #11-48) and South East Scotland Research Ethics Committee (reference number: LREC08/S1101/1).

Human fetal testis collection. First-trimester human fetal testes were recovered from the abortion aspiration products using a binocular microscope (Olympus SZX7, Lille, France). They were immediately placed in ice-cold phosphate-buffered saline (PBS) solution. Second trimester human fetal testes were recovered and placed into ice-cold 'xenograft media' containing Liebowitz L-15 with glutamine, 10% fetal bovine serum, 1% penicillin/streptomycin and 1% non-essential amino acids (all Sigma, Poole, UK).

Culture and xenograft procedures. The testes were cut into explants of less than 1 mm^3 according to a standardized protocol previously described[26,40]. For the testes younger than 8 GW, 2 wells were designed to accommodate 1 testis and either control or 10^{-5} M of ibuprofen treatment. These testes were immediately exposed to treatments. For the 8 to 10 GW group, 4 wells were prepared for 4 different culture conditions (1 control and 3 ibuprofen concentrations). These wells were each half a testis in length and contained 2 to 3 pieces of a single testis. For the older testes (10 to 12 GW), 6 wells for 6 different culture conditions (1 control and 5 ibuprofen concentrations) were created, each containing 1 or 2 testis pieces from a single testis. The explants were cultured in inserts (0.4 μm pores; Falcon, Becton-Dickinson, Le Pont de Claix, France) placed in 24-well companion culture plates (Becton-Dickinson). Human chorionic gonadotrophin (Sigma Aldrich, Saint-Quentin, France) was added at a concentration of 0.1 IU/mL[71], and the cultures were incubated at 37 °C for 96 h in a humidified atmosphere of 95% air and 5% CO2. The medium was removed every 24 h and divided into at least 2 aliquots that were immediately snap-frozen on dry ice and stored at −80 °C. To assess dose-response effects, after the first 24 h of culture (D0) the explants were exposed to either the control, DMSO at a final concentration of 0.1%, or to the ibuprofen treatment, with concentrations of 10^{-7} M to 10^{-4} M added to the medium.

For xenograft studies, human fetal testes were grafted into castrate host mice as previously described[27]. Briefly, small pieces (1 mm^3 approx; 4–6 per mouse) of testis tissue were placed subcutaneously, either side of the midline, under the dorsal skin of the mice using a 13 G cancer implant needle (Popper and Sons, US). In general, 3–6 mice were xenografted with tissue from each fetus, and mice were maintained for 7 days to ensure vascularisation before any host treatments commenced. One week after grafting, host mice commenced treatment with subcutaneous injection of human chorionic gonadotropin (20 IU hCG every 72 hours; Pregnyl, Organon Laboratories) to mimic the human *in utero* environment[72]. Host mice were also randomly allocated to receive a therapeutic regimen of either ibuprofen (10 mg/kg three times daily), or vehicle (corn oil) by daily oral administration with analysis 1 hour after the final dose. Host mice were sacrificed by cervical dislocation, and blood was obtained by cardiac puncture for assessment of plasma testosterone, AMH and ibuprofen. Testosterone production and action was assessed by measuring plasma testosterone and seminal vesicle weight. No differences were observed between vehicle- and ibuprofen-exposed host mice in terms of body weight, number of grafts retrieved or total graft weight (Fig. S1).

Immunostaining and stereology. Immunohistochemistry was performed on 4% paraformaldehyde-PBS and Bouin solution-fixed, paraffin-embedded tissues, as previously described[26]. The Sertoli cells were labeled with an AMH goat primary antibody (1:100; Santa Cruz Biotechnology, CA, USA). Leydig cells were stained with a rabbit anti-cytochrome P450, family 11, subfamily A, polypeptide 1 (CYP11A1) antibody (1:250; Sigma Aldrich). A mouse M2A primary antibody (1:100; Abcam, Paris, France) was used for gonocyte immunolabeling. For the AMH and M2A antibodies, antigens were retrieved for 40 min at 80 °C in 10 mM citrate buffer, pH 6.

A NanoZoomer 2.0-RS scanner (Hamamatsu, Tokyo, Japan) was used to capture pictures of the whole slides at 40x magnification. The surface area of 5 to 10 sections randomly selected within the whole explant were calculated with NDP.view software (Hamamatsu). ImageJ software (US National Institutes of Health, Bethesda, MD, USA) was used to perform the stereological cell counting. Germ and Sertoli cells were identified and counted as intra-cordal AMH-negative and AMH-positive cells, respectively.

Hormone assays. Testosterone was assayed using a specific radioimmunoassay (RIA): a direct testosterone RIA with an intra-assay coefficient of variation (CV) $\leq$ 8.6% and an inter-assay CV of 11.9% (Immunotech, Beckman Coulter, Villepinte, France). A specific RIA was also used for insulin-like 3: a human INSL3/RLF RIA kit with intra- and inter-assay CVs of $\leq$15 and 7%, respectively (Phoenix Pharmaceuticals, Strasbourg, France). AMH levels were assayed using an AMH/MIS Enzyme-Linked Immunosorbent Assay (ELISA) kit with an intra-assay CV of 3.2 to 12.3% and inter-assay CV of 5.8 to 14.2% (Immunotech, Marseille, France). PGD2 was measured with ELISA using a prostaglandin D2-MOX EIA Kit having an intra-assay CV of 8 to 15% and an inter-assay CV of 10 to 17% (Cayman Chemical, Ann Arbor, MI, USA). PGE2 was also assayed using a prostaglandin E2 EIA Kit (intra-assay CV 3.7 to 30.4% and inter-assay CV 6.4 to 35%) (Cayman Chemical).

The hormone assay data from the culture system using the testes of the fetuses younger than 8 GW were expressed as hormone production fold change as compared to the control testis. Since the older testes were cut into explants, the first 24 hours of culture (day 0 without treatment, or D0) served as the baseline for normalization of hormone production in each testicular sample after 24, 48, and 72 h of exposure to DMSO or ibuprofen. Depending on fetal age, we established cut-offs for normal relative testosterone production in the control experiments, calculated at D3 normalized to the D0 result in the same culture well. These were >0.7 for the 8–9.8 GW explants, and $\geq$0.1 for the 10–12 ones.

Global analysis of steroids. The procedures for applied sample preparation and GC-MS/MS measurements have been previously described[73,74]. Tissue samples were homogenized after addition of 50:50 v/v methanol and water (300 μl/10 mg tissue). Prior to extraction for quantification according to isotopic dilution, tissue homogenates, and cell culture media (200 μl) were spiked with internal standards (17β-estradiol-16,16,17-d3;

Gene	Upstream primer	Downstream primer	Product length (bp)	Annealing temp °C
ALPP	TCTGGGTACTCAGGGTCTGG	ATCGCTACGCAGCTCATCTC	101	62
AMH	CGCCTGGTGGTCCTACAC	GAACCTCAGCGAGGGTGTT	162	67
BZRP	GGCTTCACAGAGAAGGCTGT	ACTGACCAGCAGGAGATCCA	87	66
COL2A1	GGCAATAGCAGGTTCACGTACA	CGATAACAGTCTTGCCCCACTT	57	53
CYP11A1	AGACCTGGAAGGACCATGTG	TCCTCGAAGGACATCTTGCT	435	65
CYP17A1	GTGGAGACCACCACCTCTGT	GCTGAAACCCACATTCTGGT	108	67
DHH	TGATGACCGAGCGTTGTAAG	GCCAGCAACCCATACTTGTT	196	67
HSD3B2	GCCTGTTGGTGGAAGAGAAG	GCAGGCTCTTTTCAGGAATG	158	62
HSD17B3	TCCTTGGCCTCTCTACTCCA	AGACAGCATATGGGGTCAGC	125	62
INSL3	CCCAGAGATGCGTGAGAAGT	CCAGCCACTGTAGCAACTCA	229	68
KIT	TTCTTACCAGGTGGCAAAGG	AAATGCTTTCAGGTGCCATC	209	62
LIN28A	AAGCTGCACATGGAAGGGTT	CCGCCTCTCACTCCCAATAC	138	67
POU5F1	TACTCCTCGGTCCCTTTCC	CAAAAACCCTGGCACAAACT	131	67
RPLP0	TCTACAACCCTGAAGTGCTTGAT	CAATCTGCAGACAGACACTGG	167	66
RPS20	AACAAGCCGCAACGTAAAA	ACGATCCCACGTCTTAGAA	96	67
SOX9	AACGCCTTCATGGTGTGG	TCTCGCTCTCGTTCAGAAGTC	124	59
SRD5A3	AGGAATGCCTACATAACAGGGAA	CTCCAAATGGGATCCTGTGGT	181	62
STAR	GGCTGGCATGGCCACAGACT	TTGGGCAGCCACCCCTTGA	162	77
TFAP2C	CCGGTCCTTGCGGGAGAAGTT	CTGGTTTACTAGGAAATTCGGCTTCACA	164	75

Table 2. Primers used for qPCR.

5α-androstan-3α,17β-diol-16,16,17-d3; etiocholanolone-2,2,3β,4,4-d5; 17β-testosterone-16,16,17-d3; 4-androsten-3,17-dione-19,19,19-d3; 5α-androstan-17β-ol-3-one-16,16,17-d3; and 17-methyltestosterone-d3). Non-polar compounds were extracted from the aqueous phase (pH 5.2) with diethyl ether, followed by a liquid/liquid partitioning to separate androgens and estrogens. Both fractions were purified on 200 mg Upti-Clean SI-S cartridges (Interchim, Montluçon, France), then derivatized with a silylation reagent as described by Courant *et al.*[74]. Two micro-liters of each final extract were injected into the GC-MS/MS system. The detection and quantification of the targeted compounds were performed on a spectrometer (Bruker, Fremont, CA, USA). Electron impact (70 eV) was the ionization mode used for androgens, while negative chemical ionization (80 μA filament current) with methane reactant gas was applied for estrogens. The source temperature was set to 250 °C and the transfer line to 300 °C. The chromatographic conditions were previously described by Courant *et al.*[74]. The mass spectrometer was operated in multiple reaction monitoring (MRM) acquisition mode, and argon was used as collision gas at 2.0 mTorr. The diagnostic signals were monitored for the targeted compounds have been reported elsewhere[73,74].

For xenografts, testosterone and ibuprofen were extracted from mouse plasma by solid phase extraction using 10 mg HLB Oasis cartridges (Waters, UK). Briefly, 50 μL plasma was enriched with 1 ng 13C3-Testosterone (QMX, UK) as internal standard. Cartridges were conditioned with methanol and water, the sample loaded and washed with water, 5% methanol and then eluted with 1 mL methanol. The eluate was reduced to dryness under nitrogen at 40 °C and reconstituted in mobile phase (70 μL water/acetonitrile (70:30, v/v)). Chromatographic separation was achieved by injecting 30 μL sample onto an Acquity UPLC system with an ACE Excel C18-AR column (150 × 2.1 mm; 2 μm) protected by a Kinetex KrudKatcher (Phenomenex) and operated at 30 °C. The mobile phase consisted of 0.1% formic acid (Sigma Aldrich) in water and 0.1% formic acid in acetonitrile (B) at a flow rate of 0.5 mL/min. Gradient elution from 30–100% B was achieved, with a total run time of 9 mins. Testosterone, and Ibuprofen eluted at 5.40 and 5.7 min respectively. Following separation, testosterone and ibuprofen were detected on a QTrap 5500 triple quadrupole mass spectrometer (Sciex, Warrington, UK) operated in positive ion electrospray mode (5.5 kV, 550 °C, ion source gas 60/40). Transitions monitored were m/z 289.1 → 97.0, and *m/z* 156.1 → 114.1 for testosterone and ibuprofen, respectively. The ratio of the peak area of each analyte to the internal standard was used to generate a calibration curve and using linear regression analysis the amount of each analyte was calculated.

RNA extraction and quantitative Polymerase Chain Reaction (qPCR). RNA extractions from testes were done using a NucleoSpin XS kit (Macherey-Nagel, Hoerdt, France) according to the manufacturer's instructions. Total RNA (250 ng) was reverse transcribed with random primers and Moloney murine leukemia virus reverse transcriptase (Invitrogen, ThermoFisher, Courtaboeuf, France). Quantitative PCR was performed according to the manufacturer's instructions using the SYBR Green master mix (Applied Biosystems, ThermoFisher) with a 0.5 μl cDNA template in an Applied Biosystems 7500 Real-Time PCR system. The amplification program was as follows: a 2 min holding stage at 50 °C; initial denaturation of 10 min at 95 °C; 40 cycles of 15 sec denaturation at 95 °C; and 1 min at 60 °C for annealing and extension. Dissociation curves were produced using a thermal melting profile performed after the last PCR cycle. To avoid amplification of contaminating genomic DNA, primer pairs were selected on either side of an intron. *RPLP0* and *RPS20* mRNA were used as internal controls

for normalization[75] (Table 2). Results were calculated by the $\Delta\Delta C_T$ method as n-fold differences in target gene expression with respect to the reference gene and the calibration sample (made of an equal mix of each of the samples tested).

Statistical analysis. Hormone measurements (means ± SEM) are expressed either as percentages of the values as compared to the control testes (7 to 7.9 GW fetuses), as the fold change from the respective untreated first day of culture (D0; 8–12 GW fetuses), or as absolute values for serum in xenografted mice.

Testosterone and AMH production as a function of culture duration in 7–7.9 GW testes were analyzed using repeated measures analysis of variance (ANOVA) on ranks. Ibuprofen dose-response relationships were assessed for testosterone, INSL3, AMH, PGD2, and PGE2 using variance analyses, with the treatment as explanatory variable and a random fetus effect. To normalize the data, logarithm transformations were used for INSL3, AMH, PGD2 and PGE2 data. The dose was transformed into a categorical variable (ranging from 1 for the lowest dose to 4 for the highest one) then introduced into the models as continuous variables. The corresponding slope β therefore represents the change in hormone secretion for each supplementary dose unit. Pairwise differences between the ibuprofen treatments and controls were analyzed using the non-parametric Wilcoxon signed-rank test. Quantitative PCR data, GC-MS/MS data, and cell-counts were also analyzed with the Wilcoxon test. For analysis of AMH, testosterone and ibuprofen in xenografts, a two-way ANOVA was performed. Significance was defined as a confidence level of $p < 0.05$. Statistical analyses were performed using SAS software (SAS/STAT version 9.3; SAS Institute Inc., Cary, NC) and SigmaPlot 12.0 software (Systat Software, San Jose, CA, USA).

References

1. Kristensen, D. M. *et al.* Analgesic use - prevalence, biomonitoring and endocrine and reproductive effects. *Nat. Rev. Endocrinol.* doi: 10.1038/nrendo.2016.55 (2016).
2. Verlicchi, P., Al Aukidy, M., Galletti, A., Petrovic, M. & Barceló, D. Hospital effluent: investigation of the concentrations and distribution of pharmaceuticals and environmental risk assessment. *Sci. Total Environ.* **430,** 109–18 (2012).
3. Kassaw, C. & Wabe, N. T. Pregnant women and non-steroidal anti-inflammatory drugs: knowledge, perception and drug consumption pattern during pregnancy in ethiopia. *N. Am. J. Med. Sci.* **4,** 72–6 (2012).
4. Hassoun-Barhamji, R., Raia Barjat, T. & Chauleur, C. In the Era Of Self-Medication, What Do Pregnant Women Know about Anti-Inflammatory Drugs? *Therapie* **70,** 369–76 (2015).
5. Ertresvåg, J. M., Zwart, J.-A., Helde, G., Johnsen, H.-J. & Bovim, G. Headache and transient focal neurological symptoms during pregnancy, a prospective cohort. *Acta Neurol. Scand.* **111,** 233–7 (2005).
6. Werler, M. M., Mitchell, A. A., Hernandez-Diaz, S. & Honein, M. A. Use of over-the-counter medications during pregnancy. *Am. J. Obstet. Gynecol.* **193,** 771–7 (2005).
7. Kristensen, D. M. *et al.* Intrauterine exposure to mild analgesics is a risk factor for development of male reproductive disorders in human and rat. *Hum. Reprod.* **26,** 235–44 (2011).
8. Snijder, C. A. *et al.* Intrauterine exposure to mild analgesics during pregnancy and the occurrence of cryptorchidism and hypospadia in the offspring: the Generation R Study. *Hum. Reprod.* **27,** 1191–201 (2012).
9. Alano, M. A., Ngougmna, E., Ostrea, E. M. & Konduri, G. G. Analysis of nonsteroidal antiinflammatory drugs in meconium and its relation to persistent pulmonary hypertension of the newborn. *Pediatrics* **107,** 519–23 (2001).
10. Berlin, C. M., Yaffe, S. J. & Ragni, M. Disposition of acetaminophen in milk, saliva, and plasma of lactating women. *Pediatr. Pharmacol.* (*New York*). **1,** 135–41 (1980).
11. Bitzén, P. O., Gustafsson, B., Jostell, K. G., Melander, A. & Wåhlin-Boll, E. Excretion of paracetamol in human breast milk. *Eur. J. Clin. Pharmacol.* **20,** 123–5 (1981).
12. Ellfolk, M. & Hultzsch, S. In Drugs During Pregnancy and Lactation: Treatment options and risk assessment. (eds Schaeffer, C., Peters, P. & Miller, R.) 4.1, 653–670 (Elsevier, 2015).
13. Levy, G., Garrettson, L. K. & Soda, D. M. Letter: Evidence of placental transfer of acetaminophen. *Pediatrics* **55,** 895 (1975).
14. Naga Rani, M. A., Joseph, T. & Narayanan, R. Placental transfer of paracetamol. *J. Indian Med. Assoc.* **87,** 182–3 (1989).
15. Weigand, U. W., Chou, R. C., Maulik, D. & Levy, G. Assessment of biotransformation during transfer of propoxyphene and acetaminophen across the isolated perfused human placenta. *Pediatr. Pharmacol.* (*New York*). **4,** 145–53 (1984).
16. Nezvalová-Henriksen, K., Spigset, O. & Nordeng, H. Effects of ibuprofen, diclofenac, naproxen, and piroxicam on the course of pregnancy and pregnancy outcome: a prospective cohort study. *BJOG* **120,** 948–59 (2013).
17. Hammerman, C. & Kaplan, M. Patent ductus arteriousus in the premature neonate: current concepts in pharmacological management. *Paediatr. Drugs* **1,** 81–92 (1999).
18. Marsh, C. A., Cragan, J. D., Alverson, C. J. & Correa, A. Case-control analysis of maternal prenatal analgesic use and cardiovascular malformations: Baltimore–Washington Infant Study. *Am. J. Obstet. Gynecol.* **211,** 404.e1–404.e9 (2014).
19. Vieux, R., Fresson, J., Guillemin, F. & Hascoet, J. M. Perinatal drug exposure and renal function in very preterm infants. *Arch. Dis. Child. Fetal Neonatal Ed.* **96,** F290–5 (2011).
20. Sordillo, J. E. *et al.* Prenatal and infant exposure to acetaminophen and ibuprofen and the risk for wheeze and asthma in children. *J. Allergy Clin. Immunol.* **135,** 441–8 (2015).
21. Berkowitz, G. S. & Lapinski, R. H. Risk factors for cryptorchidism: a nested case-control study. *Paediatr. Perinat. Epidemiol.* **10,** 39–51 (1996).
22. Jensen, M. S. *et al.* Maternal use of acetaminophen, ibuprofen, and acetylsalicylic acid during pregnancy and risk of cryptorchidism. *Epidemiology* **21,** 779–85 (2010).
23. Fisher, B. G. *et al.* Prenatal paracetamol exposure is associated with shorter anogenital distance in male infants. *Hum. Reprod.* **31,** 2642–2650 (2016).
24. Lind, D. V. *et al.* Maternal use of mild analgesics during pregnancy associated with reduced anogenital distance in sons: a cohort study of 1027 mother-child pairs. *Hum. Reprod.* **32,** 223–231 (2017).
25. Kristensen, D. M. *et al.* Paracetamol (acetaminophen), aspirin (acetylsalicylic acid) and indomethacin are anti-androgenic in the rat foetal testis. *Int. J. Androl.* **35,** 377–84 (2012).
26. Mazaud-Guittot, S. *et al.* Paracetamol, aspirin, and indomethacin induce endocrine disturbances in the human fetal testis capable of interfering with testicular descent. *J. Clin. Endocrinol. Metab.* **98,** E1757–67 (2013).
27. van den Driesche, S. *et al.* Prolonged exposure to acetaminophen reduces testosterone production by the human fetal testis in a xenograft model. *Sci. Transl. Med.* **7,** 288ra80 (2015).
28. Jégou, B. Paracetamol-induced endocrine disruption in human fetal testes. *Nat. Rev. Endocrinol.* **11,** 453–4 (2015).
29. Glover, D. D., Amonkar, M., Rybeck, B. F. & Tracy, T. S. Prescription, over-the-counter, and herbal medicine use in a rural, obstetric population. *Am. J. Obstet. Gynecol.* **188,** 1039–45 (2003).

30. Wen, S. W. *et al.* Patterns of pregnancy exposure to prescription FDA C, D and X drugs in a Canadian population. *J. Perinatol.* **28,** 324–9 (2008).
31. Damase-Michel, C., Christaud, J., Berrebi, A., Lacroix, I. & Montastruc, J.-L. What do pregnant women know about non-steroidal anti-inflammatory drugs? *Pharmacoepidemiol. Drug Saf.* **18,** 1034–8 (2009).
32. Stephansson, O. *et al.* Drug use during pregnancy in Sweden - assessed by the Prescribed Drug Register and the Medical Birth Register. *Clin. Epidemiol.* **3,** 43–50 (2011).
33. Daniel, S. *et al.* Fetal exposure to nonsteroidal anti-inflammatory drugs and spontaneous abortions. *CMAJ* **186,** E177–82 (2014).
34. Van Marter, L. J., Hernandez-Diaz, S., Werler, M. M., Louik, C. & Mitchell, A. A. Nonsteroidal antiinflammatory drugs in late pregnancy and persistent pulmonary hypertension of the newborn. *Pediatrics* **131,** 79–87 (2013).
35. Lind, J. N. *et al.* Maternal medication and herbal use and risk for hypospadias: data from the National Birth Defects Prevention Study, 1997-2007. *Pharmacoepidemiol. Drug Saf.* **22,** 783–93 (2013).
36. Hernandez, R. K., Werler, M. M., Romitti, P., Sun, L. & Anderka, M. Nonsteroidal antiinflammatory drug use among women and the risk of birth defects. *Am. J. Obstet. Gynecol.* **206,** 228.e1–8 (2012).
37. Akre, O. & Richiardi, L. Does a testicular dysgenesis syndrome exist? *Hum. Reprod.* **24,** 2053–60 (2009).
38. Foresta, C., Zuccarello, D., Garolla, A. & Ferlin, A. Role of hormones, genes, and environment in human cryptorchidism. *Endocr. Rev.* **29,** 560–80 (2008).
39. Thorup, J., Nordenskjöld, A. & Hutson, J. M. Genetic and environmental origins of hypospadias. *Curr. Opin. Endocrinol. Diabetes. Obes.* **21,** 227–32 (2014).
40. Ben Maamar, M. *et al.* An investigation of the endocrine-disruptive effects of bisphenol a in human and rat fetal testes. *PLoS One* **10,** e0117226 (2015).
41. Mitchell, R. T. *et al.* Do phthalates affect steroidogenesis by the human fetal testis? Exposure of human fetal testis xenografts to di-n-butyl phthalate. *J. Clin. Endocrinol. Metab.* **97,** E341–8 (2012).
42. Anand-Ivell, R., Ivell, R., Driscoll, D. & Manson, J. Insulin-like factor 3 levels in amniotic fluid of human male fetuses. *Hum. Reprod.* **23,** 1180–6 (2008).
43. Rajpert-De Meyts, E. *et al.* Developmental expression of POU5F1 (OCT-3/4) in normal and dysgenetic human gonads. *Hum. Reprod.* **19,** 1338–44 (2004).
44. Hoei-Hansen, C. E. *et al.* Transcription factor AP-2gamma is a developmentally regulated marker of testicular carcinoma *in situ* and germ cell tumors. *Clin. Cancer Res.* **10,** 8521–30 (2004).
45. Shinoda, G. *et al.* Lin28a regulates germ cell pool size and fertility. *Stem Cells* **31,** 1001–9 (2013).
46. Jørgensen, N. *et al.* Expression of immunohistochemical markers for testicular carcinoma *in situ* by normal human fetal germ cells. *Lab. Invest.* **72,** 223–31 (1995).
47. Robinson, L. L., Gaskell, T. L., Saunders, P. T. & Anderson, R. A. Germ cell specific expression of c-kit in the human fetal gonad. *Mol. Hum. Reprod.* **7,** 845–52 (2001).
48. Mitchell, J. A., Akarasereenont, P., Thiemermann, C., Flower, R. J. & Vane, J. R. Selectivity of nonsteroidal antiinflammatory drugs as inhibitors of constitutive and inducible cyclooxygenase. *Proc. Natl. Acad. Sci. USA* **90,** 11693–7 (1993).
49. Simmons, D. L., Botting, R. M. & Hla, T. Cyclooxygenase isozymes: the biology of prostaglandin synthesis and inhibition. *Pharmacol. Rev.* **56,** 387–437 (2004).
50. Nef, S. & Parada, L. F. Cryptorchidism in mice mutant for Insl3. *Nat. Genet.* **22,** 295–9 (1999).
51. Hutson, J. M., Balic, A., Nation, T. & Southwell, B. Cryptorchidism. *Semin. Pediatr. Surg.* **19,** 215–24 (2010).
52. Serrano, T., Chevrier, C., Multigner, L., Cordier, S. & Jegou, B. International geographic correlation study of the prevalence of disorders of male reproductive health. *Hum. Reprod.* **28,** 1974–1986 (2013).
53. Källström, E., Heikinheimo, M. & Quiding, H. Bioavailability of three commercial preparations of ibuprofen 600 mg. *J. Int. Med. Res.* **16,** 44–9 (1988).
54. Karttunen, P., Saano, V., Paronen, P., Peura, P. & Vidgren, M. Pharmacokinetics of ibuprofen in man: a single-dose comparison of two over-the-counter, 200 mg preparations. *Int. J. Clin. Pharmacol. Ther. Toxicol.* **28,** 251–5 (1990).
55. Jost, A. A new look at the mechanisms controlling sex differentiation in mammals. *Johns Hopkins Med. J.* **130,** 38–53 (1972).
56. Pelliniemi, L. J. & Niemi, M. Fine structure of the human foetal testis. I. *The interstitial tissue. Zeitschrift für Zellforsch. und mikroskopische Anat.* (*Vienna, Austria 1948*) **99,** 507–22 (1969).
57. Chauvigné, F. *et al.* Mono-(2-ethylhexyl) phthalate directly alters the expression of Leydig cell genes and CYP17 lyase activity in cultured rat fetal testis. *PLoS One* **6,** e27172 (2011).
58. Locke, J. A. *et al.* A novel communication role for CYP17A1 in the progression of castration-resistant prostate cancer. *Prostate* **69,** 928–37 (2009).
59. Stutz, G. *et al.* Functional activity of mouse sperm was not affected by low doses of aspirin-like drugs. *Arch. Androl.* **44,** 117–28 (2000).
60. Sten, T., Finel, M., Ask, B., Rane, A. & Ekström, L. Non-steroidal anti-inflammatory drugs interact with testosterone glucuronidation. *Steroids* **74,** 971–7 (2009).
61. Zimmermann, S. *et al.* Targeted disruption of the Insl3 gene causes bilateral cryptorchidism. *Mol. Endocrinol.* **13,** 681–91 (1999).
62. Bay, K. & Andersson, A.-M. Human testicular insulin-like factor 3: in relation to development, reproductive hormones and andrological disorders. *Int. J. Androl.* **34,** 97–109 (2011).
63. Fischer, S. M., Hawk, E. T. & Lubet, R. A. Coxibs and other nonsteroidal anti-inflammatory drugs in animal models of cancer chemoprevention. *Cancer Prev. Res.* (*Phila*). **4,** 1728–35 (2011).
64. Santander, S. *et al.* Cyclooxygenase inhibitors decrease the growth and induce regression of human esophageal adenocarcinoma xenografts in nude mice. *Int. J. Oncol.* **40,** 527–34 (2012).
65. Rodríguez-Burford, C. *et al.* Effects of nonsteroidal anti-inflammatory agents (NSAIDs) on ovarian carcinoma cell lines: preclinical evaluation of NSAIDs as chemopreventive agents. *Clin. Cancer Res.* **8,** 202–9 (2002).
66. Valle, B. L. *et al.* Non-steroidal anti-inflammatory drugs decrease E2F1 expression and inhibit cell growth in ovarian cancer cells. *PLoS One* **8,** e61836 (2013).
67. Taketo, T., Thau, R. B., Adeyemo, O. & Koide, S. S. Influence of adenosine 3′:5′-cyclic monophosphate analogues on testicular organization of fetal mouse gonads *in vitro*. *Biol. Reprod.* **30,** 189–98 (1984).
68. Philibert, P. *et al.* Unilateral cryptorchidism in mice mutant for Ptgds. *Hum. Mutat.* **34,** 278–82 (2013).
69. Hirata, T. & Narumiya, S. Prostanoids as regulators of innate and adaptive immunity. *Adv. Immunol.* **116,** 143–74 (2012).
70. Dean, A. *et al.* Analgesic exposure in pregnant rats affects fetal germ cell development with inter-generational reproductive consequences. *Sci. Rep.* **6,** 19789 (2016).
71. Hallmark, N. *et al.* Effects of monobutyl and di(n-butyl) phthalate *in vitro* on steroidogenesis and Leydig cell aggregation in fetal testis explants from the rat: comparison with effects *in vivo* in the fetal rat and neonatal marmoset and *in vitro* in the human. *Environ. Health Perspect.* **115,** 390–6 (2007).
72. Mitchell, R. T. *et al.* Xenografting of human fetal testis tissue: a new approach to study fetal testis development and germ cell differentiation. *Hum. Reprod.* **25,** 2405–14 (2010).
73. Courant, F. *et al.* Exposure assessment of prepubertal children to steroid endocrine disrupters 1. Analytical strategy for estrogens measurement in plasma at ultra-trace level. *Anal. Chim. Acta* **586,** 105–14 (2007).

74. Courant, F. *et al.* Assessment of circulating sex steroid levels in prepubertal and pubertal boys and girls by a novel ultrasensitive gas chromatography-tandem mass spectrometry method. *J. Clin. Endocrinol. Metab.* **95,** 82–92 (2010).
75. Svingen, T., Jørgensen, A. & Rajpert-De Meyts, E. Validation of endogenous normalizing genes for expression analyses in adult human testis and germ cell neoplasms. *Mol. Hum. Reprod.* **20,** 709–18 (2014).

Acknowledgements

We thank all the staff of the Department of Obstetrics and Gynecology and the Department of Pediatric Surgery of the Rennes Sud Hospital (Rennes, France) and the participating women, without whom this study would not have been possible. We also thank the nursing staff of the Bruntsfield Ward at the Royal Infirmary of Edinburgh and the Human Developmental Biology Resource (www.hdbr.org) for providing some of the fetal material (Joint MRC/Wellcome Trust; Grant No: 099175/Z/12/Z). We also thank Natalie Homer from the Edinburgh CRF Mass Spectrometry Core for her assistance. This study was funded by Inserm, University of Rennes 1, EHESP – School of Public Health, by grants from the Agence Nationale de Sécurité du Médicament et des Produits de Santé (ANSM; AAP-2012–037), and the Danish Council for independent Research (Medical Sciences), and the Wellcome Trust (Grant No: 098522).

Author Contributions

M.B.M. performed experiments (organ collection, FEGA, hormone measurements, Qt RT-PCR and histology), analyzed data and wrote the manuscript draft. J-P.A., B.L.B. and K.H. performed the global steroid analyses and wrote the corresponding section of the manuscript. L.L. performed cell counts, statistics and contributed to the writing of the manuscript. C.D.L. contributed to hormone measurements and Qt RT-PCR validations. K.K. performed xenografting experiments. I.C. contributed to organ collection and tissue culture. A.D.R. designed and performed Qt-RT-PCR. C.C. performed multivariate analyses. N.D.R. and D.M.K. contributed to critical discussions. V.L. supervised the collection of the first trimester human fetal testis samples. R.T.M. designed and conducted the xenograft experiments, analyzed data, and contributed to the writing of the manuscript. S.M.G. designed and performed experiments (organ collection, FEGA, Qt RT-PCR and histology), analyzed data, and contributed to writing of the manuscript. B.J. designed the study, analyzed data, and contributed to the writing of the manuscript. All authors approved the final version.

Additional Information

Supplementary information accompanies this paper at http://www.nature.com/srep

Competing Interests: The authors declare no competing financial interests.

How to cite this article: Ben Maamar, M. *et al.* Ibuprofen results in alterations of human fetal testis development. *Sci. Rep.* **7**, 44184; doi: 10.1038/srep44184 (2017).

Publisher's note: Springer Nature remains neutral with regard to jurisdictional claims in published maps and institutional affiliations.

Nilsson et al. BMC Genomics 2013, 14:496
http://www.biomedcentral.com/1471-2164/14/496

BMC Genomics

RESEARCH ARTICLE Open Access

Gene bionetworks that regulate ovarian primordial follicle assembly

Eric Nilsson[1], Bin Zhang[2] and Michael K Skinner[1*]

Abstract

Background: Primordial follicle assembly is the process by which ovarian primordial follicles are formed. During follicle assembly oocyte nests break down and a layer of pre-granulosa cells surrounds individual oocytes to form primordial follicles. The pool of primordial follicles formed is the source of oocytes for ovulation during a female's reproductive life.

Results: The current study utilized a systems approach to detect all genes that are differentially expressed in response to seven different growth factor and hormone treatments known to influence (increase or decrease) primordial follicle assembly in a neonatal rat ovary culture system. One novel factor, basic fibroblast growth factor (FGF2), was experimentally determined to inhibit follicle assembly. The different growth factor and hormone treatments were all found to affect similar physiological pathways, but each treatment affected a unique set of differentially expressed genes (signature gene set). A gene bionetwork analysis identified gene modules of coordinately expressed interconnected genes and it was found that different gene modules appear to accomplish distinct tasks during primordial follicle assembly. Predictions of physiological pathways important to follicle assembly were validated using ovary culture experiments in which ERK1/2 (MAPK1) activity was increased.

Conclusions: A number of the highly interconnected genes in these gene networks have previously been linked to primary ovarian insufficiency (POI) and polycystic ovarian disease syndrome (PCOS). Observations have identified novel factors and gene networks that regulate primordial follicle assembly. This systems biology approach has helped elucidate the molecular control of primordial follicle assembly and provided potential therapeutic targets for the treatment of ovarian disease.

Keywords: Ovary, Primordial follicle, Assembly, Ovarian development, PCO, POI, Transcriptome, Female fertility, Genomics, System biology

Background

Complex and interconnected networks of gene expression, cellular signaling and other processes within cells and organs are what control biological processes. This raises the concern that the common reductionist experimental approach to biomedical research may not be adequate to fully understand the systems that control these processes. Reductionist experiments will commonly impose single treatments onto the biological entity under study and measure a single response parameter compared to controls. A relevant example from the authors' own laboratory is the study of the effect that treatment of neonatal rat ovaries with anti-Müllerian hormone (AMH) has on the proportion of primordial follicles formed [1]. Results from these types of experiments can provide clear information about candidate regulatory factors, but typically do not elucidate the network of factors or signals that are required for a normal biological process. A systems biology experimental approach to studying normal development can be a powerful tool that is complementary to the more reductionist methods. The goal of the current study is to use a systems biology approach to identify gene expression networks involved in the formation of ovarian primordial follicles (primordial follicle assembly), and to identify putative regulatory factors involved in this developmental process.

Primordial follicle assembly is the process by which ovarian primordial follicles are formed. A primordial

* Correspondence: skinner@wsu.edu
[1]Center for Reproductive Biology, School of Biological Sciences, Washington State University, Pullman, WA 99164-4236, USA
Full list of author information is available at the end of the article

follicle is composed of an oocyte arrested in prophase of the first meiotic division and surrounded by a single layer of pre-granulosa cells [2]. Follicle assembly in mammals occurs either during gestation (e.g. cattle and humans) or shortly after birth (e.g. rodents). The pool of assembled primordial follicles is the source of oocytes for follicle growth and ovulation over the course of a female's reproductive life [3]. When the primordial follicle pool is depleted reproduction ceases and women enter menopause [2-7]. Prior to follicle assembly, mitotic proliferation of germ cells creates groups of cells linked by intracellular bridges and surrounded by an epithelial/mesenchymal cell layer and the structures are called oocyte nests and when the surrounding stromal cells are considered ovigerous cords [8-10]. The mitotically arrested germ cells within the nests enter meiosis and progress to the diplotene stage of prophase one of meiosis and arrest at that stage until such time as ovulation occurs [5,6,11].

During the follicle assembly process oocyte nests break down and a single layer of pre-granulosa cells surrounds individual oocytes to form primordial follicles [3]. The majority of oocytes in each nest undergo apoptosis during follicle assembly [3,6,12,13]. Abnormalities in the follicle assembly process can lead to a reduced primordial follicle pool size and reproductive capacity. Abnormal pool size may lead to some types of infertility such as Primary Ovarian Insufficiency (POI) in which the follicle pool is depleted early in life and women undergo early menopause [14,15]. Previous research has shown that several extracellular signaling molecules (e. g. growth factors and hormones) can regulate follicle assembly [3,5-7]. These studies have primarily used a reductionist approach to test candidate factors one at a time for their ability to affect the assembly process. Growth factors and hormones that have been shown to regulate primordial follicle assembly include anti-Müllerian hormone (AMH) (decrease) [1], connective tissue growth factor (CTGF) (increase) [16], estradiol (E2) (increase) [17-21], activin A (increase) [21], progesterone (P4) (decrease) [17,18,22,23], tumor necrosis factor alpha (TNFa) (decrease) [23-25], members of the notch/jagged signaling pathway (increase) [26], members of the brain derived neurotrophic factor (BDNF) / NTRK2 neurotrophin signaling pathway [27,28] and kit ligand (KITL) and growth differentiation factor-9 (GDF9) (increase) [29]. Evidence suggests fibroblast growth factor-2 (FGF2) may also be a regulator of follicle assembly [1,30], although this has not been confirmed experimentally.

A systems biology experimental approach was employed in the current study to expand upon the results of these previous experiments that examined single gene effects on the follicle assembly process. A similar systems biology approach has been used previously to identify coordinately and interconnected expressed gene modules and gene networks that regulate the primordial to primary follicle transition which is the subsequent stage of ovarian follicle development [31]. This previous study used a systems approach to elucidate the suite of genes involved in initiating the development of arrested primordial follicles to initiate folliculogenesis. In the current investigation, whole rat ovaries from zero-day old rats were cultured *in vitro* in a manner that allows primordial follicle assembly to occur. The ovaries were treated with one of several different extracellular signaling factors that have been shown to regulate follicle assembly. Messenger RNA was isolated from the ovaries and used for microarray transcriptome analysis to globally survey gene expression under these different treatment conditions. The effects of each signaling factor treatment were analyzed to determine similarities and differences in gene expression between the treatments. A gene bionetwork analysis subjected all the differentially expressed genes across all treatments to a weighted co-expression cluster analysis to identify groups of genes (i.e. modules) whose expression was regulated in a coordinated and interconnected manner [32-35]. In this type of analysis biological systems are surveyed with microarrays multiple times with and without perturbations that cause the system to change. The coordinately and interconnected expressed gene modules identified are often associated with specific physiological processes and have been used to identify potential therapeutic targets [32,36,37]. In addition, the various groups and modules of genes identified were subjected to an unbiased gene network analysis that compared gene lists to databases of known gene binding and/or functional relationships. The gene expression analyses can then be interpreted from the standpoint of physiological function and important regulatory gene networks. The objective of the investigation was to use a systems biology experimental approach to identify gene expression networks involved in regulating primordial follicle assembly. Novel regulatory factors and potential therapeutic targets were identified that correlate with normal follicle assembly and associated ovarian disease.

Results

Actions on primordial follicle assembly

In the selection of regulatory factors to be used in the current study one novel factor was considered. Previous research [1,30] indicated that FGF2 might be a regulatory growth factor for the follicle assembly process. In order to determine if FGF2 would be included as a treatment in the current study, organ culture experiments were performed to empirically test the effects of FGF2 on follicle assembly. Ovaries from zero-day old rats containing un-assembled oocytes in nests (Figure 1A) were placed into an organ culture system and cultured for two days with or without FGF2. After culture ovaries

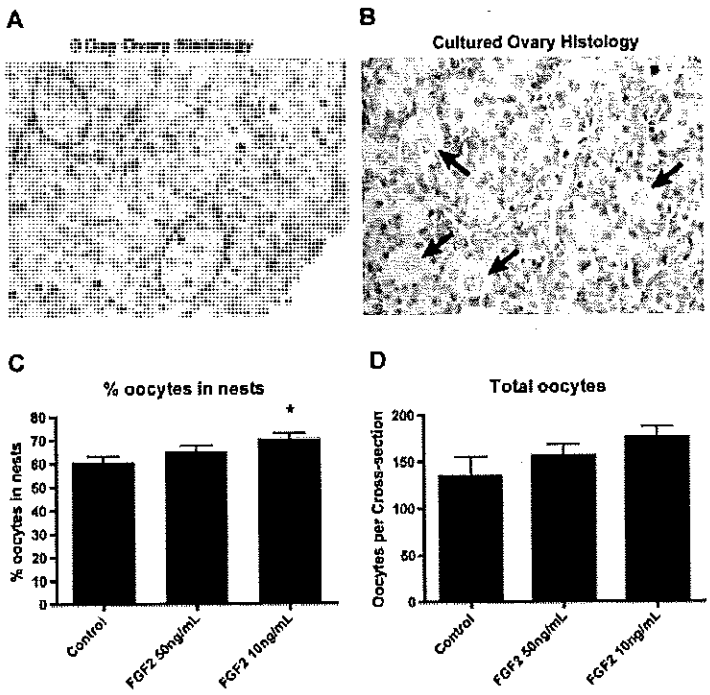

Figure 1 Validation of FGF2 as a growth factor that affects primordial follicle assembly. A) Representative image of a 0-day old rat ovary, showing oocytes in nests (circle nests). **B)** Representative image of an ovary after two days in culture, showing some oocytes assembled into primordial follicles (arrows). **C)** Proportion of oocytes still retained in nests after two days of culture with or without FGF2 treatment. **D)** Total number of oocytes per ovarian cross-section after culture. * = $p<0.05$ compared to untreated Control by Student's *t*-test.

were fixed, sectioned, stained and evaluated morphologically (Figure 1B). The number of oocytes in oocyte nests and assembled into primordial follicles was observed (see Methods). Results indicate that treatment with 10ng/ml FGF2 resulted in a modest but statistically significant increase in the proportion of oocytes retained in unassembled nests (Figure 1C). A larger duration culture of four days promotes a greater magnitude response, but is a combined effect of oocyte survival and follicle assembly, such that the shorter duration culture was used to focus on follicle assembly. A 50 ng/ml dose did not have an effect in comparison with the 10 ng/ml dose which is assumed to be due to negative feedback regulation during the 2 day culture period required. There was no statistical difference in the total number of oocytes per ovarian cross-section with FGF2 treatment (Figure 1D), although there was a trend for oocyte numbers to rise. Observations suggest FGF2 acts to inhibit the follicle assembly process. Based on these results it was decided that FGF2 be included as a treatment in the follicle assembly network experiments.

Growth factor and hormone regulation of the ovarian transcriptome

To determine the gene networks and processes involved in follicle assembly ovaries from zero-day old rats were placed into an organ culture system and exposed to different regulatory factors. The ovaries were treated for 24 hours with one of each of the following regulatory extracellular signaling factors: AMH, CTGF, E2, FGF2, activin A, P4, TNFa, or were untreated as Controls. CTGF, activin A, estradiol have been shown the increase assembly, while AMH, progesterone and TNFa decrease assembly. A 24 hour culture period was used to minimize the impact of differences in follicle numbers (morphological impact), due to the required 2 days of culture to observe detectable morphological differences. After culture the ovaries receiving the same treatment from one culture well were pooled and RNA isolated. There were three different experiments involving different ovaries for each of the seven treatment compounds, and seven different experiments with different ovaries for the controls, for a total of 28 samples (see Methods). Gene expression in the RNA samples was evaluated using Affymetrix© Rat Gene 1.0 ST microarrays. Array data pre-processing and evaluation determined that one array (P4-treated) was abnormal and an outlier, so that array was eliminated from further analysis (Additional file 1: Figure S1).

The sets of differentially expressed genes, defined as signature lists, in the treated ovary groups compared to

controls were identified using criteria as described in Methods. A total of 1081 genes were differentially expressed in ovaries treated with these known regulators of follicle assembly, suggesting these genes are involved in the ovarian primordial follicle assembly process. Whether the specific genes have an increase or decrease in expression is shown in Additional file 2: Table S1. Each treatment resulted in 50 to 303 genes being differentially expressed compared to controls. Interestingly, there were relatively few (5-10%) differentially expressed genes in common between the different treatments (Figure 2) as indicated for specific genes in Additional file 2: Table S1. Only one gene, the growth factor staniocalcin 1, was differentially expressed in as many as four different treatments, and no other genes were differentially expressed in more than three treatments (Additional file 2: Table S1). These genes in these signature lists were categorized into gene functional categories. The metabolism and transport, signaling, and receptors and binding proteins were predominant categories for all treatments (Figure 3 and Additional file 1: Table S1).

Primordial follicle assembly pathway analysis

The complete list of 1081 differentially expressed genes from the signature lists were correlated to curated cellular pathway and process gene lists from the KEGG database (see Methods) to identify physiological processes and pathways that may be regulated during follicle assembly. Pathways that were statistically over-represented within the differentially expressed gene lists included focal adhesion, chemokine signaling, cytochrome P450 metabolism, glutathione metabolism, ECM-receptor interaction and ribosomal components (Additional file 3: Table S2). There was a high degree of overlap of affected pathways between different treatments (Figure 2). The statistical analysis used both a hypergeometric probability calculation and Fishers exact test calculation to identify statistical likelihood of over-representation of differentially expressed genes in pathways (Additional file 3: Table S2). This analysis reduces the variable of data set size and potential for artifact generation by identifying those pathways with over-representation having differentially expressed genes from several treatments. As can be seen, not all pathways had statistical significance while others consistently did (Additional file 4: Figure S2). From 44% to 87% of affected pathways were common between treatments. According to Fisher's Exact test the probability that our list of differentially expressed genes randomly overlaps with the pathways is negligible (~1/2000 chance), particularly since we had many genes falling in more than one pathway. As can be seen in Additional file 3: Table S2 and Figure 4, most affected pathways contained differentially expressed genes from several different treatments. As shown in the focal adhesion pathway, five of the factors affected genes in the same pathway (Figure 4). Therefore, each of these extracellular signaling factors that were used as treatments affected similar pathways via different genes. There were isolated exceptions to this trend. For example, all of the genes present in the ribosome process pathway were induced by activin A treatment, and four of five genes in the GABAergic synapse pathway were induced by FGF2 (Additional file 3: Table S2).

Primordial follicle assembly bionetwork analysis

Gene expression level data from the entire set of 1081 differentially expressed genes was subjected to a cluster analysis to identify groups (i.e. modules) of genes whose expression is regulated in a coordinated and interconnected manner (see Methods). The cluster analysis scores each gene according to how well across different

		AMH	CTGF	E2	FGF2	Activin	P4	TNFa
	# genes	#PW 73	9	79	115	83	85	63
AMH	158		4	45	63	43	41	29
CTGF	50	2		7	8	7	7	5
E2	120	10	0		69	49	49	38
FGF2	303	13	4	9		71	70	50
ActivinA	287	11	1	4	14		52	40
P4	167	5	3	8	11	14		43
TNFa	116	6	4	4	7	9	3	

Number (#) of pathways overlapped

Number (#) of genes overlapped

Figure 2 Number of genes and physiological pathways overlapped between treatment group (signature) lists. Total number of differentially expressed genes for each treatment is shown in dark yellow column, while numbers of genes in common between each pair of treatment groups are in light yellow columns. Total number of KEGG pathways affected by each treatment is shown in dark green row; numbers of KEGG pathways in common for each pair of treatment groups are shown in light green rows. A KEGG pathway is considered affected if ≥ 3 differentially expressed genes are present in the pathway.

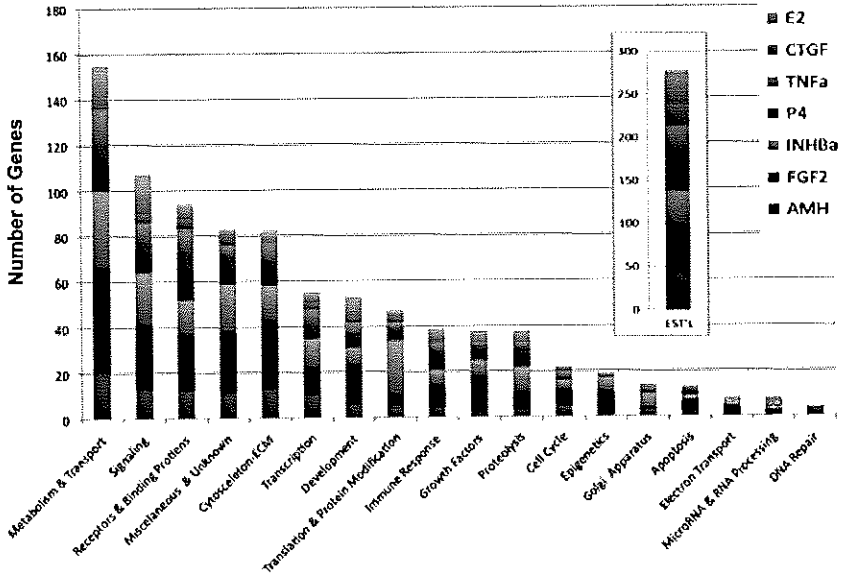

Figure 3 Numbers of genes with mRNA expression levels significantly different between Control and treated ovaries after two days of culture. Genes are placed into functional categories.

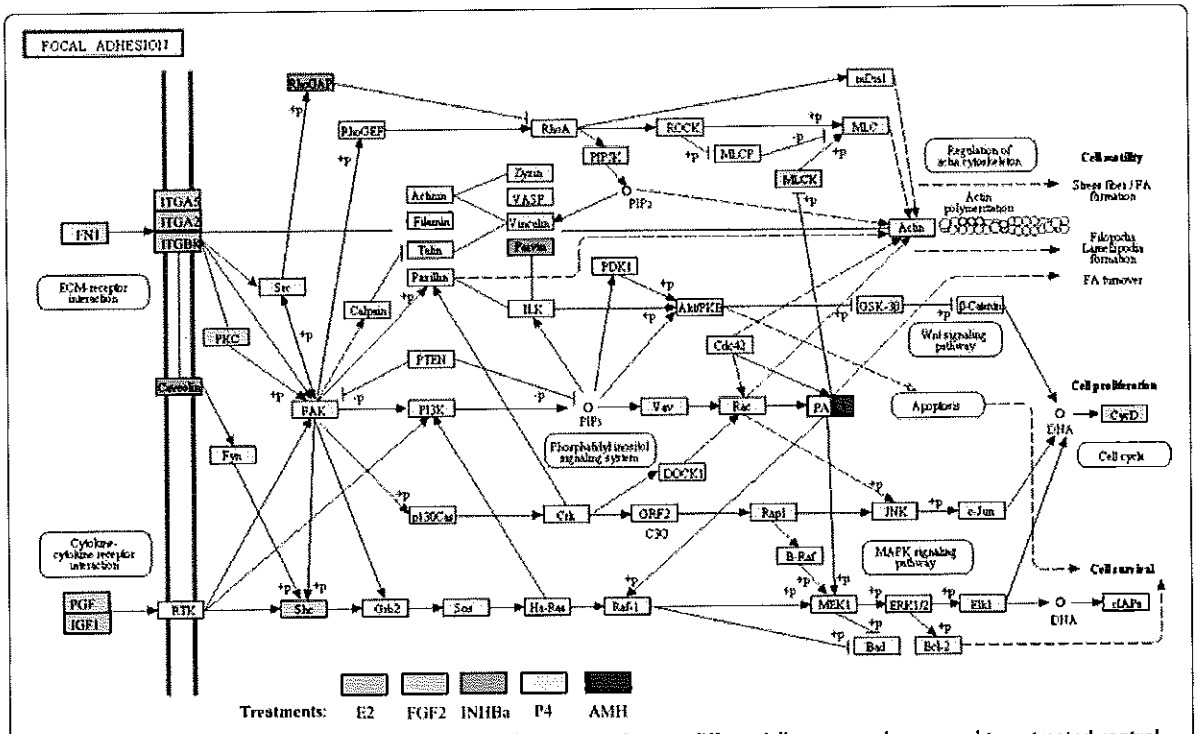

Figure 4 Focal adhesion signaling pathway highlighting those genes that are differentially expressed compared to untreated control ovaries and identifying by color the treatment group(s) from which the differentially expressed genes came. Adapted from KEGG pathway rno04510, Kanehisa Laboratories, Kyoto University, Japan.

treatments its changes in gene expression are correlated with the changes in expression of every other gene. High connectivity scores indicate that expression of a particular gene changes in concert with that of many other genes. In addition, the cluster expression analysis identifies gene modules in which the member genes have similar changes in expression in response to the various experimental treatments. Such gene modules are often associated with specific biological processes [32]. To identify gene modules, a topological overlap matrix [37] was generated that reflected connectivity scores and sorted genes based on an agglomerative hierarchical clustering algorithm (see Methods). The topological overlap matrix map with gene modules color-coded for the nine modules identified is shown in Figure 5. The module to which each gene belongs can be found in Additional file 2: Table S1. The nine modules contained collectively 851 genes with the remaining 230 genes (colored as grey) not falling into any module. The list of differentially expressed genes in each module was correlated to signaling pathway and cellular process databases to determine if specific physiological processes were associated with particular modules (see Methods). Those pathways and processes statistically over-represented for each module are shown in Table 1.

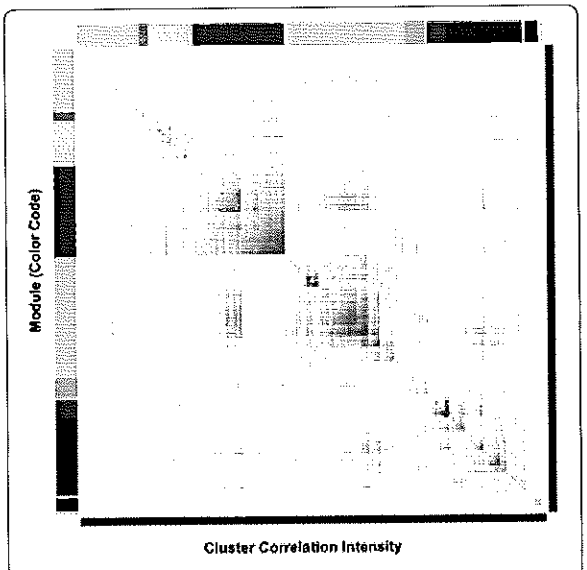

Figure 5 Gene cluster analysis and corresponding gene modules. A topological overlap matrix of the gene co-expression network consisting of the 1081 genes regulated by the various ovary treatments is shown. Genes in the rows and columns are sorted by an agglomerative hierarchical clustering algorithm (see Methods). The different shades of color signify the strength of the connections between the nodes (from white signifying not significantly correlated to red signifying highly significantly correlated). The hierarchical clustering and the topological overlap matrix indicate highly interconnected subsets of genes (modules). Modules identified are colored along both column and row and are boxed.

Table 1 Gene category overlap with modules

Module	Gene category	Gene number module overlap*	Over representation fisher P-value†
Turquoise	Ribosome	10	7.52E-08
Turquoise	cytosolic ribosome	7	2.40E-06
Turquoise	Neural tube closure	4	0.00041
Turquoise	Negative regulation of binding	5	0.00045
Turquoise	Primary neural tube formation	4	0.00056
Turquoise	Protein biosynthesis	15	0.00071
Turquoise	Glutathione metabolism	5	0.0011
Blue	Response to oxidative stress	12	1.30E-06
Blue	Regulation of anatomical structure morphogenesis	13	2.20E-06
Blue	Mesoderm development	18	1.90E-05
Blue	Angiogenesis	6	2.20E-05
Blue	Response to carbohydrate stimulus	6	3.60E-05
Blue	Regulation of axonogenesis	6	5.00E-05
Blue	Membrane raft	9	7.80E-05
Blue	negative chemotaxis	3	1.00E-04
Blue	Axon guidance	6	3.70E-03
Blue	Glutathione metabolism	3	3.10E-02
Blue	Focal adhesion	6	3.20E-02
Blue	Fc gamma R-mediated phagocytosis	4	3.60E-02
Blue	MAPK signaling pathway	6	8.50E-02
Brown	Germ cell nucleus	3	7.00E-04
Brown	Male meiosis	3	0.0015
Brown	Neurite regeneration	3	0.0031
Brown	Condensed nuclear chromosome	3	0.0041
Brown	Other oncogenesis	3	0.0074
Brown	Cell cycle	4	0.026
Brown	Olfactory transduction	12	0.065
Yellow	Hematopoietic cell lineage	3	0.0027
Yellow	Positive regulation of apoptosis	5	0.009
Yellow	Coenzyme and prosthetic group metabolism	3	0.015
yellow	Mitochondrial lumen	3	0.018
Green	proteinaceous extracellular matrix	3	0.0072
Black	Extracellular matrix	4	0.00015
Black	extracellular region	7	0.00042
Black	Response to stress	8	0.002
Black	Cell communication	6	0.0029
Black	Negative regulation of apoptosis	4	0.0029
Pink	Apical plasma membrane	3	0.0011
Pink	Protein glycosylation	3	0.0018
Magenta	Calcium mediated signaling	2	0.0066

*Gene Number Module Overlap is the number of genes from that module that are in common with those in the listed physiological process or pathway (see Methods).
†Fisher's Exact test was used to calculate a p-value reflecting the probability that the specified module and pathway/process would have listed number of overlapped genes.

The turquoise module predominately contains genes coding for ribosomal components and genes involved in protein and glutathione metabolism. The blue module contains genes involved in processes related to tissue morphogenesis. The red module has genes involved with germ cells and meiosis. Some physiological processes, such as apoptosis and extracellular matrix function, were over-represented in several modules. However, in general the genes of different modules were over-represented in different cellular pathways and processes (Table 1).

Genes whose expression altered in response to treatments were correlated with the genes assigned to each module to determine if specific modules were heavily influenced by particular regulatory factors (Figure 6). In most cases, differentially expressed genes from each treatment group could be found in each of the modules. However, some modules had strikingly high numbers of genes in common with specific treatments. For example, among the 240 genes of the turquoise module and the 287 genes of the activin A treatment group, 184 genes were in common. Interestingly, these included 10 of the 11 differentially expressed genes that populated the ribosomal component process. In addition, among the 209 genes of the blue module and the 303 genes of the FGF2 treatment group, 169 genes were in common. Similarly, there were 58 genes in common between the brown module and the P4 treatment group, and these included 8 of the 19 genes that populated the olfactory transduction pathway (Figure 6).

Primordial follicle assembly gene network analysis

In order to determine what functional relationships and gene networks exist between the differentially expressed genes identified, the complete list of 1081 genes was subjected to an automated unbiased analysis of published literature using Pathway Studio software (Elsevier Inc. Rockville, MD USA), (see Methods). A total of 326 genes were found to form a gene network that linked neighboring genes together with regulatory or binding relationships. While this network was too large and complex for easy visual interpretation (Additional file 4: Figure S2), inferences about the genes involved can be obtained. Genes with the greatest number of putative regulatory connections to neighbors in the network were considered to be important in controlling the follicle assembly process, either as upstream regulators of the assembly network or as downstream targets of the network. The genes with the most connections to neighbors in the network of 326 genes were *Il1b* (interleukin 1 beta; 144 connections), *Fn1* (fibronectin 1; 100 connections) and *Igf1* (insulin-like growth factor 1; 99 connections) (Additional file 4: Figure S2).

Each module of coordinately regulated genes was subjected to gene network analysis to determine which genes within a module formed a gene network as shown in Figure 7. A network for the turquoise module identified *Fn1*, *Stat1* (signal transducer and activator of transcription 1) and *Vcam* (vascular cell adhesion molecule 1) as having many connections, suggesting they may play a role in controlling the physiological processes mediated by the turquoise module. For the blue module (Additional file 5: Figure S3A) *Cav1* (caveolin), *Anxa2* (annexin A2), *F3* (coagulation factor 3, thromboplastin) and *Ccnd1* (cyclin D1) have the most neighbor connections. *F3* and *Ccnd1* are seen to be primarily the recipients of the regulatory relationships suggesting their regulation may be an important output of the blue module network. Although relatively small, the black module also formed a network of connected genes (Additional file 5: Figure S3B). The growth factors *Igf1* and *Il1b* have the most neighbor connections. The remaining modules did not form significant networks of genes related to each other, even though many of these modules had more genes than were present in the black module.

Each treatment signature list of differentially expressed genes was analyzed to determine which genes formed a gene network of regulatory relationships. For the genes of the E2 treatment group, *Igf1* is seen to have many

		turquoise	blue	brown	yellow	green	red	black	pink	magenta
	# genes	240	209	176	65	45	43	27	26	20
AMH	158	14	7	28	19	25	0	0	7	3
CTGF	50	0	4	8	1	1	5	2	3	4
E2	120	1	6	3	20	8	14	15	9	4
FGF2	303	4	169	44	28	9	1	0	2	4
INHBa	287	184	24	26	5	2	15	0	14	1
P4	167	16	5	58	11	0	8	6	7	4
TNFa	116	36	10	19	6	4	2	4	0	6

Figure 6 Numbers of genes found to be in common when comparing genes differentially expressed in various ovary culture treatment groups (left column) with differentially expressed genes assigned to co-expression modules (top row). Numbers in bold type indicate a high number of genes in common with a treatment compared to others for that module (column). Underlined numbers indicate a high number of genes in common with a module compared to others for that treatment (row).

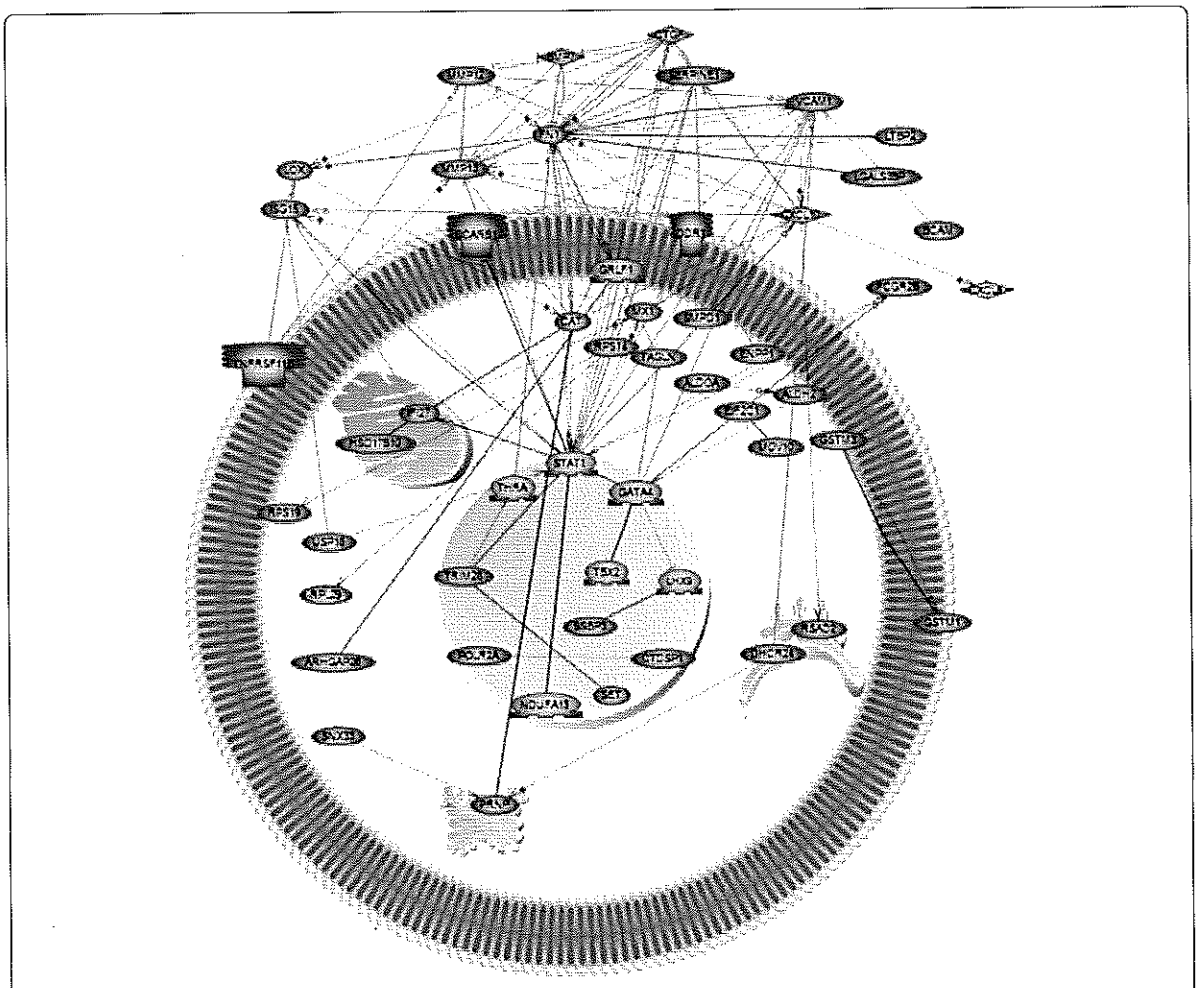

Figure 7 Gene network of known relationships among those differentially expressed genes assigned to the turquoise module. Node shapes code: oval – protein; diamond – ligand; irregular polygon – phosphatase; circle/oval on tripod platform – transcription factor; ice cream cone – receptor. Grey arrows represent regulation, lilac – expression, green – promoter binding, olive – protein modification, purple - binding. Plasma membrane, cell nucleus, mitochndria, golgi apparatus and endoplasmic reticulum are indicated for gene expression localization.

neighbor connections (Additional file 6: Figure S4A). For the FGF2 treatment network *Vcam*, *Vim* (vimentin) and *Tgfb2* (transforming growth factor beta 2) have many neighbor connections, while *Ccnd1* and *F3* appear to be outputs of the network (Additional file 6: Figure S4B). For the activin A treatment group, the transcription factor *Stat1* and the growth factor *Cxcl10* have many connections, while *Fn1* appears to be an output (Additional file 6: Figure S4C).

In order to determine those genes whose actions are likely to be the most important in regulating the control of primordial follicle assembly, a combined approach was taken that determined the gene network associated with the most highly interconnected genes. For each module, the top 10% of genes with the highest connectivity index (k.in.) (i.e., those that are the most tightly co-regulated within their module) were selected. These genes were then screened for whether they were present in the large network of 326 genes with known regulatory connections derived from the entire list of 1081 differentially expressed genes (Additional file 4: Figure S2). Those genes from the top 10% of each module (tightly co-expressed) that also had the most neighbor connections (regulatory relationships) are presented in Table 2. These included the transcriptions factors *Ppargc1a* and *Gata4*, the growth factor *Tgfb2*, the transferrin receptor (*Tfrc*), *Mdm2* and *Prkcb* (protein kinase C beta). These genes formed a regulatory network among themselves, and were associated with specific pathways and cellular processes. As can be seen in Figure 8, these genes have been previously shown to influence the processes of apoptosis, vascularization, contraction, cell migration, proliferation and differentiation.

Table 2 Gene connectivity ranking information

Name / symbol gene	Gene description	Local connectivity *
TNFRSF1A	Tumor necrosis factor receptor superfamily, member 1A	37
TGFB2	Transforming growth factor, beta 2	36
MDM2	Mdm2 p53 binding protein homolog (mouse)	27
GATA4	GATA binding protein 4	27
PPARGC1A	Peroxisome proliferator-activated receptor gamma, coactivator 1 alpha	26
PRKCB	Protein kinase C, beta	25
TFRC	Transferrin receptor (p90, CD71)	23
ANXA5	Annexin A5	20
ANXA2	Annexin A2	20
SDC4	Syndecan 4	16
LRP2	Low density lipoprotein-related protein 2	16
GRLF1	Glucocorticoid receptor DNA binding factor 1	15
GSTP1	Glutathione S-transferase pi 1	14
HSD11B1	Hydroxysteroid (11-beta) dehydrogenase 1	13
UCP2	Uncoupling protein 2 (mitochondrial, proton carrier)	12
THRA	Thyroid hormone receptor, alpha (erythroblastic leukemia viral (v-erb-a) oncogene homolog, avian)	10
ANPEP	Alanyl (membrane) aminopeptidase	10
IL1R1	Interleukin 1 receptor, type I	9
EPHA2	EPH receptor A2	9
CTSK	Cathepsin K	8
SMPD1	Sphingomyelin phosphodiesterase 1, acid lysosomal	8

*Local connectivity is the number of regulatory connections which that gene has with other genes, identified in published literature, within the gene network of 326 genes derived from the complete set of 1081 differentially expressed genes (see Additional file 4: Figure S2).

Other groups of differentially expressed genes examined were the growth factor, hormone and receptor families. These genes provide novel regulatory factors to be investigated in future studies in their role in controlling ovarian primordial follicle assembly. A subset of the entire set of 1081 differentially expressed genes, comprised of growth factors, hormones and their receptors was evaluated for their ability to form a sub-network of regulatory connections. A sub-network of 52 genes was identified showing the regulatory connections between these growth factors and receptors (Figure 9).

Primordial follicle assembly signaling pathway modulation and validation

As described above, specific physiological processes and pathways are over-represented in the lists of differentially expressed genes identified in these studies (Table 1 and Additional file 3: Table S2), and so are predicted to be important in regulating follicle assembly. The MAPK signaling, focal adhesion and chemokine signaling pathways are over-represented in particular gene modules or in the global set of all 1081 differentially expressed genes. ERK1/2 (MAPK1) is a kinase that plays a prominent role in these pathways (Figure 4). ERK1/2 activity is inhibited by Dusp6 (dual specificity phosphatase 6; MKP-3) [38]. In order to test if these physiological pathways are in fact important to the assembly process, ovaries from 0-day old rats were treated in vitro for 2 days with the inhibitor of DUSP6: BCI ((E)-2-benzylidene-3-(cyclohexylamino)-2,3-dihydro-1H-inden-1-one [39,40]. Dusp6 inhibition resulted in a significant increase in the proportion of assembled follicles at the end of ovary culture with no effect on oocyte numbers (Figure 10). Therefore, alteration of ERK1/2 signaling in physiological pathways predicted to be important for follicle assembly resulted in a change in the rate of assembly of primordial follicles.

Primordial follicle assembly regulated gene correlation with ovarian disease

The final analysis identified those differentially expressed genes associated with ovarian disease. The genes within the differentially expressed gene lists (Additional file 2: Table S1) that have previously been shown to be linked in the literature with primary ovarian insufficiency (POI) and polycystic ovarian syndrome (PCOS) were identified (Figure 11). Seventeen genes associated with POI and PCOS were identified and two genes, Igf1 and Tgfbr3 were common to both POI and PCOS.

Discussion

A systems biology approach was used to elucidate how regulatory factors alter gene expression to influence ovarian primordial follicle assembly. Neonatal rat ovaries were treated with different growth factors or hormones and changes in gene expression at the transcriptome level were assayed and analyzed. The strength of a systems biology approach is that it is unbiased and examines the genome wide complexity of gene expression to elucidate regulatory networks that control developmental processes. These genes are identified regardless of whether they have known functions consistent with the follicle assembly process or whether they have known functions at all. The unbiased systems analysis allows the complexity of the biology to be considered to elucidate the developmental process. Future investigations can now target identified genes to further characterize their specific actions in the networks regulating follicle assembly.

Primordial follicle assembly growth factors and hormones investigated

Ovaries were treated with several different growth factors or hormones that affect the assembly process to get a more complete view of the gene expression changes

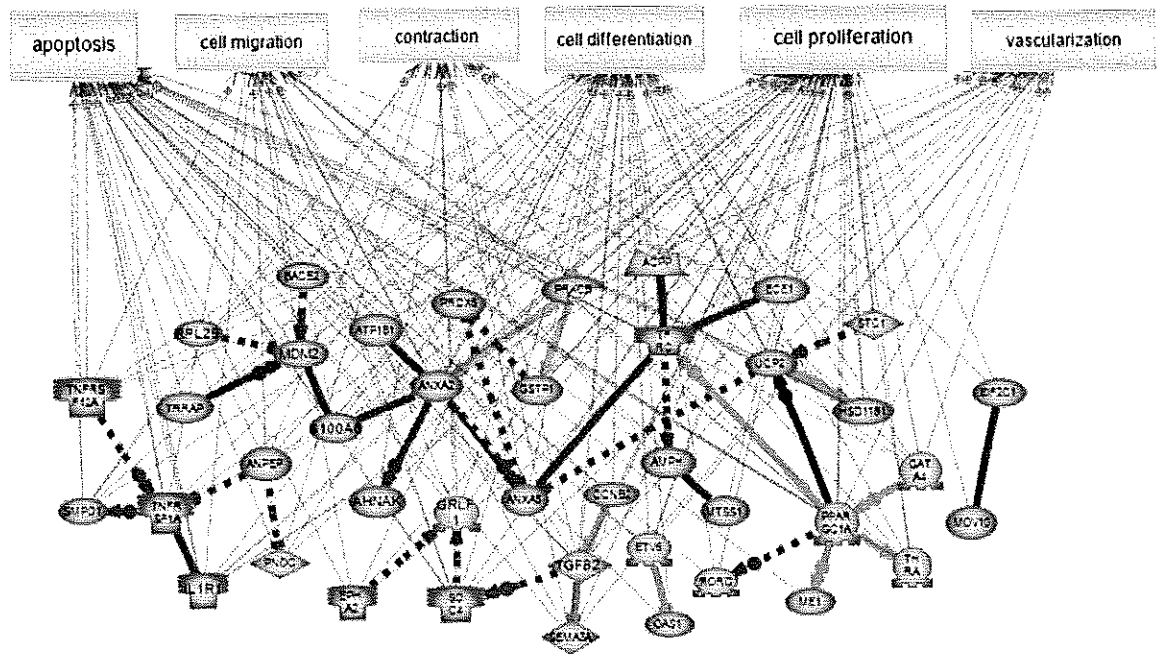

Figure 8 Gene network of known relationships and associations with specific cell processes for those differentially expressed genes from the top 10% of each module that also had the most neighbor connections (see Table 2 for list). Node shapes code: oval and circle – protein; diamond – ligand; irregular polygon – phosphatase; circle/oval on tripod platform – transcription factor; ice cream cone – receptor. Grey rectangles represent cell processes; arrows with plus sign show positive regulation/activation, arrows with minus sign – negative regulation/inhibition. Grey arrows represent regulation, lilac – expression, green – promoter binding, olive – protein modification.

accompanying primordial follicle assembly. A number of growth factors and hormones previously shown to influence primordial follicle assembly were selected including: AMH [1], CTGF [16], estradiol [17-21], progesterone [18,22,23], activin A [21], and TNFa [23,24]. The combined actions of factors on assembly has not been thoroughly investigated, but studies on follicle transition have shown combined stimulatory or inhibitory factors does not provide an additional response different from the individual factors [3]. All of the growth factors and corresponding receptors, as well as hormone receptors, associated with the factors used have been shown to be expressed in the ovary during primordial follicle assembly. For example, AMH is expressed in the stromal/interstitial cells of the 0 day ovary followed by expression later in development by the secondary and developing follicles [1]. Interestingly, some of the factors promote follicle assembly (CTGF, activin A, estradiol), while others (AMH, progesterone, TNFa, FGF2) inhibit follicle assembly. Therefore, both positive and negative regulation of follicle assembly is considered when characterizing the regulatory gene networks. Comparison of the stimulatory versus inhibitory factors did not show any major differences in regards to regulated genes or gene networks.

In addition to these known regulatory agents, a novel factor was examined and included in the analysis. Previous research suggested FGF2 may be a regulator of follicle assembly. A receptor for FGF2, FGFR2B, has previously been shown to be differentially expressed in 0-day old rat ovaries with oocyte nests compared to 4-day old ovaries that had completed assembly [30]. Treatment of neonatal rat ovaries with the known inhibitor of follicle assembly AMH resulted in differential expression of *Nudt6* (*nudix 6*) [41], which acts as an antisense inhibitor of *Fgf2* expression [42]. In order to determine if FGF2 would be included as a treatment in the current investigations, organ culture experiments were performed to empirically test the effects of FGF2 on follicle assembly. It was found that FGF2 acts as an inhibitor of follicle assembly (Figure 1). The magnitude of the inhibitory actions can be increased with an extended culture duration (four days), but then alterations in follicle number and ovarian morphology become confounders influencing data interpretation. A short 2-day culture was used to reduce these confounder effects. The optimal dose for the analysis of in vitro follicle assembly analysis was lower than that for the short-term 24-hour culture gene expression analysis, in part due to the negative feedback of the extended culture duration.

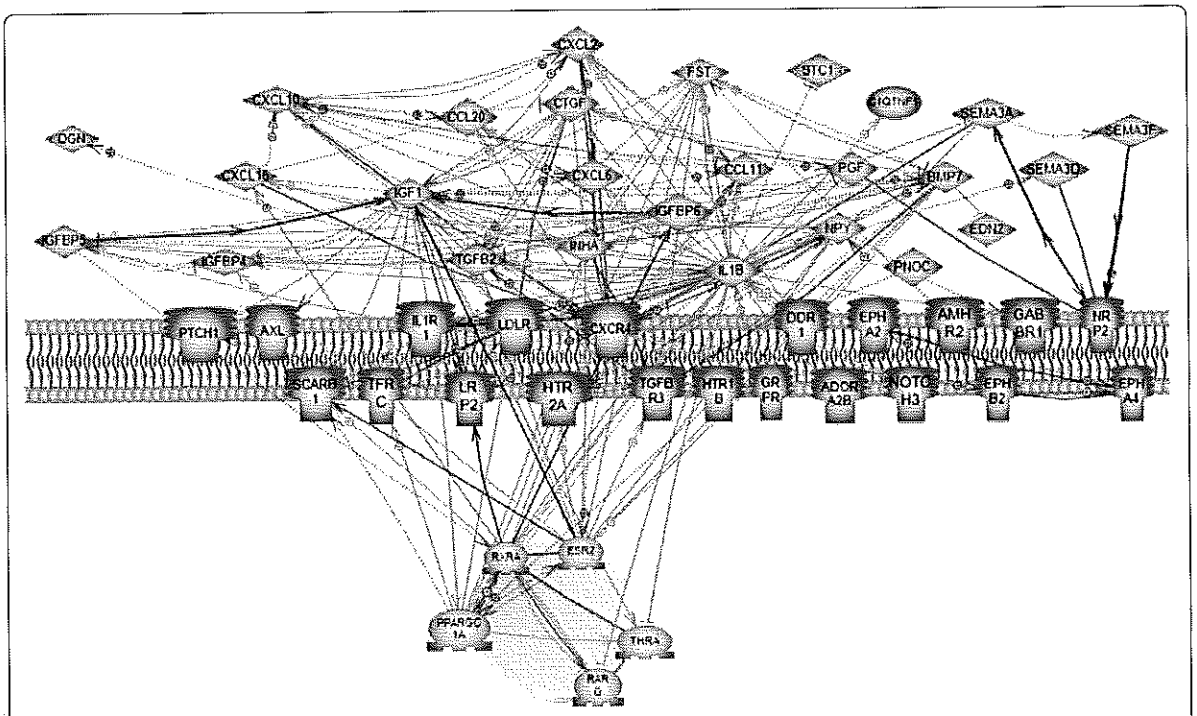

Figure 9 Gene network of known relationships among those differentially expressed genes that were extracellular signaling factors, growth factors, growth factor binding proteins, growth factor receptors or hormone receptors (see Additional file 2: Table S1: categories 'Growth Factors' and 'Receptors & Binding Proteins'). Node shapes code: oval – protein; diamond – ligand; circle/oval on tripod platform – transcription factor/hormone receptor; ice cream cone – receptor. Grey arrows represent regulation, lilac – expression, green – promoter binding, olive – protein modification, purple - binding. Plasma membrane and cell nucleus are indicated for gene expression localization.

The FGF2 was found to alter the expression of 303 genes with approximately 10% of these genes in common with the differentially expressed gene sets of the other features. Although the differentially expressed genes influenced by FGF were unique, 50–70 different pathways were affected and in common with other factors investigated, (Figure 2). Therefore FGF2 was included as one of the seven treatments used to perturb the neonatal rat ovary experimental system.

Primordial follicle assembly differentially expressed genes

One thousand and eight-one genes were found to be differentially expressed compared to controls when results were combined across the different treatment groups. These genes were predominantly from the functional categories of metabolism and transport, signaling proteins and receptors. The genes differentially expressed in response to each growth factor or hormone treatment were compared across the different treatments. Interestingly, only a small proportion of differentially expressed genes (<10%) were found to be common between any two treatments (Figure 2). This is somewhat surprising in light of the fact that all the treatments affect the same process of follicle assembly. However, this same finding was observed in a systems biology investigation of genes regulating ovarian primordial to primary follicle transition [31]. In that study different treatments, all known to regulate the transition of arrested primordial follicles to developing primary follicles, were found to have few differentially expressed genes in common. Although neither this previous study nor the current study found a high degree of overlap between the specific treatment signature gene lists, there was a high degree of overlap among the specific signaling pathways and cellular processes impacted by the differentially expressed genes of each treatment (Figures 2 and 3). This indicates that all the treatments affect similar cellular pathways and processes as follicle assembly occurs (44% to 87%), but that each treatment affects different genes in those pathways. As shown in Additional file 2: Table S2, some pathways had a highly statistically significant over-representation of differentially expressed genes while others did not, suggesting the analysis was not unduly influenced by data set size or simply an artifact of the analysis. An example of this is shown in Figure 4 where five of the different factors affected different genes in the focal adhesion pathway. Similar observations have shown this phenomena in other biological systems [43]. Multiple

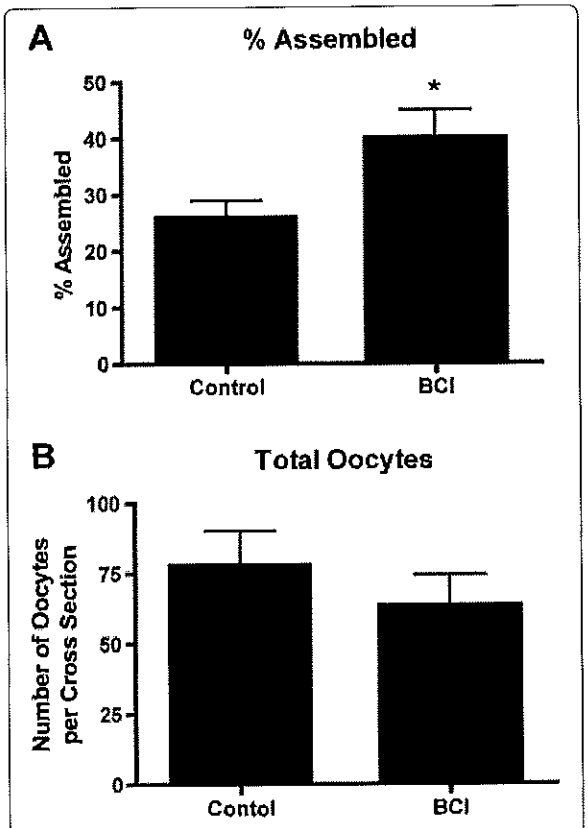

Figure 10 Results of experiments in which 0-day old ovaries were cultured two days with or without BCI (an inhibitor of DUSP6 that results in increased ERK12/MAPK1 activity). A) Proportion of oocytes still assembled into follicles. **B)** Total number of oocytes per ovarian cross-section after culture. * = $p<0.05$ compared to untreated vehicle-treated Control by Student's *t*-test. Mean ± SEM from three different experiments is presented.

input points into these cellular pathways and processes may allow for more precise regulation and for a more robust regulatory network in the face of disruptions.

A cluster analysis of coordinated gene expression grouped the differentially expressed genes into gene modules containing genes whose expression responded in concert to the different growth factor and hormone treatments. This approach of generating a weighted gene network and then clustering genes making use of a topological overlap matrix has been used extensively for uncovering biologically meaningful gene modules [31,32,44-46]. The gene modules identified in the current study were, on the whole, each enriched with genes associated with differing cellular pathways and processes (Table 1). For example, the turquoise module contains genes coding for ribosomal components, while the blue module contains genes involved in processes related to tissue morphogenesis, and the red module has genes associated with meiosis. This suggests that these modules of genes are each responsible for controlling distinct functions necessary for primordial follicle assembly. In contrast, most modules were enriched for genes involved in apoptosis and extracellular matrix function, perhaps underscoring the importance of these processes to follicle assembly. Oocyte apoptosis is known to have a vital role in the assembly of primordial follicles [3,6,12,13]. Identification and examination of the gene modules helps elucidate the molecular control of follicle assembly.

When genes whose expression changed in response to treatments were cross-matched with the genes assigned to each module, it was found that in most cases differentially expressed genes from each treatment group could be found in all the gene modules (Figure 6). This is consistent with the idea that all the treatments affect the same cellular processes, but that each treatment affects different genes within those pathways. However, it should be noted that in some cases a particular treatment shared a disproportionate number of genes within a specific module. For example, the activin A treatment resulted in differential expression of 287 genes, of which 184 were in common with the 240 genes assigned to the turquoise module, and these included almost all the genes that coded for ribosomal components. Therefore, in some cases signaling from a particular growth factor will induce a suite of genes that may be targeted toward specific physiological tasks.

Primordial follicle assembly gene networks

In order to identify functional relations among differentially expressed genes, an analysis of published literature was used to detect connections among listed genes to form gene networks of putative regulatory relationships. Examination of these networks can yield inferences about how genes interact to regulate primordial follicle assembly, and can identify potentially important control points within these regulatory networks. When the entire list of genes found to be differentially expressed during follicle assembly was analyzed in this way it was found that the genes *Il1b* (interleukin 1 beta), *Fn1* (fibronectin 1) and *Igf1* (insulin-like growth factor 1) had the most regulatory connections to neighbors. These genes are considered important in controlling the follicle assembly process as either regulators of the assembly network or as downstream effectors of the network. However, it should be kept in mind that genes that have been extensively studied are more likely to have relationships with other genes in the published literature, and that un-studied genes may in fact be important. Nonetheless, gene networks of regulatory connections provide a good starting point toward understanding the control of processes such as follicle assembly.

Since the genes of each module may act in concert to accomplish distinct cellular processes during follicle

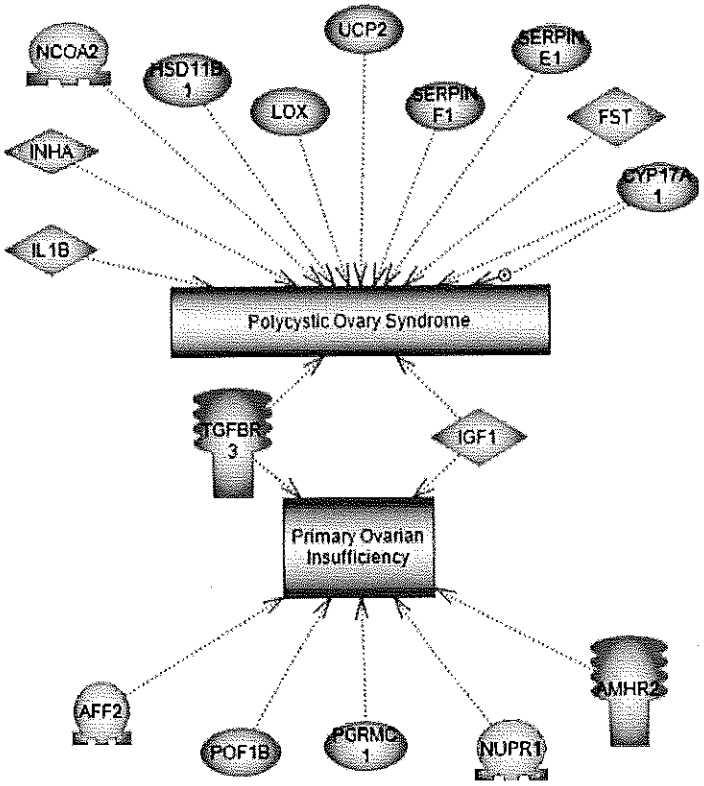

Figure 11 Genes differentially expressed during follicle assembly that are also known to be associated with the adult-onset diseases primary ovarian insufficiency and polycystic ovarian syndrome. Node shapes code: oval – protein; diamond – ligand; circle/oval on tripod platform – transcription factor; ice cream cone – receptor.

assembly, each module was analyzed separately for gene networks of putative regulatory relationships. The genes of the turquoise, blue and black modules each formed distinct gene networks (Figure 7 and Additional file 5: Figure S3), implicating the genes *Fn1*, *Stat1* (signal transducer and activator of transcription 1), *Vcam* (vascular cell adhesion molecule 1), *Cav1* (caveolin), *Anxa2* (annexin A2), *F3* (coagulation factor 3), *Ccnd1* (cyclin D1), *Igf1* and *Il1b* as being important within their respective modules. Interestingly, genes of the brown, yellow, green, red, pink and magenta modules did not contain gene networks of known regnlatory relationships, even though some of these modules contained many more genes than the black module, which did have such a network. This suggests that the genes within each of these modules may have as yet un-characterized regulatory relationships with each other. Furthermore, the genes of the red module were not found to be over-represented in association with any particular known cellular pathways or processes, and many of the red module genes are poorly characterized expressed sequence tags (ESTs). However, genes of the red module had relatively high connectivity scores (k. in.), indicating that this group of genes was quite tightly co-regulated (Figure 5). Observations suggest that groups of poorly characterized genes are likely playing important roles in primordial follicle assembly. Further research is needed to uncover the functions of these genes and their roles in developmental processes such as follicle assembly.

The most highly interconnected (k. in.) genes from each module were compared to databases of genes present in specific cellular pathways and processes. This group of highly interconnected genes was found to be over-represented in the processes of apoptosis, cell migration, cell differentiation and cell proliferation (Figure 8). This is consistent with the activities that occur during follicle assembly and supports the idea that these highly interconnected genes contribute to follicle assembly. Genes were also over-represented in the process of vascularization which is not known to be a part of follicle assembly. Investigations into the role vascularization plays in follicle assembly are suggested in future studies.

Analysis of a specific gene sub-network of differentially expressed genes in the growth factor, hormone and

receptor functional gene categories identified a large number of such regulatory signaling factors that appear to regulate ovarian primordial follicle assembly (Figure 9). Many of these growth factors and receptors in this sub-network have multiple connections with each other, indicating that these genes are known to regulate other signaling factors within the sub-network. The growth factors IL1B, IGF1 and CXCL10, and the receptor CXCR4 have the most connections to other genes, so these are candidates in the regulation of follicle assembly to investigate in future studies. The CXCR4 and IGF1 genes have been shown to be involved in primordial follicle transition [47,48], but not previously been associated with assembly.

Primordial follicle assembly modulation and pathway validation

Analyses of the differentially expressed genes of the current study implicate specific physiological pathways and gene networks as being important to the follicle assembly process. In order to test the validity of some of these predictions, organ culture experiments were preformed in which neonatal rat ovaries were treated with BCI. BCI has the effect of increasing ERK1/2 (MAPK1) activity *via* inhibition of DUSP6 [38,39]. ERK1/2 plays a prominent role in the MAPK signaling, focal adhesion and chemokine signaling pathways, all of which were implicated as important to follicle assembly (Figure 4, Additional file 3: Table S2, Table 1). BCI-treated ovaries with increased ERK1/2 activity were shown to have an increase in assembled follicles (Figure 10), supporting the predicted role of these physiological pathways in primordial follicle assembly. This experiment helps validate the systems biology approach used in the current study.

Primordial follicle assembly and ovarian disease

Since follicle assembly provides each female mammal with the pool of primordial follicles from which their ovulated eggs are derived, abnormal follicle assembly could result in defective primordial follicles that may lead to a reduced follicle pool size. This in turn can lead to infertility and the cessation of reproduction early in life, as is seen in women with primary ovarian insufficiency (POI). Women with POI deplete their pool of primordial follicles prior to age 40 and undergo early menopause [14,15]. Forty-nine genes that have been implicated in POI in humans have been compiled and are listed with the Ovarian Kaleidoscope Database (http://ovary.stanford.edu/). Seven of these genes were found to be in common with the 1081 differentially expressed genes found in the current study to be associated with follicle assembly (significant at $p<0.05$ by Fisher's Exact test). These genes were *Tgfbr3* (transforming growth factor beta receptor type 3), *Amhr2* (anti-Müllerian hormone receptor type 2), *Pgrmc1* (progesterone receptor membrane component 1), *Nupr1* (nuclear protein transcriptional regulator 1), *Pof1b* (premature ovarian failure 1b), IGF1 and AFF2 (AF4/FMR2 family, member 20). AMH, progesterone and *Pgrmc1* are known to play roles in follicle assembly [1,17,18,22,23]. It is notable that *Pof1b*, the gene named for its association with premature ovarian failure (i.e. POI), is linked to follicle assembly in the current study. These observations suggest that some cases of POI may have abnormal follicle assembly as an underlying cause. In addition to specific gene links with POI, a number of links were also made to polycystic ovarian syndrome (PCOS) (Figure *11*). PCOS is the most predominant female reproductive disease affecting 7-18% of the female population [49]. A number of the differentially expressed genes identified in the current study correlated to previously known genes linked to PCOS (Figure *11*). Observations suggest abnormal ovarian primordial follicle assembly may be a component of POI and PCOS later in life as some of the genes involved are in common. Future analysis of these genes and the gene networks identified is anticipated to help elucidate the molecular etiology of POI and PCOS, as well as provide novel therapeutic targets.

Conclusions

In summary, a systems biology experimental approach can provide an unbiased global view of the relationships important to a particular developmental process. For the primordial follicle assembly process the systems approach evaluated genes that were differentially expressed in response to growth factor and hormone treatments. It was found that different treatments all affected similar cellular pathways and processes, but that each treatment affected expression of different genes within those pathways. Cluster analyses identified modules of coordinately regulated genes and the different modules appear to accomplish distinct cellular functions during follicle assembly. The regulatory gene networks identified provide predictions about important regulatory genes, signaling pathways and cellular processes involved in ovarian primordial follicle assembly. An organ culture experiment in which ovaries were treated to increase ERK1/2 activity confirmed some of the predicted physiological pathways were in fact important in follicle assembly regulation. The regulatory genes and gene networks identified as controlling primordial follicle assembly, when disrupted or altered, were suggested to be linked to the etiology of ovarian diseases such as primary ovarian insufficiency POI and polycystic ovarian syndrome PCOS. Future investigations can now utilize the observations from this systems approach to further elucidate the molecular control of ovarian primordial follicle development and associated diseases.

Methods

Ovarian organ culture

Zero-day old female Sprague–Dawley rats (Harlan Laboratories, Inc., USA) were euthanized within six hours after birth according to Washington State University IACUC approved (#02568) protocols and the ovaries removed and cultured whole as described previously [50]. Zero-day old rat ovaries contain primarily oocytes in nests, prior to being assembled into follicles. For ovary culture experiments in which ovarian RNA was collected, 2–3 ovaries per well were cultured for one day in the absence (controls) or presence (treated) of either AMH (human Anti-Müllerian hormone)(50 ng/ml, R&D Systems Inc., USA), FGF2 (rat Fibroblast growth factor 2)(50 ng/ml, R&D Systems Inc., USA), CTGF (human Connective Tissue Growth Factor)(500 ng/ml, PeproTech Inc., NJ USA), TNFa (rat Tumor Necrosis Factor alpha)(1ng/ml, R&D Systems Inc., USA), activin A (human/mouse/rat activin beta-A homodimer)(100 ng/ml, R&D Systems Inc., USA), E2 (Estradiol)(1×10^{-6}M, Sigma-Aldrich, USA), or P4 (Progesterone)(1×10^{-6}M, Sigma-Aldrich, USA). After only one day of culture there are few morphological differences between control and treated ovaries, so measurements of whole-ovary gene expression reflect differences in RNA transcription, rather than differing proportions of cell types due to differing cell proliferation between treatments. After culture the 2–3 ovaries receiving the same treatment from one culture well were pooled and homogenized in one ml Trizol™ reagent (Sigma-Aldrich, USA), then stored at −70°C. There were three different biological experiments (biological replicates) for each of the seven treatment compounds, and seven replicates of the controls, for a total of 28 RNA samples.

In order to determine the effect of FGF2 on primordial follicle assembly, ovaries were cultured as above for two days in the absence or presence of FGF2 (50 ng/ml). Similarly, in order to determine the effect of increased ERK1/2 signaling on follicle assembly, ovaries were cultured in the presence or absence of BCI (1μM; Sigma-Aldrich #B4313). After 2 days culture ovaries were fixed with Bouin's solution, paraffin embedded, sectioned onto microscope slides and stained with hematoxylin and eosin as described previously [50].

Morphometric analysis

The number of oocytes at each developmental stage was counted and averaged in two serial sections from the largest cross-section through the center of the ovary. Oocytes in ovarian cross sections were classified as unassembled, or as assembled into primordial (stage 0), or developing follicles (stages 1–4: early primary, primary, transitional and preantral) as previously described [1,51]. Oocytes in nests are contiguous with other oocytes, without intervening stromal cells. An oocyte was still considered to be part of a nest if, for any region of its perimeter, one quarter of its circumference or more was contiguous with other oocytes. Primordial follicles consist of an oocyte arrested in prophase I of meiosis that is encapsulated by squamous (i.e. flattened) pregranulosa cells. Early transition primary follicles have initiated development (i.e., undergone primordial to primary follicle transition) and contain at least two cuboidal granulosa cells. Primary and preantral follicles exhibit one or more complete layers of cuboidal granulosa cells [30,52]. Hematoxylin/eosin stained ovarian sections were analyzed at 400× magnification using light microscopy. Degenerating red eosin-stained oocytes were not counted. Oocytes in which the cell nucleus was not clearly visible in the plane of section were not counted.

RNA preparation

RNA was isolated from whole rat ovaries after homogenization in one ml Trizol™ reagent (Sigma-Aldrich, USA), according to manufacturer's instructions. Two or three ovaries from the same culture well (from different rat pups) and receiving the same treatment were pooled and homogenized together. Homogenized samples were stored at −70°C until the time of RNA isolation. After isolation from Trizol, RNA was further purified using RNeasy MinElute Cleanup Kits (Qiagen, USA) and stored in aqueous solution at −70°C.

Microarray analysis

The microarray analysis was performed by the Genomics Core Laboratory, Center for Reproductive Biology, Washington State University, Pullman, WA using standard Affymetrix reagents and protocol. Briefly, mRNA was transcribed into cDNA with random primers, cRNA was transcribed, and single-stranded sense DNA was synthesized which was fragmented and labeled with biotin. Biotin-labeled ssDNA was then hybridized to the Rat Gene 1.0 ST microarrays containing 27,342 transcripts (Affymetrix, Santa Clara, CA, USA). Hybridized chips were scanned on Affymetrix Scanner 3000. CEL files containing raw data were then pre-processed and analyzed with Partek Genomic Suite 6.3 software (Partek Incorporated, St. Louis, MO) using an RMA GC-content adjusted algorithm. Comparison of all array histogram graphs demonstrated that the data for 27 of 28 chips were similar and appropriate for further analysis. One chip, from a P4-treated sample, was an outlier and so was discarded (Additional file 1: Figure S1). In addition, a batch effect associated with RNA processing date was noted and incorporated into the analysis. The data from the remaining 27 chips were again pre-processed and analyzed as a group, with the RNA processing batch used as a blocking factor.

The microarray quantitative data involves over 10 different oligonucleotides arrayed for each gene and the hybridization must be consistent to allow for a statistically significant quantitative measure of gene expression and regulation. In contrast, a quantitative PCR procedure only uses two oligonucleotide primers, and primer bias is a major factor in this type of analysis. Therefore, we did not attempt to use PCR based approaches as we feel the microarray analysis is more accurate and reproducible without the primer bias of PCR based approaches.

All microarray CEL files (MIAME compliant raw data) from this study have been deposited with the NCBI gene expression and hybridization array data repository (GEO, http://www.ncbi.nlm.nih.gov/geo) (GEO Accession number: Pending), all arrays combined with one accession number, and can be also accessed through www.skinner.wsu.edu. For gene annotation, Affymetrix annotation file RaGene-1_0-st-v1.na32.rn4.transcript.csv was used unless otherwise specified.

Gene bionetwork analysis

The cluster coordinated expression analysis was restricted to genes differentially expressed between the control and the treatment groups based on previously established criteria: (1) fold change of group means ≥1.2 or ≤0.83; (2) *T* test p-value ≤0.05 compared to control; and (3) absolute difference of group means ≥10. The less stringent cutoff for fold change avoids loss of important genes at such an early stage of analysis since these candidate genes will go through subsequent systems-level coexpression network and pathway analyses that can further filter noisy signal, as we have shown in the previous study [53]. The union of the differentially expressed genes from the different treatments resulted in 1081 genes (i.e. Affymetrix probesets) being identified and used for constructing a weighted gene co-expression network [32,44]. Unlike traditional un-weighted gene co-expression networks in which two genes (nodes) are either connected or disconnected, the weighted gene co-expression analysis assigns a connection weight to each gene pair using soft-thresholding and thus is robust to parameter selection. The weighted network analysis begins with a matrix of the Pearson correlations between all gene pairs, then converts the correlation matrix into an adjacency matrix using a power function $f(x) = x^{\beta}$. The parameter β of the power function is determined in such a way that the resulting adjacency matrix (i.e., the weighted co-expression network), is approximately scale-free. To measure how well a network satisfies a scale-free topology, we use the fitting index proposed by Zhang & Horvath [32] (i.e., the model fitting index R^2 of the linear model that regresses $log(p(k))$ on $log(k)$ where k is connectivity and $p(k)$ is the frequency distribution of connectivity). The fitting index of a perfect scale-free network is 1. For this dataset, we select the smallest β (= 7) which leads to an approximately scale-free network with the truncated scale-free fitting index R^2 greater than 0.75. The distribution $p(k)$ of the resulting network approximates a power law: $p(k) \sim k^{-1.29}$.

To explore the modular structures of the co-expression network, the adjacency matrix is further transformed into a topological overlap matrix [37]. The topological overlap between two genes reflects not only their direct interaction, but also their indirect interactions through all the other genes in the network. Previous studies [32,37] have shown that topological overlap leads to more cohesive and biologically meaningful modules. To identify modules of highly co-regulated genes, we used average linkage hierarchical clustering to group genes based on the topological overlap of their connectivity, followed by a dynamic cut-tree algorithm to dynamically cut clustering dendrogram branches into gene modules [54]. A total of nine modules were identified and the module size was observed to range from 20 to 240 genes.

To distinguish between modules, each module was assigned a unique color identifier, with the remaining, poorly connected genes colored grey. In this type of map, the rows and the columns represent genes in a symmetric fashion, and the color intensity represents the interaction strength between genes (Figure 5). This connectivity map highlights the fact that differentially expressed genes fall into distinct network modules, where genes within a given module are more interconnected with each other (blocks along the diagonal of the matrix) than with genes in other modules. There are several network connectivity measures, but one particularly important one is the within module connectivity (k.in). The k.in of a gene was determined by taking the sum of its connection strengths (co-expression similarity) with all other genes in the module to which the gene belonged.

In order to compile a shorter list of the most tightly co-regulated genes from each module, the top 10% of genes from each module with highest k.in. scores (connectivity within module) were selected. Additional genes were added from each module, above 10%, if those genes had k. in. scores >8. If the list for any module did not include enough named genes (i.e. genes that were not EST's) to equal 10% of the module size, then additional genes with the highest k.in. scores were added until 10% named genes was achieved.

Pathway analysis

Lists of differentially expressed genes for each regulatory factor treatment, as well as for each module generated in the network analysis, were analyzed for KEGG (Kyoto Encyclopedia for Genes and Genome, Kyoto University, Japan) pathway enrichment using Pathway-Express, a web-based tool freely available as part of the Onto-Tools

(http://vortex.cs.wayne.edu) [55]. Additionally, gene lists were analyzed using the KEGG website (http://www.genome.jp/kegg/pathway.html). KEGG pathways were considered 'impacted' and were included in analyses for this manuscript if three or more differentially expressed genes were present within a KEGG pathway. Statistical over-representation of differentially expressed genes within a pathway was determined by Fischer's exact test for two by two contingency tables, and by calculating hypergeometric probability of obtaining exactly the listed number of genes in common with that pathway.

Global literature analysis of various gene lists was performed using Pathway Studio (Ariadne, Genomics Inc. Rockville MD) software, which performs pathway and interaction analysis and identifies genes that have regulatory or binding relationships. Pathway Studio was also used to identify cellular functions and diseases (including polycystic ovarian syndrome) linked in the published literature to the genes in these lists. In addition, Pathway Studio was used to determine over-represented physiological processes for gene lists based on KEGG, PANTHER (Protein ANalysis THrough Evolutionary Relationships) and NCBI GO (National Center for Biotechnology Information Gene Ontology) databases.

Additional files

Additional file 1: Figure S1. Sample histograms and box plots for ovary RNA sample microarray signal values prior to pre-processing and normalization. Note that one of the P4-treated samples was an outlier, and was discarded. X-axis shows hybridization intensity value. Y-axis (Hybridization Frequency) shows the number of genes having a given hybridization intensity.

Additional file 2: Table S1. Differentially expressed genes: A) Genes influenced by treatment with anti-Müllerian hormone (AMH). B) Genes influenced by treatment with CTGF. C) Genes influenced by treatment with FGF2. D) Genes influenced by treatment with ActivinA. E) Genes influenced by treatment with P4. F) Genes influenced by treatment with TNFa. G) Genes influenced by treatment with E2.

Additional file 3: Table S2. Treatment and module differentially expressed genes correlated to cellular pathways and processes.

Additional file 4: Figure S2. Gene network of known relationships among all 1081 genes found to be differentially expressed in treated *versus* Control ovaries. Genes with the greatest number of connections (relationships) to other genes have enlarged gene symbols. Network is derived from an un-biased search of literature using Pathway Studio™. Node shapes code: oval – protein; diamond – ligand; irregular polygon – phosphatase; circle/oval on tripod platform – transcription factor; ice cream cone – receptor. Grey arrows represent regulation, lilac – expression, green – promoter binding, olive – protein modification, purple - binding.

Additional file 5: Figure S3. Gene network of known relationships among differentially expressed genes assigned to specific co-expression modules. A) Blue module. B) Black module. Network is derived from an un-biased search of literature using Pathway Studio™. Node shapes code: oval – protein; diamond – ligand; irregular polygon – phosphatase; circle/oval on tripod platform – transcription factor; ice cream cone – receptor. Grey arrows represent regulation, lilac – expression, green – promoter binding, olive – protein modification, purple - binding.

Additional file 6: Figure S4. Gene network of known relationships among genes differentially expressed in ovaries receiving specific treatments, compared to controls. A) E2 (estrogen). B) FGF2. C) Activin A. Network is derived from an un-biased search of literature using Pathway Studio™. Node shapes code: oval – protein; diamond – ligand; irregular polygon – phosphatase; circle/oval on tripod platform – transcription factor; ice cream cone – receptor. Grey arrows represent regulation, lilac – expression, green – promoter binding, olive – protein modification, purple - binding.

Abbreviations

POI: Primary ovarian insufficiency; PCOS: Polycystic ovarian disease syndrome; AMH: Anti-Müllerian hormone; CTGF: Connective tissue growth factor; E2: Estradiol; P4: Progesterone; TNFa: Tumor necrosis factor alpha; BDNF: Brain derived neurotrophic factor; KITL: Kit ligand; GDF9: Growth differentiation factor-9; FGF2: Fibroblast growth factor-2; k.in.: Connectivity index.

Competing interest

The authors declare that no competing interests exist.

Authors' contribution

MKS designed the study. EN performed the ovary cultures and microarray analysis and network design. BZ performed the bionetwork analysis and bioinformatics. EN wrote the manuscript and all authors edited the manuscript. All authors read and approved the final manuscript.

Acknowledgements

We thank the expert technical assistance of Ms. Rebecca Tracey, Ms. Renee Espinosa Najera, Ms. Jessica Shiflett, Ms. Chrystal Bailey, Ms. Colleen Johns, and Mr. Md. Haque. We thank Ms. Heather Johnson for assistance in preparation of the manuscript.

Financial disclosure

This study was supported by a grant from the NIH, NIEHS to MKS.
The funders had no role in study design, data collection and analysis, decision to publish, or preparation of the manuscript.

Author details

[1]Center for Reproductive Biology, School of Biological Sciences, Washington State University, Pullman, WA 99164-4236, USA. [2]Department of Genetics & Genomic Sciences, Mount Sinai School of Medicine, New York, NY, USA.

Received: 4 February 2013 Accepted: 4 July 2013
Published: 23 July 2013

References

1. Nilsson EE, Schindler R, Savenkova MI, Skinner MK: Inhibitory actions of Anti-Mullerian Hormone (AMH) on ovarian primordial follicle assembly. *PLoS One* 2011, 6(5):e20087.
2. Hirshfield AN: Development of follicles in the mammalian ovary. *Int Rev Cytol* 1991, 124:43–101.
3. Skinner MK: Regulation of primordial follicle assembly and development. *Hum Reprod Update* 2005, 11(5):461–471.
4. Rajah R, Glaser EM, Hirshfield AN: The changing architecture of the neonatal rat ovary during histogenesis. *Dev Dyn* 1992, 194(3):177–192.
5. Sarraj MA, Drummond AE: Mammalian foetal ovarian development: consequences for health and disease. *Reproduction* 2012, 143(2):151–163.
6. Pepling ME: Follicular assembly: mechanisms of action. *Reproduction* 2012, 143(2):139–149.
7. Richards JS, Pangas SA: The ovary: basic biology and clinical implications. *J Clin Invest* 2010, 120(4):963–972.
8. Pepling ME, Spradling AC: Female mouse germ cells form synchronously dividing cysts. *Development* 1998, 125(17):3323–3328.
9. Gondos B: Germ cell degeneration and intercellular bridges in the human fetal ovary. *Z Zellforsch Mikrosk Anat* 1973, 138(1):23–30.
10. Byskov AG: Differentiation of mammalian embryonic gonad. *Physiol Rev* 1986, 66(1):71–117.
11. Borum K: Oogenesis in the mouse. A study of the meiotic prophase. *Exp Cell Res* 1961, 24:495–507.

12. McGee EA, Hsu SY, Kaipia A, Hsueh AJ: Cell death and survival during ovarian follicle development. *Mol Cell Endocrinol* 1998, 140(1–2):15–18.
13. Pepling ME, Sundman EA, Patterson NL, Gephardt GW, Medico L Jr, Wilson KI: Differences in oocyte development and estradiol sensitivity among mouse strains. *Reproduction* 2010, 139(2):349–357.
14. De Vos M, Devroey P, Fauser BC: Primary ovarian insufficiency. *Lancet* 2010, 376(9744):911–921.
15. Maclaran K, Panay N: Premature ovarian failure. *J Fam Plann Reprod Health Care* 2011, 37(1):35–42.
16. Schindler R, Nilsson E, Skinner MK: Induction of ovarian primordial follicle assembly by connective tissue growth factor CTGF. *PLoS One* 2010, 5(9):e12979.
17. Chen Y, Jefferson WN, Newbold RR, Padilla-Banks E, Pepling ME: Estradiol, progesterone, and genistein inhibit oocyte nest breakdown and primordial follicle assembly in the neonatal mouse ovary in vitro and in vivo. *Endocrinology* 2007, 148(8):3580–3590.
18. Yang MY, Fortune JE: The capacity of primordial follicles in fetal bovine ovaries to initiate growth in vitro develops during mid-gestation and is associated with meiotic arrest of oocytes. *Biol Reprod* 2008, 78(6):1153–1161.
19. Wang C, Roy SK: Development of primordial follicles in the hamster: role of estradiol-17beta. *Endocrinology* 2007, 148(4):1707–1716.
20. Zachos NC, Billiar RB, Albrecht ED, Pepe GJ: Developmental regulation of baboon fetal ovarian maturation by estrogen. *Biol Reprod* 2002, 67(4):1148–1156.
21. Bristol-Gould SK, Kreeger PK, Selkirk CG, Kilen SM, Cook RW, Kipp JL, Shea LD, Mayo KE, Woodruff TK: Postnatal regulation of germ cells by activin: the establishment of the initial follicle pool. *Dev Biol* 2006, 298(1):132–148.
22. Nilsson EE, Skinner MK: Progesterone regulation of primordial follicle assembly in bovine fetal ovaries. *Mol Cell Endocrinol* 2009, 313(1–2):9–16.
23. Nilsson EE, Stanfield J, Skinner MK: Interactions between progesterone and tumor necrosis factor-alpha in the regulation of primordial follicle assembly. *Reproduction* 2006, 132(6):877–886.
24. Marcinkiewicz JL, Balchak SK, Morrison LJ: The involvement of tumor necrosis factor-alpha (TNF) as an intraovarian regulator of oocyte apoptosis in the neonatal rat. *Front Biosci* 2002, 7:d1997–d2005.
25. Morrison LJ, Marcinkiewicz JL: Tumor necrosis factor alpha enhances oocyte/follicle apoptosis in the neonatal rat ovary. *Biol Reprod* 2002, 66(2):450–457.
26. Trombly DJ, Woodruff TK, Mayo KE: Suppression of Notch signaling in the neonatal mouse ovary decreases primordial follicle formation. *Endocrinology* 2009, 150(2):1014–1024.
27. Spears N, Molinek MD, Robinson LL, Fulton N, Cameron H, Shimoda K, Telfer EE, Anderson RA, Price DJ: The role of neurotrophin receptors in female germ-cell survival in mouse and human. *Development* 2003, 130(22):5481–5491.
28. Kerr B, Garcia-Rudaz C, Dorfman M, Paredes A, Ojeda SR: NTRK1 and NTRK2 receptors facilitate follicle assembly and early follicular development in the mouse ovary. *Reproduction* 2009, 138(1):131–140.
29. Wang J, Roy SK: Growth differentiation factor-9 and stem cell factor promote primordial follicle formation in the hamster: modulation by follicle-stimulating hormone. *Biol Reprod* 2004, 70(3):577–585.
30. Kezele PR, Ague JM, Nilsson E, Skinner MK: Alterations in the ovarian transcriptome during primordial follicle assembly and development. *Biol Reprod* 2005, 72(1):241–255.
31. Nilsson EE, Savenkova MI, Schindler R, Zhang B, Schadt EE, Skinner MK: Gene bionetwork analysis of ovarian primordial follicle development. *PLoS One* 2010, 5(7):e11637.
32. Zhang B, Horvath S: A general framework for weighted gene co-expression network analysis. *Stat Appl Genet Mol Biol* 2005, 4:17.
33. Lum PY, Chen Y, Zhu J, Lamb J, Melmed S, Wang S, Drake TA, Lusis AJ, Schadt EE: Elucidating the murine brain transcriptional network in a segregating mouse population to identify core functional modules for obesity and diabetes. *J Neurochem* 2006, 97(Suppl 1):50–62.
34. Millstein J, Winrow CJ, Kasarskis A, Owens JR, Zhou L, Summa KC, Fitzpatrick K, Zhang B, Vitaterna MH, Schadt EE, *et al*: Identification of causal genes, networks, and transcriptional regulators of REM sleep and wake. *Sleep* 2011, 34(11):1469–1477.
35. Wang IM, Zhang B, Yang X, Zhu J, Stepaniants S, Zhang C, Meng Q, Peters M, He Y, Ni C, *et al*: Systems analysis of eleven rodent disease models reveals an inflammatome signature and key drivers. *Mol Syst Biol* 2012, 8:594.
36. Schadt EE, Lamb J, Yang X, Zhu J, Edwards S, Guhathakurta D, Sieberts SK, Monks S, Reitman M, Zhang C, *et al*: An integrative genomics approach to infer causal associations between gene expression and disease. *Nat Genet* 2005, 37(7):710–717.
37. Ravasz E, Somera AL, Mongru DA, Oltvai ZN, Barabasi AL: Hierarchical organization of modularity in metabolic networks. *Science* 2002, 297(5586):1551–1555.
38. Arkell RS, Dickinson RJ, Squires M, Hayat S, Keyse SM, Cook SJ: DUSP6/MKP-3 inactivates ERK1/2 but fails to bind and inactivate ERK5. *Cell Signal* 2008, 20(5):836–843.
39. Molina G, Vogt A, Bakan A, Dai W, de Queiroz Oliveira P, Znosko W, Smithgall TE, Bahar I, Lazo JS, Day BW, *et al*: Zebrafish chemical screening reveals an inhibitor of Dusp6 that expands cardiac cell lineages. *Nat Chem Biol* 2009, 5(9):680–687.
40. Li G, Yu M, Lee WW, Tsang M, Krishnan E, Weyand CM, Goronzy JJ: Decline in miR-181a expression with age impairs T cell receptor sensitivity by increasing DUSP6 activity. *Nat Med* 2012, 18(10):1518–1524.
41. Nilsson E, Rogers N, Skinner MK: Actions of anti-Mullerian hormone on the ovarian transcriptome to inhibit primordial to primary follicle transition. *Reproduction* 2007, 134(2):209–221.
42. MacFarlane LA, Murphy PR: Regulation of FGF-2 by an endogenous antisense RNA: effects on cell adhesion and cell-cycle progression. *Mol Carcinog* 2010, 49(12):1031–1044.
43. Yang D, Li Y, Xiao H, Liu Q, Zhang M, Zhu J, Ma W, Yao C, Wang J, Wang D, *et al*: Gaining confidence in biological interpretation of the microarray data: the functional consistence of the significant GO categories. *Bioinformatics* 2008, 24(2):265–271.
44. Zhu J, Wiener MC, Zhang C, Fridman A, Minch E, Lum PY, Sachs JR, Schadt EE: Increasing the power to detect causal associations by combining genotypic and expression data in segregating populations. *PLoS Comput Biol* 2007, 3(4):e69.
45. Gargalovic PS, Imura M, Zhang B, Gharavi NM, Clark MJ, Pagnon J, Yang WP, He A, Truong A, Patel S, *et al*: Identification of inflammatory gene modules based on variations of human endothelial cell responses to oxidized lipids. *Proc Natl Acad Sci U S A* 2006, 103(34):12741–12746.
46. Horvath S, Zhang B, Carlson M, Lu KV, Zhu S, Felciano RM, Laurance MF, Zhao W, Qi S, Chen Z, *et al*: Analysis of oncogenic signaling networks in glioblastoma identifies ASPM as a molecular target. *Proc Natl Acad Sci U S A* 2006, 103(46):17402–17407.
47. Holt JE, Jackson A, Roman SD, Aitken RJ, Koopman P, McLaughlin EA: CXCR4/SDF1 interaction inhibits the primordial to primary follicle transition in the neonatal mouse ovary. *Dev Biol* 2006, 293(2):449–460.
48. Slot KA, Kastelijn J, Bachelot A, Kelly PA, Binart N, Teerds KJ: Reduced recruitment and survival of primordial and growing follicles in GH receptor-deficient mice. *Reproduction* 2006, 131(3):525–532.
49. Dunaif A: Polycystic ovary syndrome in 2011: Genes, aging and sleep apnea in polycystic ovary syndrome. *Nat Rev Endocrinol* 2012, 8(2):72–74.
50. Dole G, Nilsson EE, Skinner MK: Glial-derived neurotrophic factor promotes ovarian primordial follicle development and cell-cell interactions during folliculogenesis. *Reproduction* 2008, 135(5):671–682.
51. Oktay K, Schenken RS, Nelson JF: Proliferating cell nuclear antigen marks the initiation of follicular growth in the rat. *Biol Reprod* 1995, 53(2):295–301.
52. Parrott JA, Skinner MK: Kit-ligand/stem cell factor induces primordial follicle development and initiates folliculogenesis. *Endocrinology* 1999, 140(9):4262–4271.
53. Skinner MK, Manikkam M, Haque MM, Zhang B, Savenkova M: Epigenetic Transgenerational Inheritance of Somatic Transcriptomes and Epigenetic Control Regions. *Genome Biol* 2012, 13(10):R91.
54. Langfelder P, Horvath S: Eigengene networks for studying the relationships between co-expression modules. *BMC Syst Biol* 2007, 1:54.
55. Draghici S, Khatri P, Tarca AL, Amin K, Done A, Voichita C, Georgescu C, Romero R: A systems biology approach for pathway level analysis. *Genome Res* 2007, 17(10):1537–1545.

doi:10.1186/1471-2164-14-496
Cite this article as: Nilsson *et al.*: Gene bionetworks that regulate ovarian primordial follicle assembly. *BMC Genomics* 2013 14:496.